Phase change materials encapsulation in crosslinked polymer-based monoliths : syntheses, characterization and evaluation of pullulan and black liquor based-monoliths for the encapsulation of phase change materials

Juan Ángel Moreno Balderrama

université de BORDEAUX

THÈSE PRÉSENTÉE

POUR OBTENIR LE GRADE DE

DOCTEUR DE

L'UNIVERSITÉ DE BORDEAUX

ÉCOLE DOCTORALE

SPÉCIALITÉ CHIMIE DE POLYMERES

Par Juan Ángel MORENO BALDERRAMA

PHASE CHANGE MATERIALS ENCAPSULATION IN CROSSLINKED POLYMER-BASED MONOLITHS

Syntheses, characterization and evaluation of pullulan and black liquor based-monoliths for the encapsulation of phase change materials

Sous la direction de : Hervé DELEUZE

Soutenue le 14 Décembre 2018

Membres du jury :

M. ESQUENA Jordi	Centro de Química Coloidal Interficial (QCI)	Président
Mme. CHARRIER Fatima	Université de Pau et des Pays de l'Adour	Rapporteur
M. LEAL Fernando	Centre de Colloïdes et Lipides pour l'Industrie et la Nutrition, Bordeaux, France	Rapporteur
M. MAHEO Laurent	Université de Bretagne Sud	Invité

" No hay nada repartido de modo más equitativo que la razón; todo el mundo está convencido de tener suficiente"

Descartes

Title : Phase change materials encapsulation in crosslinked polymer-based monoliths

Abstract : Emulsion-templated polymer based (pullulan, lining and hemicelluloses) monoliths encapsulating butyl stearate as bio-based phase change material (PCM) were synthesized. Polymer-bases were crosslinked with sodium trimetaphosphate (STMP) under alkaline aqueous conditions leading to an interconnected porous network. The influence of the drying process on the obtained composite materials morphology was studied indicating freeze-drying as the most effective technique. Differential Scanning Calorimetry (DSC) studies allow to assess that encapsulation of butyl stearate onto matrices do not alter its phase change thermal properties. Mechanical compression and strain resistance tests allowed to evaluate monoliths potential as heat storage panels installed directly in buildings and greenhouses, STMP crosslinking products were identified by solid-NMR characterization, this allowed to synthetize monoliths at different crosslinking yields to find a formulation that improves PCM encapsulation. Polymer matrices were studied by scanning electron microscopy to identify the pore size distribution obtained in STMP crosslinked materials. This new one-step encapsulating approach appears as efficient and cost-effective and is expected to find a broad development in energy storage applications.

Keywords : Encapsulation, phase change materials, pullulan, black liquor, STMP crosslinking, STMP- NMR reaction products, porous materials.

Polymers Chemistry

[Institut des Sciences Moléculaires, Ecole Doctoral de Chimie, Université de Bordeaux]

Titre : Encapsulation de matériaux à changement de phase dans des monolithes réticulés à base de polymères

Résumé : Le stéarate de butyle, un matériau de changement de phase biosourcé (MCP), a été encapsulés dans des matrices polymères (pullulane, lignine, hémicelluloses) par la technique des émulsions concentrées. Les matrices polymères ont été réticulées avec du trimetaphosphate de sodium (STMP) dans des conditions alcalines afin d'obtenir un réseau poreux interconnecté rigide. L'influence du processus de séchage sur les matériaux composites obtenus a été étudiée, indiquant la lyophilisation comme la technique la plus efficace. Des études de calorimétrie à balayage différentiel (DSC) ont permis de déterminer que l'encapsulation de stéarate de butyle dans des matrices polymères ne modifiait pas ses propriétés thermiques de changement de phase. Des essais de compression mécanique et de résistance à la déformation ont permis d'évaluer le potentiel des monolithes en tant que panneaux de stockage de chaleur installés directement dans des bâtiments et des serres. Les produits de réticulation par le STMP ont été identifiés et caractérisés par RMN solide du 31P. Il a ainsi été possible de synthétiser des monolithes ayant différents taux de réticulation afin d'optimiser la formulation d'encapsulation de MCP. Les matrices polymères vidée de tous leurs contenus liquides ont été étudiées par microscopie électronique à balayage afin d'étudier leur structure poreuse (distribution de taille des pores). Cette nouvelle approche d'encapsulation en une étape apparaît comme efficace et devrait permettre un développement important des applications énergétiques.

Mots-clés : Encapsulation, Matériaux à changement de phase, Isolation thermique, Pullulane, Liqueur noire

Index

Index of figures

Index of tables

1 Economic impact of thermal insulation in energy savings

1.1 Introduction

One of the most important challenges of future buildings is the reduction of energy consumptions in all their life phases, from construction to demolition. Several regulations have been created in the recent years to improve the use of energy in buildings and in general, their efficiency in the resources utilization. A list of recently created regulations and their objectives have been indicated in **Table 1-1**.

Table 1-1. Regulations concerning energy efficiency in buildings

Regulation concerning the improvement of energy efficiency in buildings	Buildings resources consumption	Main regulations objectives	References
✓ U.S. Department of Energy ✓ United Nation Environmental Program ✓ European Commission ✓ EU Energy Performance of Buildings directive (EPBD) ✓ 2010 / 31 EU directive ✓ Energy Efficiency Directive (EED)	Consumption of: ⌖ 40 % of world global energy ⌖ 25 % global water ⌖ 40 % of global resources ⌖ $^1/_3$ of global greenhouse emissions	Development of insulating materials and energy-efficient systems Enhance thermal performance of buildings, passive cooling techniques and thermal capacity of materials Building renovation following the zero-energy buildings measures Reduce by 2020, 20 % of the EU energy consumption	(1) (2) (3) (4) (5) (6) (7)

Regulations agreed with the level of impact of buildings, identifying the energy market as the most affected since 40 % of world global energy is consumed by them. Additionally, high investment costs, lack of information on energy-efficient solutions and a lack of specific available solutions have been identified as the main obstacles to energy building improvement.

Predictions for the coming years indicate that heating and cooling are the main energy building consumers, followed by electric appliances and water heating (**Figure 1-1**).

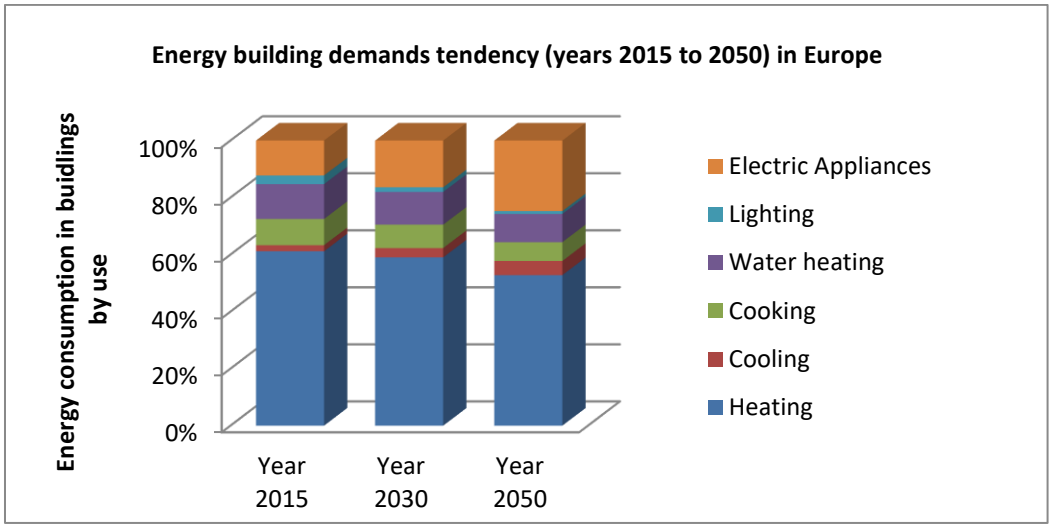

Figure 1-1. Trend of the European energy demand in the residential sector by energy use.

After considering the main energy consumers, lighting is in the last position probably for the efficiency of new lighting technologies [1-3].

Buildings have a large energy-savings potential through renovation and upgrading [2]. At this point the necessity to implement effective measures for reducing building energy consumption is evident. The potential and cost-effective energy savings in buildings are focused in reducing the heat transfer through building envelopes (walls, roofs and windows) and the adoption of efficient installations for heating, cooling, ventilation, water heating, lighting and electricity [3].

1.2 The global market of thermal insulation materials

Residential and non-residential thermal insulation market is expected to keep increasing according to economic predictions made by [8] for the year 2027 the European Union, North America and the Asia Pacific region (APAC) will occupy the first three places concerning thermal insulation investments and building renovation as exemplified in **Figure 1-2**.

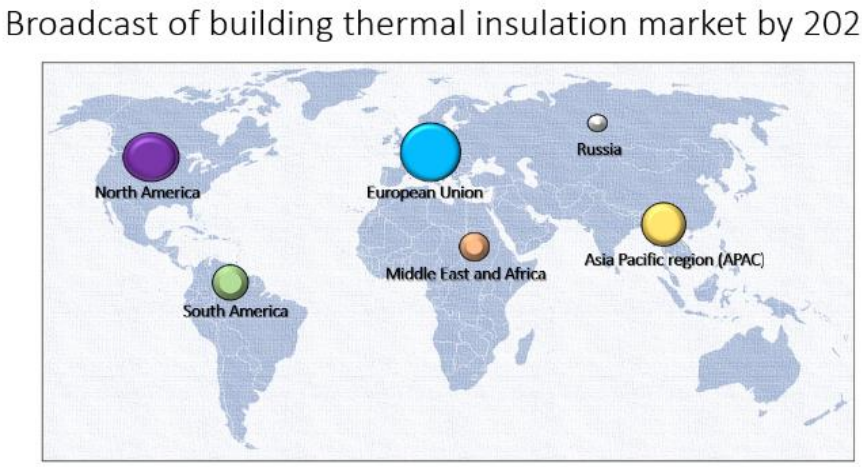

Figure 1-2. Broadcast of thermal insulation market by 2027.

Government regulations to increase energy efficiency seems to be the most important reason to explain this prediction; however, this behavior depends of each country. In the case of the EU it is expected to make the biggest contribution regarding thermal insulation and energy efficiency investments by 2027.

Globally, the most required thermal insulation materials are based on wool (glass and stone wool) and plastic foams (EPS, XPS and PUR), the building thermal insulation market size by type of material has been exemplified in **Figure 1-3**. Mineral wool has advantages such as efficient heat barrier, fire safety, dimensional stability, ecological compatibility, chemical resistance and vapor permeability. The thermal properties of expanded polystyrene (EPS) for energy efficient are well known and have been recognized by standards such as the SANS-204 for South Africa, EPS is also non-toxic and completely recyclable [3].

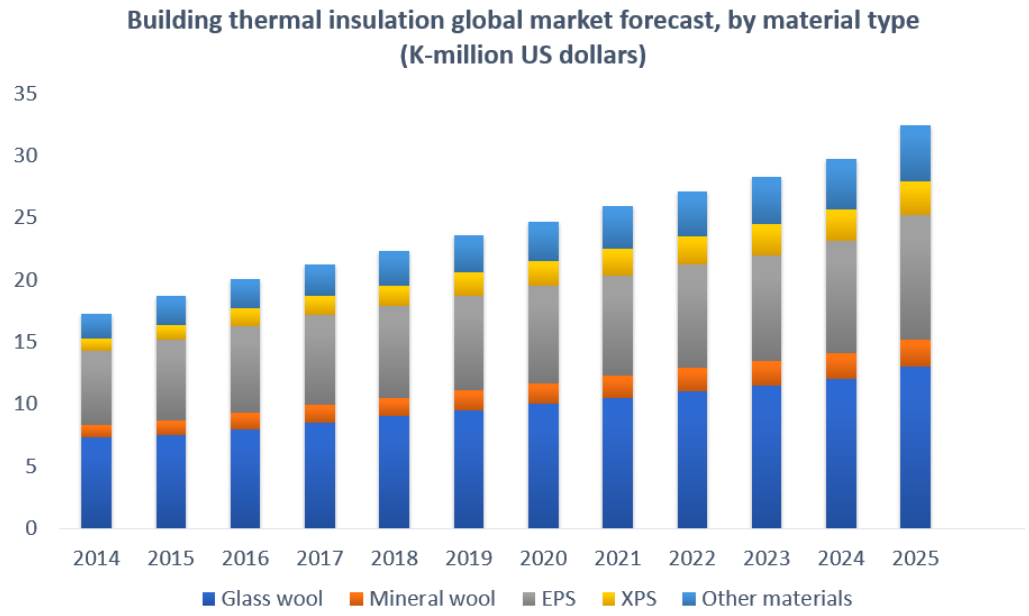

Figure 1-3. Global thermal insulation market forecast by material type (K-million US dollars).

Innovative materials (aerogels, advance insulation foams, vacuum insulation panels and phase change materials) with superior insulation properties are currently under development and the EU represents a potential market [1]. The introduction of the sustainability concept is leading to a gradual change regarding insulation technologies with the development of natural or recycled materials as well as the ones development in research laboratories under green-chemistry principles.

1.3 Materials thermal performance

Thermal insulation systems and materials aim at reducing the transmission of heat flow, main material thermal properties are shown in **Table 1-2**, usually these kinds of materials are used in internal and external building walls, floors and roofs.

Table 1-2. Materials thermal properties

Material	Thermal conductivity (λ) $W.m^{-1}.K^{-1}$	Thermal diffusivity (D) $m^2 s^{-1}$	Specific heat (C) $J\ Kg^{-1}\ K^{-1}$
EPS	0.041	0.030x10-6	1250
Mineral wool	0.050	0.023x10-6	850
Foam glass	0.045	0.023x10-6	1130
Sheep wool	0.046	0.020x10-6	1300 – 1700
XPS	0.040	0.035x10-6	1450 – 1700
Air	0.025	$2x10^{-5}$	718
Silver (pure)	418	149x10-6	234
Copper	388	113x10-6	387
Aluminum	167	97.5x10-6	900
Iron	55	22.8x10-6	448

[9,10].

The preference for one material over the other depends on factors like weather conditions and the level of insulation required. Ceiling and wall insulation are the largest applications in the market followed by windows and floor [9,10]. The typical heat losses and gains in a residential building have been exemplified in **Figure 1-4**.

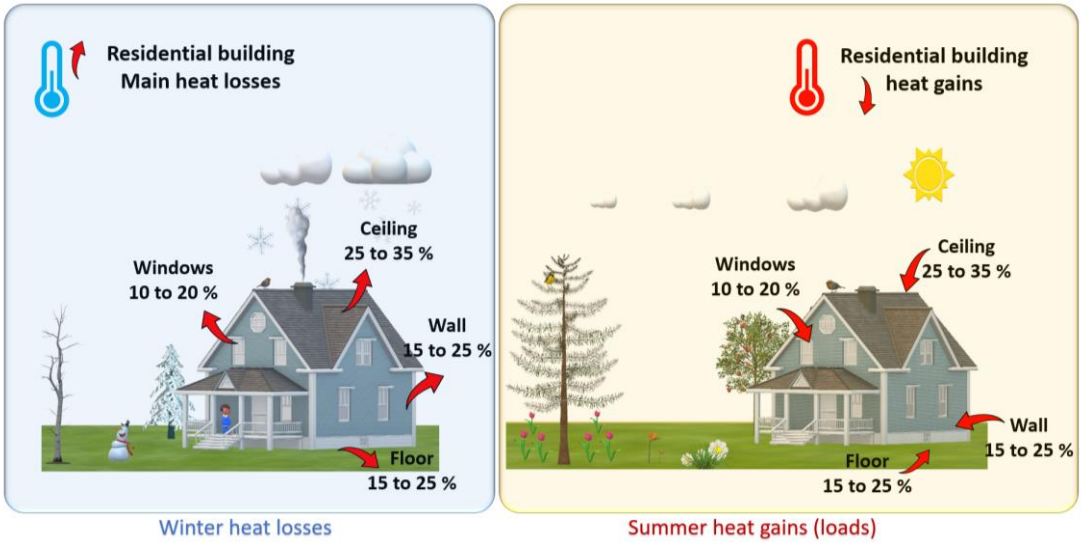

Figure 1-4. Typical heat gains (summer) and losses (winter) in a residential building without insulation

Building insulation market is dominated by few categories, more environmentally friendly buildings outlines developing opportunities for new sustainable materials. These new materials can be manufactured by recycled products or industrial plants byproducts. The need for the development of new environmentally friendly materials and the support to material science is clear; it represents an opportunity area with high impact in the present and future [11].

In response to this problematic and with the aim to contribute to the development and innovation of new environmentally friendly materials, this research work has been developed and it's presented in the following chapters.

The encapsulation of phase change materials in polymeric matrices for building thermal insulation is proposed, following green-chemistry principles and giving a second use to industrial by-products such as black liquor (paper Kraft byproduct). A contribution to energy efficiency in buildings is expected.

Phase change materials (PCMs) are utilized to design thermal energy storage systems, they have been included in buildings ceiling, inside coolers for drinks refrigeration and research is done in order to include them in cooling systems for industrial applications. A review of energy storage systems and PCMs generalities is presented below.

1.4 Technology for Energy Storage

Storage technologies are being develop and implemented as a solution to the disadvantages of typical systems such as lead batteries, the development and implementation of other storage technologies from renewable sources, allowing energy to be released when needed it is becoming more valuable than last decades.

Many attempts have been made to compare ES technologies based on efficiency, cost, application and many other characteristics. Nevertheless, each system is different in terms of specifications that they are difficult to compare. A general description of some of them is presented below.

1.4.1 Hydro storage (pumped storage) systems

Hydro storage system involves the pumping of water from a lower part to an upper part of water to create stored energy for future use. When that energy is needed, the water is then released, and the pumps are reversed allowing the water to run through hydroelectric turbines generating energy. This is a reversible technique that represents the simplest form of pump storage systems widely utilized and well known, it has been described as one of the first techniques used because of its simplicity and easy utilization since it does not require high technology equipment [12].

1.4.2 Compressed air energy storage

Air compressor driven into underground storage (natural salt cave) have a common volume of 600 m^3 up to a pressure of 80 atm, shown in **Figure 1-5**. When the power consumption in the network increases, the storage air goes up and sends a power system. Emptying the air tank to lower the operating pressure 40 atm takes 26 hours giving in general 150 MW [13].

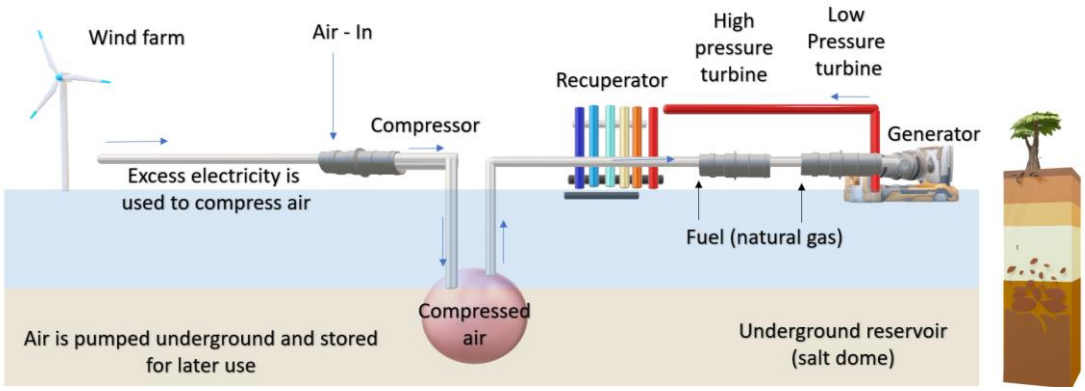

Figure 1-5. Compressed air storage system

The compressed air turns the turbine itself and enters the gas turbine. Since usually $^2/_3$ of power of the gas turbine is consumed to drive a compressor which pumps air into it, it turns into economic savings. Before entering the turbine, air is heated in the flow heat recovery combustion, which adds efficiency [13].

1.4.3 Phase change materials tubes design

PCM-tubes are based on custom made plastic containers filled with PCM with an operating temperature according with the chosen PCM. The range can go from -50 °C to 117 °C, for example. Tubes can be stacked in either cylindrical or rectangular tanks for atmospheric pressurized systems for a variety of thermal energy storage applications. PCM-tubes are sealed after filled with PCM. Its design incorporates internal support columns and external guides so that the containers can be stacked on the top of each other, forming a self-assembling large heat exchanger within the tank, as shown in **Figure 1-6** [14].

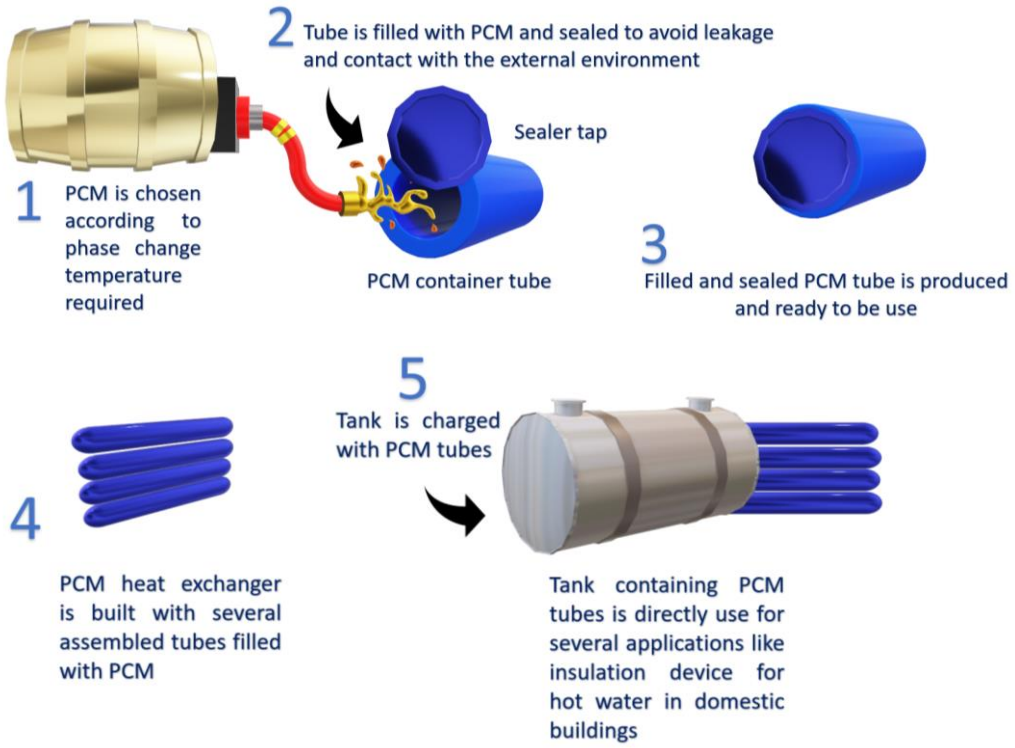

Figure 1-6. Phase change materials in heat exchangers

The self-stacking tubes concept can be applied for both water and air circuits and the gap between each container provides an ideal flow passage with a large heat exchange surface.

Tanks can be of any shape or form to suite site requirements. Tank volumes are calculated based on the required thermal energy system (TES). They can be constructed with plastic, steel or concrete and installed under or above the ground. Tanks can be supplied with flow headers to assure ideal flow conditions within them and a better heat exchange. PCM filled tanks can be installed in domestic houses as shown in **Figure 1-7**. Cold water enters into the tank by the action of pumps and when getting in contact with PCM-tubes, it absorbs the heat from them. The

system is connected to natural gas source or electric source to contribute into water heating. Heated water goes out of the system to the house. Both heat thermal heat storage and external water heat source contribute for the development of better heat water efficiency [14] .

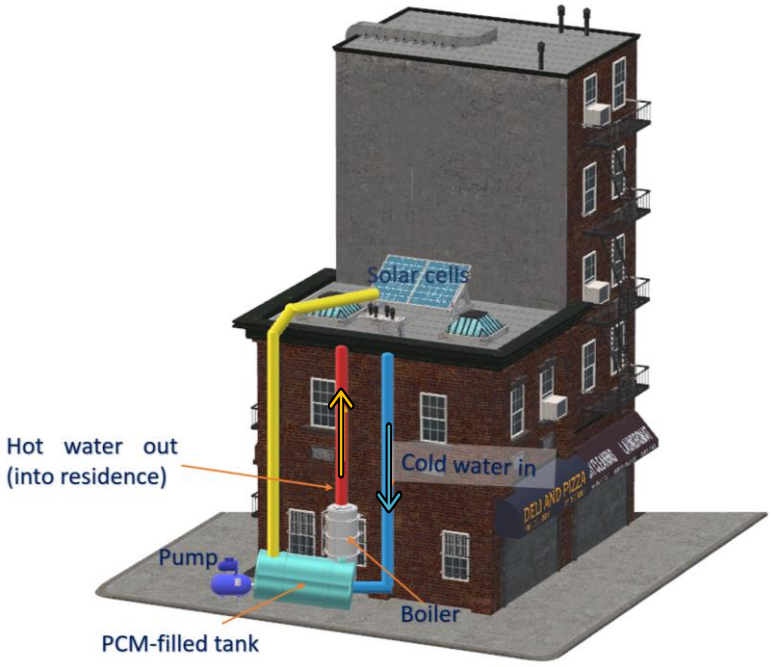

Figure 1-7. PCM-tanks as thermal energy storage systems in domestic residences.

In this case PCM stored heat as latent heat of fusion or also called latent heat of fusion, this offers a higher heat storage capacity per volume / mass and a higher stability of stored hot water. PCM absorbs heat during its phase transition from solid to liquid during daytime solar cycle. The amount of heat a water tank absorbs is higher with the presence of PCM. Sometimes PCM can be encapsulated in polypropylene or high-density polyethylene balls if filled-tubes are not utilized. Latent heat maintains the stored heat for longer periods of time and reduces water temperature fluctuations. The above heat transfer can also be organized for air circuits to store energy during off-peak periods (night), heat is transfer in the same way. The system is illustrated in **Figure 1-8** [14].

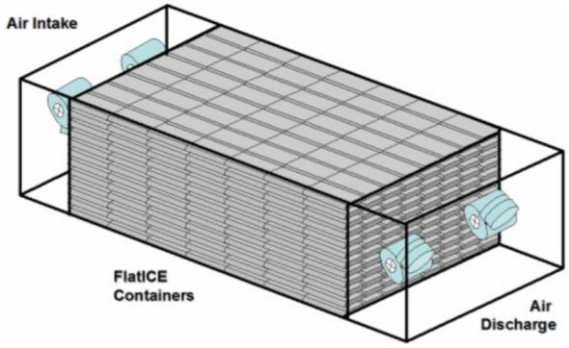

FIGURE 1-8. AIR HEAT ENERGY STORAGE SYSTEM .

1.4.4 Greenhouse insulation with phase change materials filled PVC-pipes.

Similar to the application mentioned before concerning PCM tanks (**Figure 1-6**), the insulation of greenhouses with PCV pipes previously filled with PCM is beginning to emerge. The objective is to insulate the greenhouse walls to avoid heat losses and capture solar heat for night-time utilization. If the greenhouses have a heater-device inside, this heat will be kept for longer time than without PCM panels and the heat device will be less use. This application has been exemplified in **Figure 1-9**.

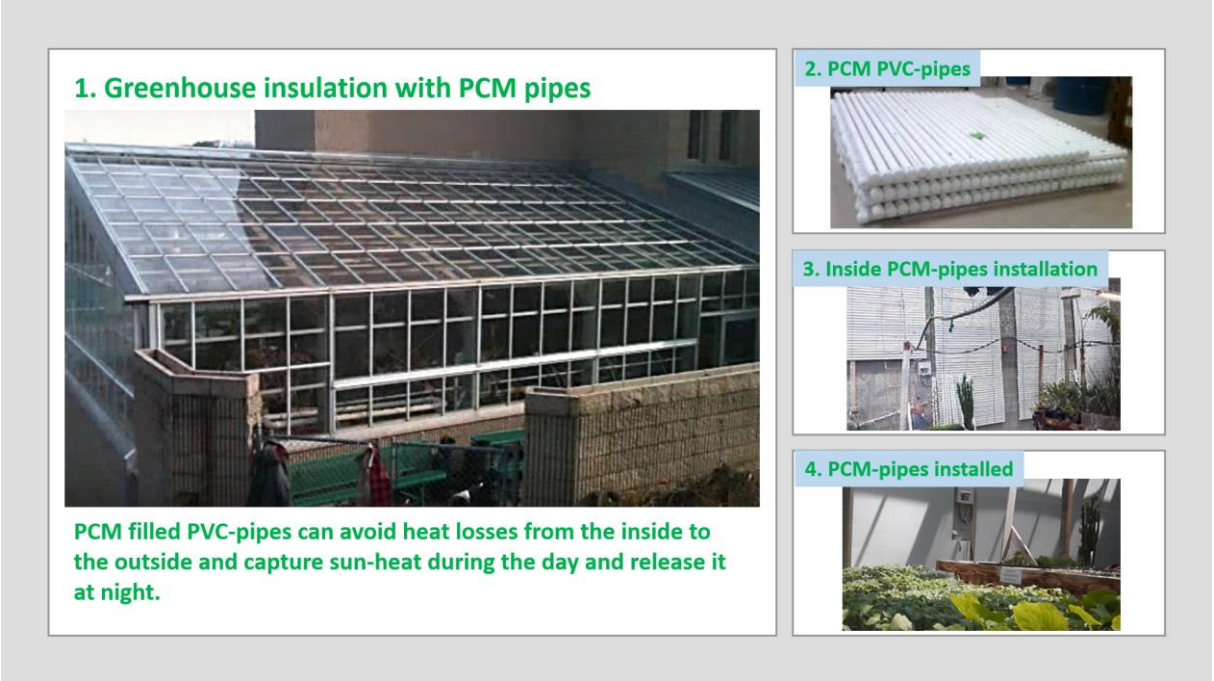

Figure 1-9. Greenhouse insulation with PCM filled PVC-pipes.

PCM-panels are installed inside the greenhouse directly expose to sunlight, in this way the heat is capture during the day and release at night to keep a nice temperature inside the greenhouse, panels are installed in certain walls leaving access to natural light. This kind of systems is under development mostly in U.S. Alternatively, they could be movable in order to installed them when desire.

In general, main advantages of these systems are:

- Temperature of stored water decreases at much slower rates
- PCM can pre-heat cold inlet water during extreme consumption of evening hours
- Total heat storage is more efficient with PCM in solar thermal storage tanks

Storage technologies are being develop and implemented as a solution to the disadvantages of typical systems such as lead batteries which cannot withstand high cycling rates, nor can they store large amounts of energy in a small volume. They must be considered as methods that working together will provided a significant improvement in energy efficiency.

In the following section emphasis will be made in thermal energy storage systems (TES) to present their more remarkable characteristics, advantages and applications. TES thought phase change materials were studied during this research work.

1.5 Thermal energy storage systems (TES)

Renewable energy is an intermittent energy source. For example, intermittence of solar energy is caused by day-night cycles, seasons and weather conditions. Similar problems arise for waste heat recovery systems, where the waste heat availability and utilization periods are different. Therefore, thermal energy storage (TES) is an essential technique for thermal energy utilization to solve the intermittence problems and leveling energy supply and demand. A large volume of TES materials can store the entire daily and annual energy requirement. The optimum size is mainly dependent upon meteorological conditions, storage temperature, storage heat losses, economic viability of storage medium, collector area and efficiency.

Irrespective of their sizes, all TES system must satisfy certain characteristics. The desired characteristics of TES are as follows [15]:

- ✓ Compact, large storage capacity per unit mass and volume
- ✓ Heat storage medium with suitable properties in the operating temperature range,
- ✓ Capability to charge and discharge with largest heat input/output rates but without large temperature gradients
- ✓ Able to undergo large number of charging/discharging cycles without loss in performance and storage capacity
- ✓ Small self-discharging rate (ex. negligible heat losses due to surroundings)
- ✓ Long life
- ✓ Inexpensive

The selection of a TES system for an application depends on many factors, including storage duration, economics, supply and utilization temperature requirements, storage capacity, heat losses and available spaces. Common benefits of TES are well known and listed in **Figure 1-10** [15]:

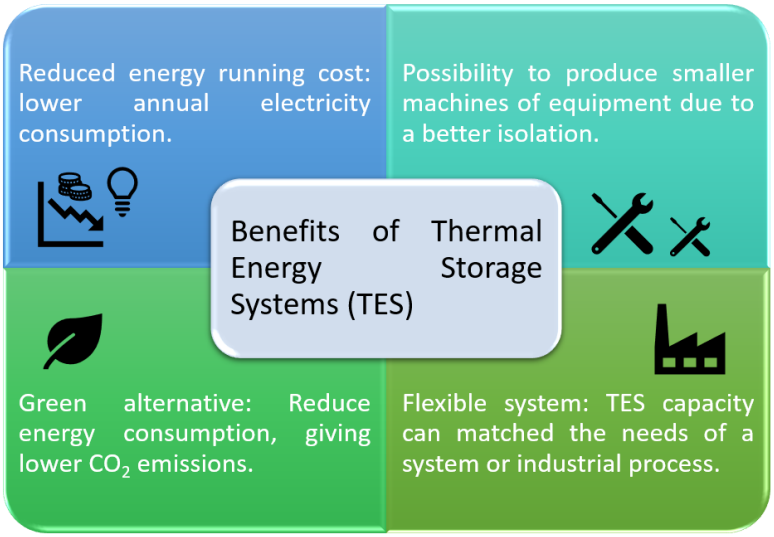

Figure 1-10. Benefits of energy storage systems.

Energy demands in the commercial, industrial, and utility sectors vary on daily, weekly, and seasonal bases. These demands can be matched with the help of thermal energy storage systems (TES) that operate synergistically. The use of TES for thermal applications such as space and

water heating, cooling, air-conditioning, and so on has received much attention. TES systems have an enormous potential to make the use of thermal energy equipment more effective and for facilitating large-scale energy substitutions from an economic perspective. In general, a coordinated set of actions in several sectors of the energy system is needed if the potential benefits of thermal storage are to be fully realized [16].

For thermal energy storage, there are two alternatives: sensible or latent heat utilization, some of the media available for sensible and latent heat TES systems are shown in **Figure 1-11**.

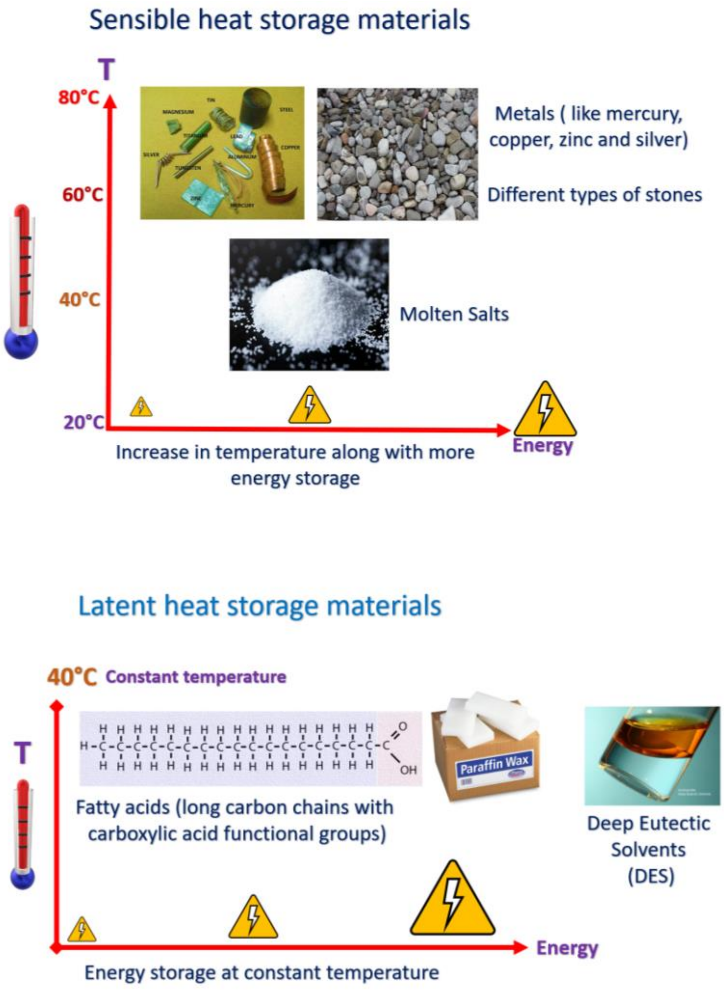

Figure 1-11. Available media for sensible and latent TES systems.

1.5.1 Sensible heat storage

Sensible heat storage has been used for centuries by builders to store or release passively thermal energy, but a much larger volume of material is required to store the same amount of energy in comparison to latent heat storage. Sensible TES systems store energy by changing the temperature of the storage medium, which can be water, brine, rock, etc. The amount of energy input to TES by a sensible heat device is proportional to the difference between the storage final and initial temperatures, the mass of the storage medium, and its heat capacity [16].

A typical example of a sensible heat systems is water, ceramics and rocks. Water is utilized to cool down industrial machines and equipment, like in the case of electricity production. Then the resulted hot water is cooled down by air-flows in cooling-towers (**Figure 1-12**).

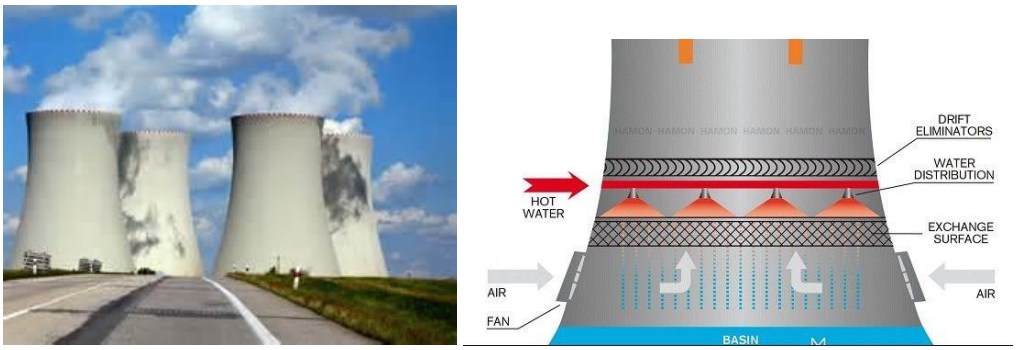

FIGURE 1-12 COOLING TOWERS. WATER IS UTILIZED TO COOL DOWN INDUSTRIAL MACHINES AND EQUIPMENT, THEN IT IS COOLED DOWN BY AIR-FLOWS IN COOLING TOWERS.

The success of water as a thermal energy storage material finishes at the moment it begins to evaporate, at that point it cannot absorb more, in consequence large amounts are often necessary. Its relatively quick phase transition is explained for its specific heat capacity of 4.2 kJ Kg^{-1} $°C^{-1}$, higher in comparison with ceramics and rocks (0.84 kJ Kg^{-1} $°C^{-1}$) [17].

In the case of ceramic and rocks, they have been utilized as filled materials in packaged cooling towers to improve heat transfer with the entering hot-liquid (near to 200 °C). In this case water with the highest heat capacity is useful for heating and cooling while rock and ceramics for high temperature applications. The relatively low heat capacity of rocks and ceramics is somewhat

compensated by the large temperature changes possible with these materials, and their relatively high densities. Sensible TES consists of a storage medium, a container, and input/output devices. Containers must both retain the storage material and prevent losses of thermal energy. Thermal stratification, the existence of a thermal gradient across storage, is desirable. Maintaining stratification is much simpler in solid storage media than in fluid [17].

1.5.2 Latent heat storage

The heat transfer which occurs when a substance changes from one phase to another is called *latent heat*. The latent heat change is usually much higher than the sensible heat change for a given medium, which is related to its specific heat [18].

A representation of a material's heat absorption is shown in **Figure 1-13**, where the material specific heat (cp) is absorbed as sensible heat while the material's temperature increase, when the material absorbed heat as latent heat the temperature remains constant while a phase change occurs. Finally, when the phase change ends, sensible heat is absorbed again with an increase of the material's temperature. This process involves a material phase transition represented in **Figure 1-14**.

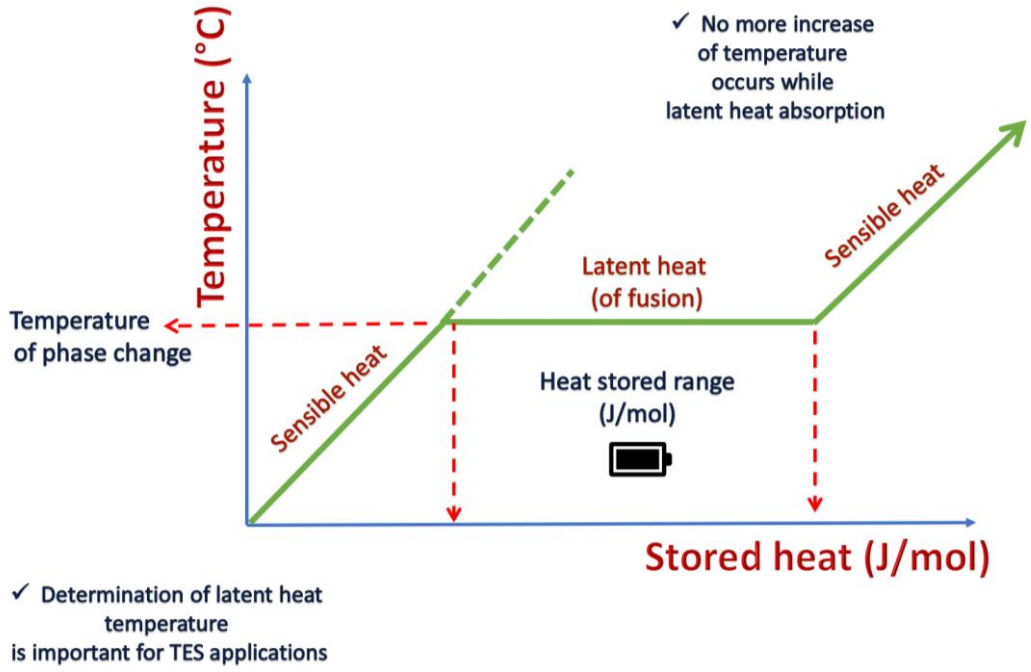

Figure 1-13. Sensible and latent heat absorption systems.

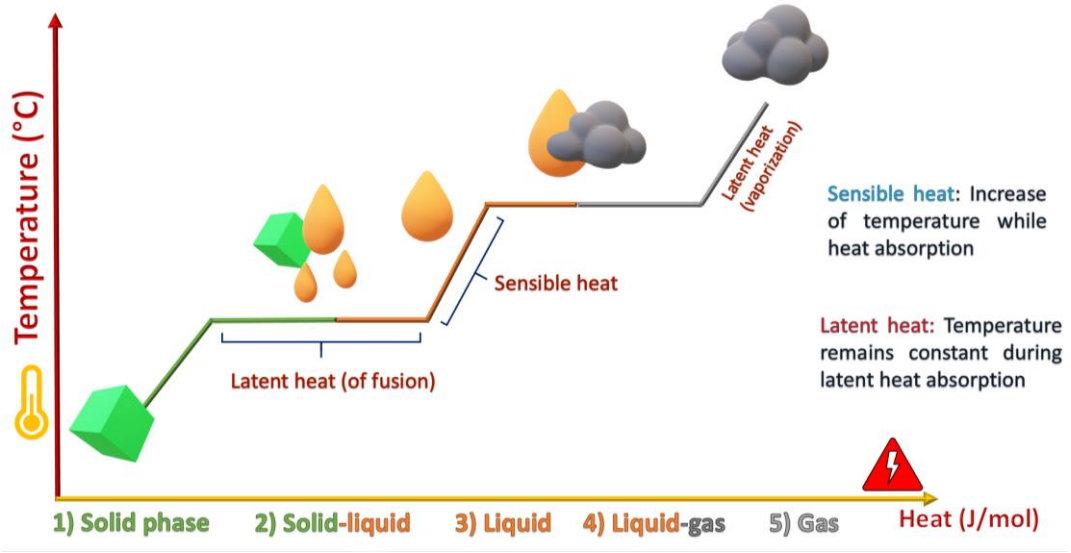

Figure 1-14. Phase change transitions during a latent and sensible heat absorption.

Most practical systems using phase change energy storage involve solutions of salts in water. Several problems are associated with such systems, which includes the following:

- Supercooling of the PCM may take place, rather than crystallization with heat release. This problem can be avoided partially by adding small crystals as nucleating agents;
- It is difficult to build a heat exchanger capable of dealing with the agglomeration of varying sizes of crystals that float in the liquid;
- The system operation cannot be completely reversed [19].

Any latent heat TES system must possess at least the following three components:

- A heat storage substance that undergoes a phase transition within the desired operating temperature range, and wherein the bulk added is stored as latent heat;
- A containment for the storage substance;
- A heat-exchange surface for transferring heat from the heat source to the storage substance and from latter to the heat sink, for example, from a solar collector to the latent TES substance to the load loop.

The main advantages of latent TES are high heat capacities per unit mass compared to those of sensible heat systems, and a small temperature range of operation since the heat interaction occurs at constant temperature. There is no gradual decline in temperature as heat is removed

from the PCM. Salt compounds that absorb a large amount of heat during melting are useful for energy storage. Eutectic salts and salt hydrates are widely used. Glauber's salt (sodium sulfate decahydrate) is a leading phase change material (PCM), because it has a high heat storage capacity (280 $kJ.kg^{-1}$) and a phase change temperature that is compatible with solar energy systems (31, 5 °C) (19). Typical eutectic salts are listed in **Table 1-3.**

Table 1-3. Common eutectic salts.

Eutectic salts

Type I	Type II	Type III	Type IV
Metal salt + Organic salt	Metal salt hydrate + Organic salt	Organic salt + Hydrogen bond donor	Metal salt (hydrate) + Hydrogen bond donor
Examples			
$ZnCl_2$ + choline chloride	$CoCl_2 . 6H_2O$ + choline chloride	Choline chloride + Urea	$ZnCl_2$ + Urea

Common PCMs such as eutectic salts have been widely used because of its longevity, after several freeze/thaw cycles during years they keep their thermal properties intact. Because it is a passive system with no mechanical parts, the storage system is maintenance free. PCMs can be contained in rods or plastics envelopes to facilitate the freeze-thaw cycle. These small modules, and the small number of modules required for storage, make phase change storage especially suitable for use in conventional design and for retrofitting. Experimental houses are being tested including Glauber's salt in the ceiling, the objective is to heat it up to 60 % of its surface. The phase change storage has been demonstrated to lower the peak indoor temperatures. Table salt can be added to the PCM lowering the melting point to about 22.7 °C. because heat is then absorbed at a lower temperature, the house only reaches about 26.6 °C on a clear winter's day instead of the 29.4 °C or as often seen in passive solar structures. Like ice and water, eutectic salts have been used as storage media for many decades.

A material with a high transition enthalpy can absorb more heat during phase transition, as well its ability to fully reverse the transition, adequate transition temperature, chemical stability and compatibility with the container (if present) are parameters to consider. Finally, a non-toxic, low cost material in relation to the foreseen application would be more desirable. A phase change material is then, any material capable of absorbing heat (thermal energy) in the form of latent or sensible heat. The choice of one depends on the temperature change requirement, for room temperature applications latent heat are desirable because of their phase transition temperature and more portability, since it is not necessary to use large amount of them to achieve a high heat storage. This last characteristic is related to their specific heat capacity. Phase change materials are classified as shown in **Figure 1-15**.

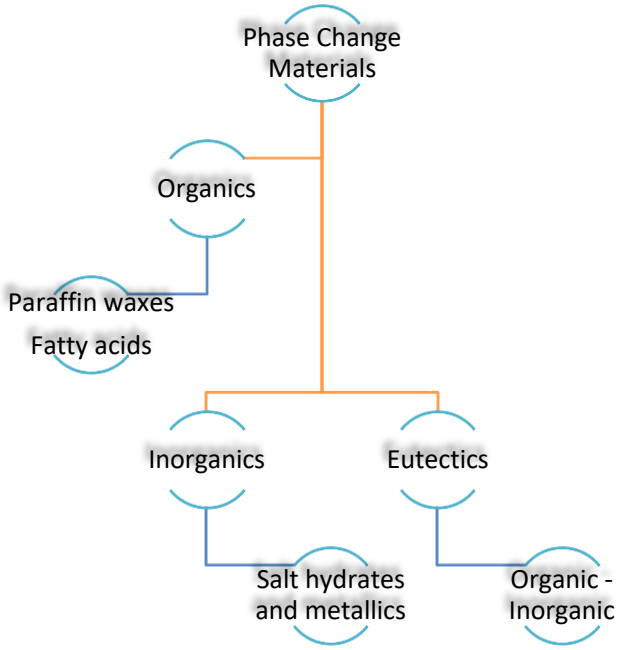

Figure 1-15. Phase change materials classification.

A preference is given for organic types because they are nontoxic, commercially available, chemically stable and they have a wide range of temperature transition.

When phase change materials are liquid, it said that they are cold because they can absorb heat from the environment, that is at a higher temperature [20]. This heat absorption has been exemplified in **Figure 1-16**.

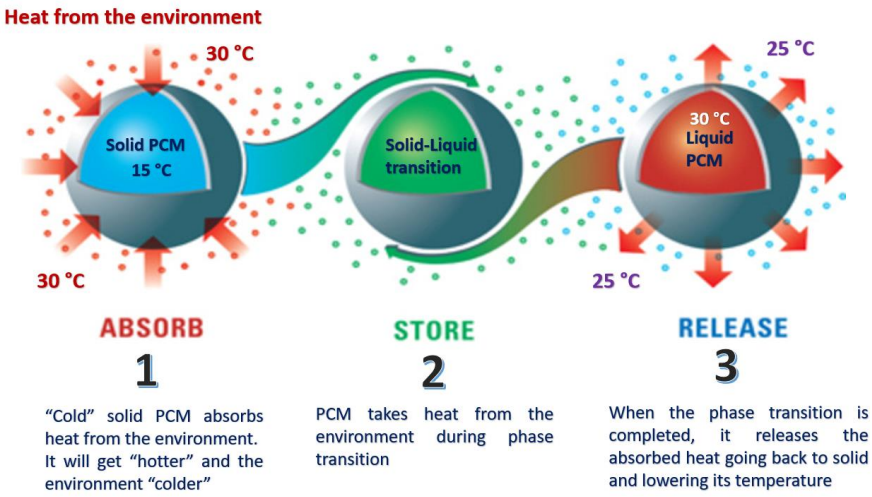

Figure 1-16. Heat absorption during phase transition.

When a material melts of vaporizes it absorbs heat; when it changes to a solid (crystallizes) or to a liquid (condenses), it releases this heat. This phase change is used for storing heat in PCMs. Typical PCMs are water/ice, salt hydrates and certain polymers.

When PCM has been melted, it cannot store more heat (**Figure 1-16-2**) and its ready to release the absorbed energy (heat) to the environment (**Figure 1-16-3**). Once this is done, its phase transition from liquid to solid is finished and the PCM is ready to start the heating absorption again.

In this thesis organic fatty acids phase change materials were utilized because of their commercial availability, wide phase transition temperature possible to use them liquid at 28 °C, environmentally friendly, inert and had no interaction with any chemical utilized for material synthesis. They had a high latent heat of fusion that allowed the use of relatively low quantities and at the same time assure a high heat absorption. Their thermal properties are well known, in consequence their identification though experimental characterization was possible. This phase change materials have been tested to insulate buildings in several ways, through its directly inclusion into concrete walls.

All these techniques have the same objective: building thermal insulation. Research is getting closer to the development of an efficient building insulation system, although improvements need to be done to avoid leakage problems, supercooling and lack of heat transfer to the whole PCM. For theses reasons this thesis has been developed, with the aim to provide clear information about PCMs and to propose the synthesis of a new material that can overcome the limitations seem so far like the necessity to contain PCMs into capsules (to prevent leakage when liquid) or the use of bags.

1.6 Molecular heat storage of phase change materials

The most commonly used latent heat storage system is solid – liquid phase transition due to large heat storage density and small volume change between phases. Solid – liquid phase change materials change their molecular arrangement from an ordered crystalline structure to a disordered amorphous one, when the temperature exceeds a critical threshold (for example, the phase transition temperature). **Figure 1-17** exemplifies this case [21] .

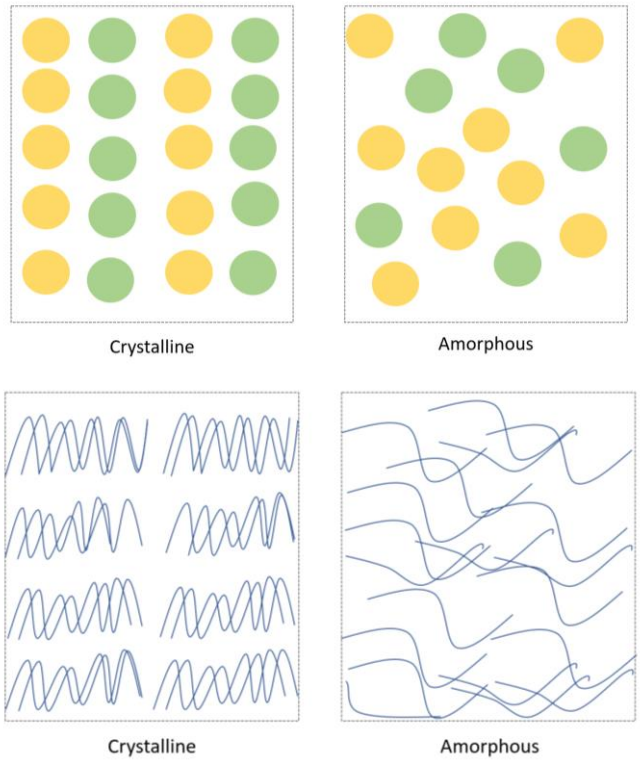

Figure 1-17. Schematic representation of solid - liquid PCMs phase change processes.

(a) salt hydrate type system going from an ordered crystalline phase to a disordered non-crystalline phase and (b); Paraffin type system going from a lamellar crystal phase to a random disordered phase.

An increase in vibrational energy breaks the supramolecular bonds between individual molecules, causing the crystalline arrangement to become a randomly oriented liquid state. In the contrary, when temperature fall below the phase transition temperature, a nucleation process starts whereby molecules re-arrange into a crystalline lattice. The shape and number of crystals that form during crystallization depends on factors such as cooling-rate, molecule's type and the presence of impurities that can serve as nucleating agents. These phase changes are

accompanied by a volume change, with volume typically increasing when the material becomes liquid. Solid – liquid PCMs commonly used for thermal energy storage include organic PCMs (paraffins) and inorganics (salt hydrates) or various mixtures (eutectics). Strategies are used to enhance their performance like for example, the phase transition temperature of paraffin can be tailored by changing the length of the carbohydrate chain; powder; graphite, metal (foams) were used to enhance thermal response of solid – liquid PCMs, many of which have low thermal conductivity [21].

1.6.1 Eutectic mixtures

Organic materials such as fatty acids and their eutectic mixtures have been explored for their good properties over inorganic materials (like super cooling, high latent heat, less volume change, good thermal and chemical stability after repeated cycles, etc.). Fatty acids and alcohols like series of palmitic acid (PA) and tetradecanol (TD) mixture, have been studied [22]. Phase change temperature of PA-TD mixture was of 29 °C, possible to be changed by modifying its ratio or one of the mixture components. These kinds of systems are also known as binary systems.

1.6.2 Binary systems

They are formed of two components mixed forming a solution. They main characteristic is that their extensive properties (volume, enthalpy, entropy, etc.) are not the sum of those of the single components. Volume for example in thermodynamics is measured by partial molar quantities:
-Partial molar volume of component *i* is defined as:

$$v_i = (dv / dn_i)_{P, T, Nj}$$

where n_i is the amount of component *i* present in the mixture and n_j constraint to the partial derivative means that all amounts of components other *i*, are to remain fixed. Then, the total volume of the mixture would be:

$$V = n_1 v_1 + n_2 v_2$$

A similar set of equations exists for all other extensive quantities.

A partial molar quantity of great importance is the chemical potential expressed by:

$$\mu_i = (dG / dn_i)_{P, T, nj}$$

where G correspond to Gibss free energy.

The thermodynamics of binary systems is linked to predict the system properties, the simplest way is by the ideal mixture model [23]:

$$\mu_i (P, T, x) = \mu°_i (P, T) + RT \, In \, (x_i)$$

for each component *i* in the mixture (μ_i is the chemical potential of component *i* in the mixture of mole fraction composition *x*, $\mu°_i$ is the chemical potential of pure component *i*) *R* is the universal gas constant.

Then: the equation for Gibbs free energy, entropy, enthalpy and volume, are respectively:

$$G = \Sigma n_i \, \mu_i° + RT \, \Sigma n_i \, In \, x_i$$

$$S = \Sigma n_i s_i° - R \, \Sigma n_i \, In \, x_i$$

$$H = \Sigma n_i h_i°$$

$$V = \Sigma n_i v_i°$$

Where *s*, *h* and *v* are molar quantitites of the pure components *i* and n_i are the number of moles of each component present in the mixture. Whereas enthalpies and volumes are additive, this is not the case for *G* and *S*. In the gas state, it is often to use the ideal mixtures model assuming that components are really similar between each other. However, it is not the case for liquids. When ideal model is inadequate more precise expressions must be studied [23] .

The deviations from ideality are extremely large for mixtures of non-polar molecules and most theories of liquid mixtures fail to predict the correct magnitude of the deviations plus there is a lack of agreement between theory and practice regarding for example aliphatic hydrocarbons. An explanation for this behavior has been that fluorocarbon – hydrocarbon interaction is much weaker than the value predicted by theoretical medias [24] . The existence of molecular complexes

between mixture components (such as hexafluorobenzene and aromatic hydrocarbons) of charge – tranfer type, are the responsibles of the intermolecular bonding leading to a mixture.

Binary systems forming more than one complex with incongruent melting points are common (carbon tetrachloride – benzene and/or pentafluorobenzene – benzene). The existence of a compound with a congruent or incongruent melting point does not necessarily imply any specific interaction in the liquid state. Mixtures of isomers frequently form compounds with congruent melting points. When in the solid state the molecules in such mixtures are able to pack in a more stable, lower energy configuration than in either of the pure substances. It is probable that in the hexafluorobenzene – n-hexane system the weak complexes formed are due to this packing and any specific interaction is extremely weak, this system is exemplified in **Figure 1-18** [25].

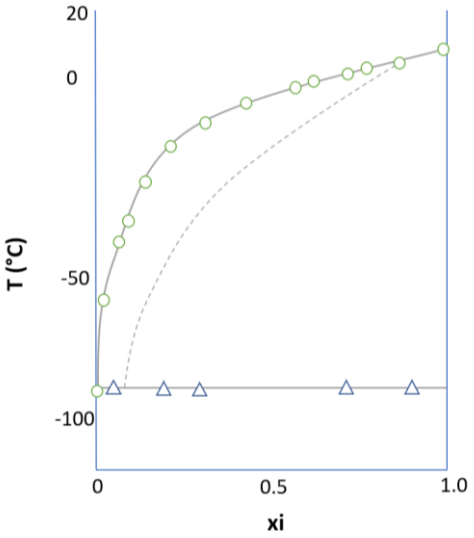

Figure 1-18. Hexafluorurobenzene - n-hexane phase diagram

The broken line represent the ideal behavior, the system exhibits a considerable positive deviation from ideality. At this point the Gibbs-Duhem equation can be used to calculate an approximate value for the excess Gibbs free energy of the liquid system of +160 cal.mol^{-1} at – 15 °C. this is of the expected sign and magnitude, being insufficiently large to cause liquid – liquid immiscibility [25] .

In this way phase diagrams and Gibbs free energy equations are utilized to determine eutectic mixtures properties. This is an exploring field because any mixtures can be done and it's difficult to characterize them.

1.7 Phase change materials encapsulation

The utilization of phase change materials requires their encapsulation unless they are used directly like in concrete. When that is not the case, encapsulation its necessary. Encapsulation allows the incorporation of PCM in walls, boards, plasters or other wall covering keeping its light weight, solve the liquid migration problem and creates small packages of different sizes for PCMs. Depending of the size of this containers formed the process is called: macro-encapsulation or micro-encapsulation. For PCMs, usually the term microencapsulation is utilized because smaller capsules tend to improve PCM dispersion and homogeneity in the media. In this way the heat transfer can be homogenous all along its surface. Microencapsulation is a process in which tiny particles are coated by a shell to form small capsules with many useful properties. Particles could be solid, liquid or in gas state, while the shell is of a polymer or inorganic material. The main purpose of the shell is to maintain the shape of the capsules and prevent leakage. The products obtained by the process are called: microparticles or microcapsules and they are differentiated by their morphology and inner structure, as it can be seen in **Figure 19** [25].

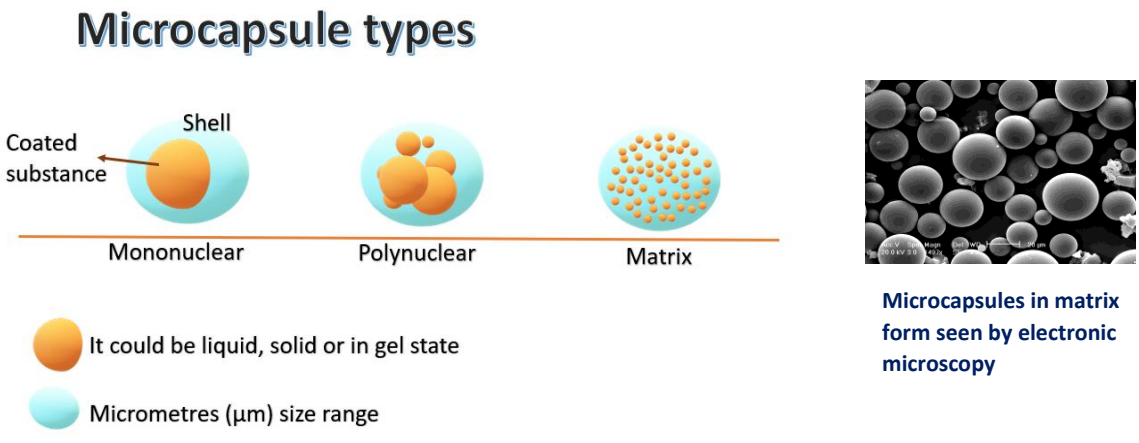

Figure 19. Microcapsules differentiated by their sizes, it goes from 1 to 1000 µm.

In its simplest form, a microparticle is a small sphere with a uniform wall around it. The material inside the microcapsule is referred to as the core, internal phase, or fill, whereas the wall is sometimes called a shell, coating or membrane [26].

Most microcapsules have diameters in the range between 1 and 1 000 µm. Through a selection of the core and shell material, it is possible to obtain microcapsules with a variety of functions. Then the choice of mononuclear, polynuclear or matrix microencapsulation depends of the desire applications. Mononuclear (core-shell) microcapsules contain the shell around the core, while polynuclear capsules have many cores enclosed within the shell. In matrix encapsulation, the core material is distributed homogeneously into the shell material.

Main advantages of encapsulation are:

1. To protect reactive substances from the environment;
2. To convert liquid active components into a dry solid system;
3. To separate incompatible components for functional reasons;
4. To mask undesired properties of the active components;
5. To protect the immediate environment of the microcapsules from the active components;
6. To control the release of the active components.

Coating materials are numerous and must be capable of forming a film that is cohesive with the active substance, chemically compatible and nonreactive with the environment nor with the encapsulated substance while strength, flexibility, impermeability and stability must be kept.

1.7.1 Encapsulation methods

Preparation of microcapsules should satisfy certain criteria, like basic understanding of the general properties of microcapsules, such as the nature of the core and coating materials, the stability and release characteristics of the coated materials and the microencapsulation methods. A summary of encapsulation methods is presented in **Figure 1-20** [27].

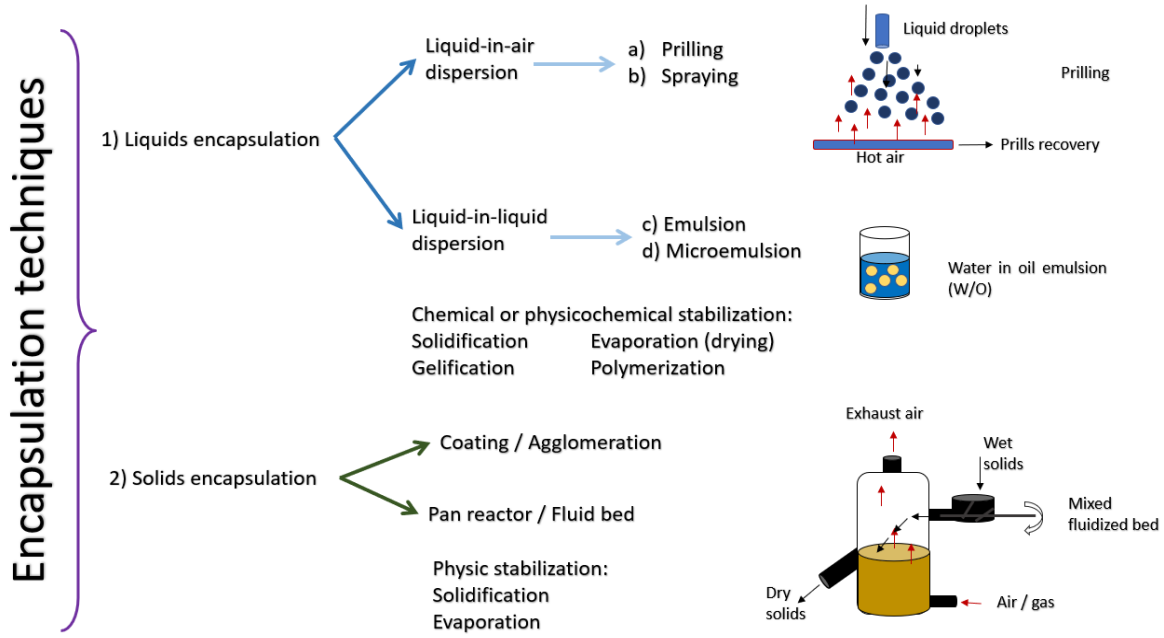

Figure 1-20. Encapsulation methods according to the matter state of the substances.

The proposed system in this thesis deals with the encapsulation of phase change materials by emulsion templating technique. An oil in water (O/W) emulsion is formed by the addition of the PCM into the aqueous phase. the advantages are that substances like solid particles, polymers and surfactants can be added in the aqueous and in the oil phase to improve the system properties and stability. Once the emulsion is formed a chemical crosslinker is added to react with the previously dissolve polymer and crosslinked it to give a closed, interconnected three-dimensional network encapsulating the dispersed PCM without affecting its thermal properties, in this way an encapsulation matrix is synthetized. The produce material is called a poly-HIPE for high internal phase emulsion porous material. This methodology will be explained in the coming section.

2 Porous Materials

Existing materials can be classified in two general categories:

Massive materials formed by a single solid matrix like metals, glass or plastics. The second one corresponds to the ones formed by two phases; one can be solid and the other a gas or a liquid. Porous materials are considered in this second category, its solid matrix is empty from the inside. These holes are called pores. All solid materials with hole inside, cavities or channels can be considered to be porous like for example sponges or polyurethanes like the ones in **Figure 2-1** [28].

Figure 2-1. Polyurethane as porous materials

Usually their porosity is superior to 20 % and there are characterized by their pore geometry, pore size and their structure inside the solid matrix. The terminology pore is utilized to define their cavities and pore-interconnections as illustrated in **Figure 2-2**.

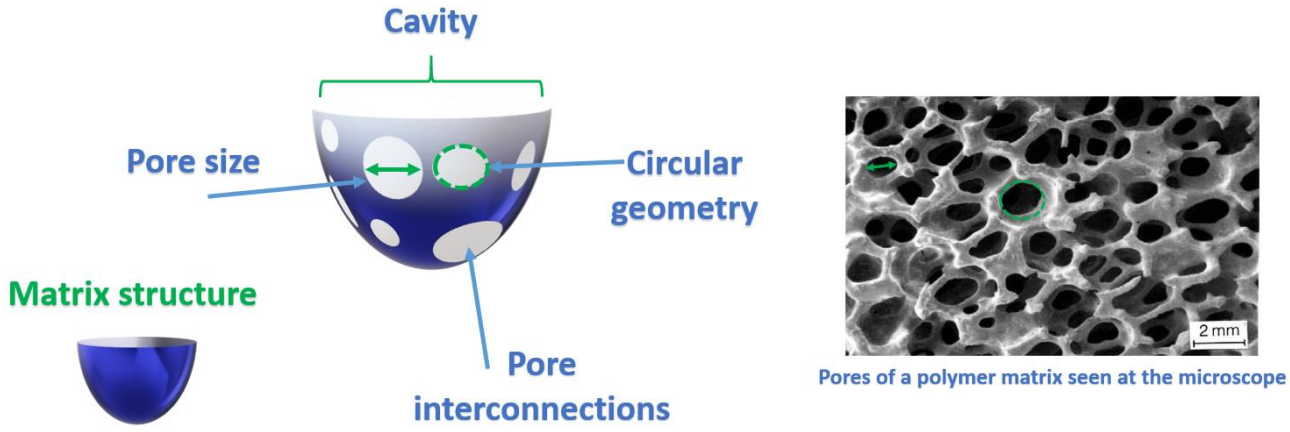

Figure 2-2. Illustration of a porous material with open porosity. Pore size, geometry and interconnections have been exemplified.

The porosity of a material (ϕ) is calculated considering the pores volume over the total material, that is: $\phi = \frac{Vp}{Vs+Vp}$, where Vp is the volume occupied by the pores and Vs the one corresponding to the solid matrix [28].

In order to describe the porosity of a material the terminology shown in **Figure 2-3** is utilized. The isolated pores (A) are considered closed-porosity, this kind of pores are going to have an effect over the density of a material because sometimes they are not measured by the characterization equipment, their mechanic properties and their thermal conductivity. Besides these porosities do not influence in gas absorption. Pores (B), (C), (D), (E) and (F) represent the open porosity because they are in contact with the external surface of the matrix. Open porosity can be divided in two categories:

1) Open pores only by an extreme size (B) and (F);
2) Open pores from two or more extreme sizes like (E).

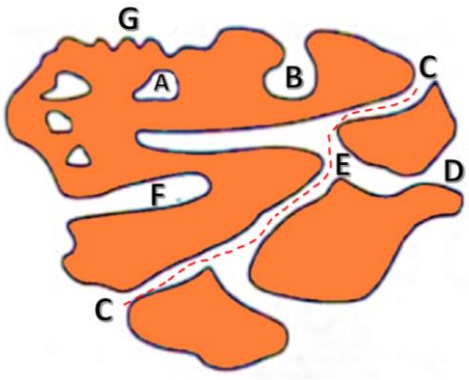

Figure 2-3. Representation of the transversal section of a porous material.

Physicochemical properties of porous materials (density, thermal conductivity and mechanical resistant) depend of their porous structure, this is the reason why the control of its pore morphology its of great importance during their synthesis. Nevertheless, pore morphology control is complex and the obtention of a perfect pore geometry it's difficult to achieve every time. Pore size represents another important parameter which is going to determine the type of applications given to the synthetized porous material. A general pore size classification given by the International Union of Pure and Applied Chemistry (IUPAC) is given in **Table 2-1** [29].

Table 2-1. Pores classification according to their diameter (IUPAC).

Pore type	**Size**
Micro pore	< 2 nm
Meso pore	2 – 50 nm
Macro pore	> 50 nm

This pore classification is the result of physicochemical phenomena like for example the hydrodynamic behavior that occurs in the pores by liquids flow in open porosity materials. This liquid flow depends of the pores dimension [29].

The main methods of porous materials characterization have been listed in **Table 2-2**.

Table 2-2. Main techniques for porous materials characterization .

Technique	Equipment measure parameters	Advantages	Limitations
Scanning electron microscopy (SEM)	Pore size observed depends of equipment performance	-Size, pore morphologies and distribution are observable	-Samples have to be metallized -2D images are obtained
Mercury Intrusion Porosity (MIP)	0.01 – 150 µm	-Total porosity -Interconnected pore sizes -Pore size distributions	-Impossible to analyze closed pore materials -May caused physical damaged to samples -Invasive method
Helium pycnometer	-	-Matrix density -Porous volume	-Impossible to analyzed closed porous materials

A porous material is characterized by its skeletal density or real density (ρ_{sq}), it depends of the molecular structure of the solid matrix while the apparent density (ρ_{ap}) accounts for the materials porosity. Both densities are related to the equation: $\phi = 1 - \frac{\rho_{ap}}{\rho_{sq}}$. the skeletal density

(ρ_{sq}) can be known considering the densities of the single materials that forms the matrix. This parameter can also be known by pyrometry helium characterization [29].

2.1.1 Gravimetric methods

The materials volume can be determined mathematically if its structure is geometrically regular. The apparent density (ρ_{ap}) is obtained considering the materials mass and its volume and the skeletal density (ρ_{sq}) depends of the matrix molecular structure. As well the Archimedes principle can be utilized over a geometrical structure or when samples are destroyed during mercury intrusion characterization [30].

2.1.1.1 Helium pycnometry

Helium pycnometry is a method that allows to determine a solid samples volume by detection of a pressure change caused by a gas in contact with the sample. Generally, the gas is helium because its small molecular size allows it to penetrate inside the smallest solid sample cavities. The materials are placed in a room of known volume full of helium, then the room's pressure is measured. An empty reference room is at the same time full of helium but at a higher pressure than the one with the sample. After an equilibrium period both rooms are put in contact by opening the valve that joins them, as a consequence the gas from the empty room passes to the one with the sample. The resulting pressure is then measure, the samples volume is obtained by measuring the pressure difference between both rooms. In this way the skeletal density can be known [30].

2.1.1.2 Mercury intrusion porosimetry

Mercury intrusion porosimetry is a technique that allows to determine the pore volume distributions of a porous material and as well, its total porosity. The sample is placed in a capillary tube under vacuum (**Figure 2-4**) and filled with mercury [30].

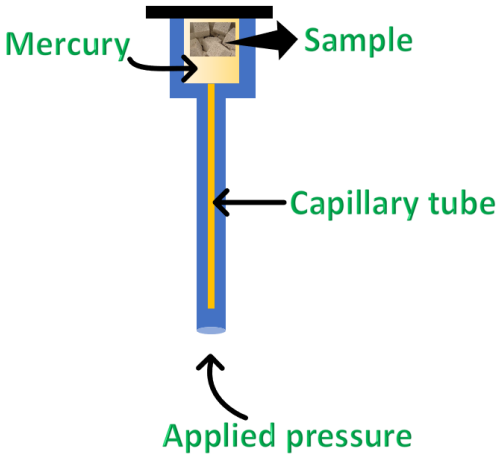

Figure 2-4. Capillary mercury tube for mercury intrusion characterization.

The test in done in two steps:

1- Low pressure is applied to fill the macropores.
2- High pressure is applied to fill the smallest pores, sometimes a lubricant oil is necessary to help mercury penetration.

The mercury volume utilized, and the pressure applied are measure simultaneously, the pore size distribution is determined by the following equation: $D = -\frac{4\gamma\cos\theta}{P}$. D is the pore diameter, γ is the superficial tension of mercury and θ the contact angle. Total porosity is obtained from the total volume of mercury introduced.

2.1.1.3 Pore morphology characterization: Scanning electron microscope

It was commercially available for the first time in the 1960's, developed by the scientists Ernst Ruska (German physicist) and Max Knoll (German electrical engineer) in response to increase the magnification potential of the available microscopes of that time (light-based microscopes) and perform studies with more detail [31].

The development of SEM involved the collaboration of scientists of different fields, its applications include biology, chemistry, medicine, forensics and physics to discover, investigate and understand new morphological details that allow the identification of different species and may help to clarify the functions of body parts in the case of living organisms [32],

reveal information about a sample including external morphology (texture), chemical composition and crystalline structure of materials [33].

Science has had huge advances due to the sheer level of detail that can be seen with SEM in comparison with optical microscope, they can exceed light-based microscopes by 1 000 times due to magnification ranges from 20x to 30 000x and a spatial resolution of 50 to 100 nm.

An electron-beam is utilized to magnify a given sample; an electron gun directs the beam to an anode (ring-shaped device with a positive electrical charge), magnetic lens focuses the stream of electrons as they travel through a vacuum chamber within the microscope. These focused electrons strike the sample on the stage and bounce off of it, creating X-rays in the process. The bounced or scattered electrons as well as the X-rays are converted into a signal that feeds an image to a screen where scientists view the sample. Additionally, the magnetic lens can be adjusted like any other lens to focus an image. SEM limitations are the black and white resulting images, highly sensible to movements giving blurred images and in the case of living samples they must be killed to analyze [34].

2.2 Obtention of porous materials by emulsion templated polymerization

2.2.1 Emulsion generalities

Theoretical basis of emulsions comprises a great study of colloids and surface science, naturally occurring systems and man-made ones are useful for different applications [35-37]. Emulsions success is highly because of their formulation versatility and the possibility to increase their stability and resistance to external factors like pH and temperature. An emulsion is a heterogeneous system consisting of at least one immiscible liquid intimately dispersed in another in the form of droplets, whose diameters in general exceed 0.1 µm. Such systems possess a minimal stability, which may be accentuated by additives such as surface-active agents, finely divided solids, etc [35-37].

A list of common emulsion stabilizers is given in **Table 2-3**, along with their usual application in recent research fields. Novel stabilizers such as nanoparticles are used in systems called Pickering-emulsions, they allow the preparation of porous materials with a smaller pore size

than with other methods by significantly reducing the pore size diameter of the dispersed phase droplets. It is possible to modify the surface nanoparticles through coordination via carboxylic acids and silane coupling agents to provide greater stability for O/W emulsions prepared with non-polar or weakly polar oils. In the other case where the oil phase is strongly polar, silane coated Fe_3O_4 nanoparticles are commonly useful in stabilizing the system. The chain length of the modifying agent plays an important role on the stability of emulsions [38].

Table 2-3. Surfactants and additives to stabilize an emulsion.

Emulsion additive	Additive nature	Application	Ref.
⦿ Mixture of micellar solutions (surfactants)	Non-ionic surfactants: Pluronic, Brij, Tetronic	Synthesis of porous silica materials	(39)
⦿ l-carrageenan	Polysaccharide extracted from red algae	Canola O/W emulsion to encapsulate epigallocatechin-3-gallate to enhanced drugs anticancer activity	(40)
⦿ β-lactoglobuline	Albumin milk protein	Resveratrol and antioxidants encapsulation	(40)
⦿ Synthetic non-ionic surfactant: polyethoxylated castor oil	Cremophor EL	Use to stabilize emulsions of non-polar substances Preparation of bio-based emulsions	(41)
⦿ Nanoparticles	Iron oxide particles (Fe3O4)	Pickering emulsions: stabilization by solid particles for porous materials preparation	(38)
⦿ Starch	Pullulan Octenyl-succinate (OSA)	Modified starch as stabilators and thickening agents. Common in cosmetics, drugs and food products.	(42)

Starch such as pullulan have been widely used in cosmetic as thickening agents, since they increase the viscosity of the constant phase and generate a denser matrix for the dispersed phase distribution. However, this kind of agents have remained almost exclusively for cosmetic, pharmaceutic and food applications. The dispersion of an immiscible liquid called dispersed

phase or oil phase in the water or constant phase, have been exemplified in **Figure 2-5** along with emulsion basic components.

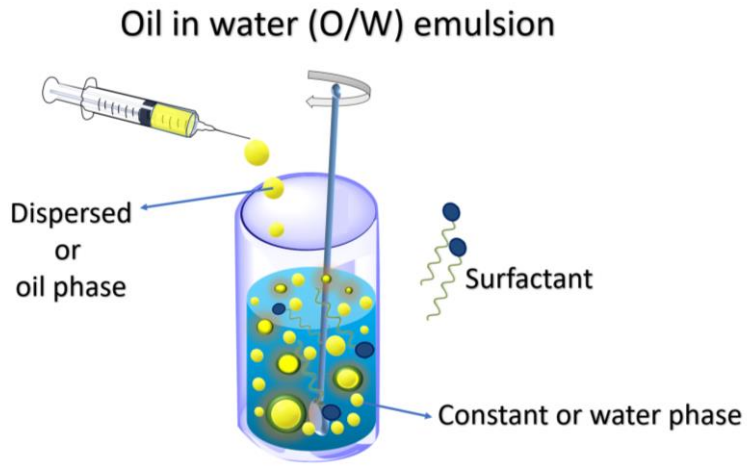

Figure 2-5. Formation of an oil-in-water (O/W) emulsion.

The components of an emulsion are water and oil, naming them as water-in-oil (W/O) or oil-in-water (O/W). The water phase may contain other substances like electrolytes or alcohols or not be water at all. The oil phase may be any liquid insoluble in the water phase like silicones, fluorocarbons or even nitroglycerine. The dispersing liquid is known as the continuous or external phase, while the dispersed liquid is called discontinuous or internal phase. Additionally, a third component is often considered, that is the surface-active agent [37]. Emulsions may contain droplets much smaller than 0.1 µm. Information regarding the droplet sizes and their distribution in emulsions is of considerable importance because these properties may impact on their properties like rheology, color or opacity and serve as a measure for their stability. Several particle sizes could be present in the same system since not always it gets to be totally homogeneous. In **Figure 2-6**, it can be seen different particle sizes obtained in a homogenous system but also in an heterogenous one [38].

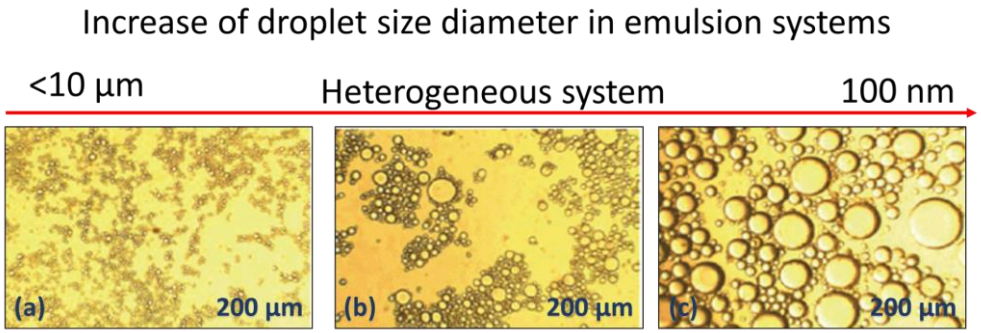

Figure 2-6. Microscope images showing different droplet sizes in a dodecane-in-water emulsion.

A macroemulsions is considered to have a droplet size between 1 to 100 µm, nanoemulsions from 0.1 to 1 µm and microemulsions from 10 to 200 µm.

Dispersion of an oil phase or dispersed phase in the constant phase is done by several methods, in **Figure 2-5** the syringe method has been exemplified. The syringe allows a drop-by-drop dispersion while controlling its size. Surfactant stabilizes the system in a thermodynamic point of view creating micelles around the oil droplets after a complete dispersion has occurred. An emulsion looks like the one pictured in **Figure 2-7**, usually with an opaque color where one phase is only identified. If it is not stable it might get divided in two phases showing the immiscibility of the constant and dispersed phase with each other [38] .

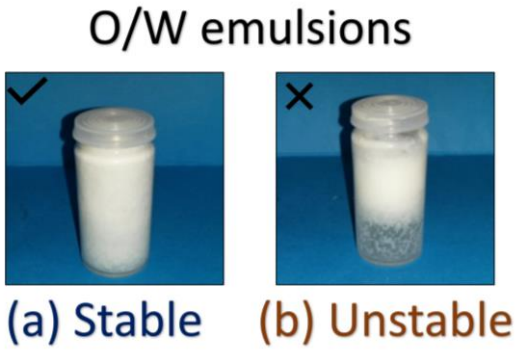

Figure 2-7. Stability of O/W emulsions by the action of a surfactant.

If the surfactant or its concentration used is not the adequate the emulsion phases separate producing an unstable emulsion visible by phase separation after some hours if preparation, sometimes it could occur even after some minutes.

The phases making up an emulsion are, liquids at the time the emulsion is formed. However, if one or both phases are solids at room temperature, it may be necessary to produce the emulsion at an elevated temperature, then; at ambient temperatures one or the other (or both) phases could be solid [35-37] .

2.2.2 Emulsions types

An emulsion oil in water (O/W) is known as direct emulsion and water in oil (W/O) as indirect. Other types are non-aqueous oil in oil (O/O) composed by a non-polar organic solvent dispersed in a polar organic solvent (**Figure 2-8**) like for example N, N-Dimethyl formamide (DMF) in dodecane [43].

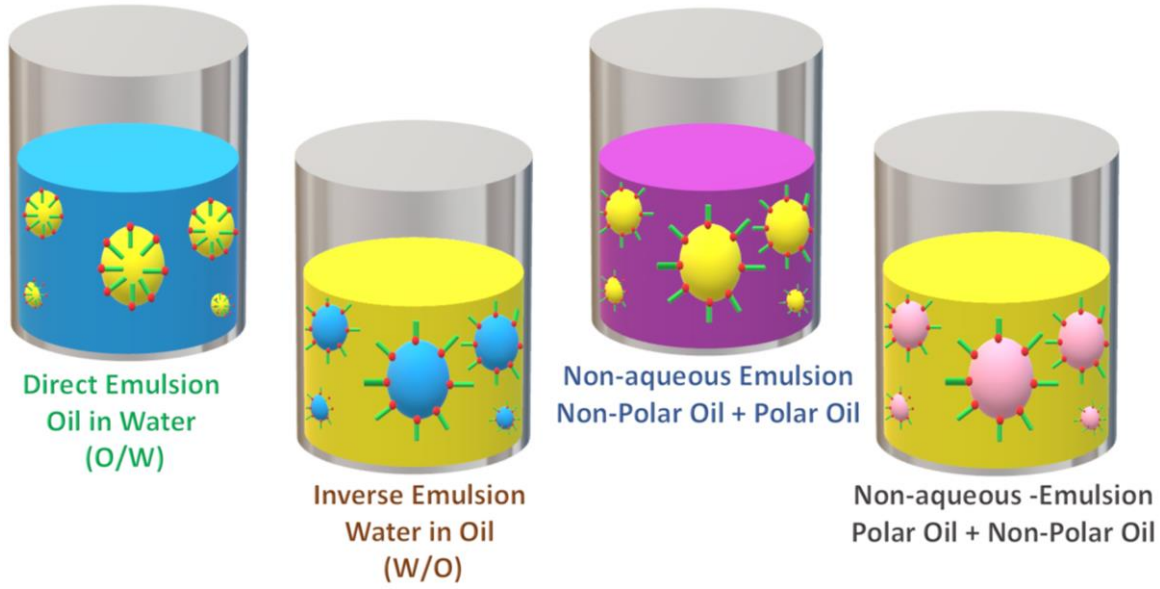

Figure 2-8. Emulsion types.

The second type correspond to a polar organic solvent dispersed into a non-polar organic solvent like dodecane in DMF. However, oil in oil emulsions are non-stable within time. An alternative to organic solvents is the utilization of ionic liquids or deep eutectic solvents to substitute one of the phases in emulsions formulation [43].

Emulsions can be classified by their oil ratio, that is:

1) Diluted emulsions with a oil ratio of 30 %, often called LIPEs (low internal phase emulsions). As consequence the dispersed oil droplets do not interact between them.
2) MIPEs or middle internal phase emulsions with an oil ratio between 30 and 74 %, dispersed droplets acquired a compacted accommodation.

3) HIPEs or high internal phase emulsions with a 74 % or more of oil phase. As consequence of their high concentration droplets shape gets deformed to occupy less space (space optimization) and be able to be present all together.

2.3 Emulsions stabilization by surfactants

An emulsion gains stability by the action of surfactants or also called emulsifiers, their body structure is shown in **Figure 2-9**. Surfactants stabilizes an emulsion by forming a film around the dispersed phase droplets that acts as a mechanical barrier that encapsulates the droplets and prevent coalescence. Presence of the emulsifier molecules at the oil-water interface is accompanied by a decrease in the interfacial tension between both phases, as it will be discussed further on this work.

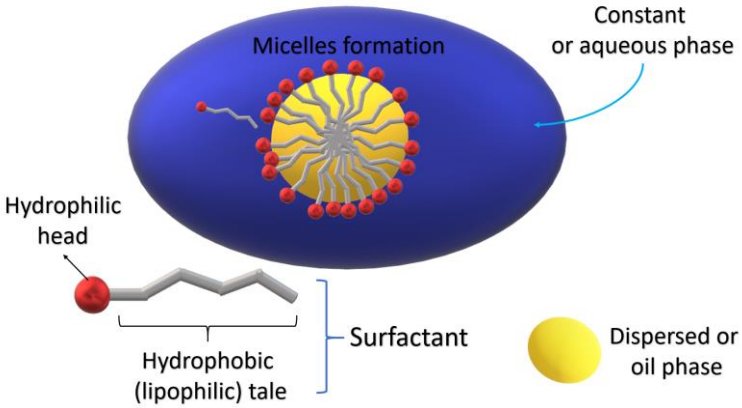

Figure 2-9. Surfactant body structure and its role in an emulsion for the stabilization of immiscible liquids.

A surfactant possesses a hydrophilic head that remains in contact with the aqueous phase while its hydrophobic tale joins the oil phase acting as a barrier or frontier between both liquids and avoiding their interaction. Without surfactant both liquids will separate forming an heterogenous system. The structure a surfactant takes depends on the other materials in the mixture and the concentration of the surfactant. At low concentrations, they adsorb at the interface forming a single layer. As their concentration increase, they form clusters known as micelles and progressively transformed into more organized structures, such as a bilayer. These structures develop because of the orientation of the surfactant molecules: the hydrophilic part of the molecule will maintain contact with water, while the lipophilic part will move away from

water. Presence of these surfactant molecules at the oil-water interface keeps the oil and water from separating into two distinguished layers [44].

Oil-in-water emulsions can also be stabilized by water-soluble polymers. Thus, in commercial emulsions, often surfactant system is not one but a mixture of them plus proteins and polymers. The composition of the system, thickness and viscoelasticity of the adsorbed layer stabilizing the oil-water interface, and the strength and nature of the interactions between adsorbed layers on different droplets affect the emulsion structure, stability and rheological properties. The strength of this interfacial film will prevent coalescence, which is the merging of the droplets when the interfacial film is broken. There are number of factors that have been shown to be important in determining emulsion stability. First, the nature of the oil phase; the most stable emulsions are formed with more polar compounds. This is attributed to its high polarity and ability to form water-like hydrogen bonded network. Second, the interfacial behavior of the surfactant employed; interfacial data can be obtained from the hydrophilic-lipophilic (HLB) value of surfactants. Particle size is an important indication of emulsion stability. It depends not only on the oil/water/surfactant system types and concentration but also on homogenization conditions. The temperature during homogenization, the pressure or the speed of the homogenizer and the duration would influence the particle size. In general, emulsion having smaller initial particle size appears more stable than that with bigger initial particle size. One of the reasons is that the emulsion containing lower number of big droplets creamed lesser than that containing high number of big oil droplets. According to Stoke's law, a decrease in particle size is very important in reducing the rate of creaming; the rate of creaming being a square root function of the particle diameter. The creaming rate is also reduced by increasing viscosity of the medium. This explains the widely used water-soluble polymers in emulsification [44].

2.3.1 Surface and interfacial tension theory

Surfactants act directly on the surface tension forces (or simply surface tension) of the dispersing liquid. Surfactants agglomerate on the surface of a liquid and form an elastic skin which resists stretching and increases the attraction forces of the liquid molecules; these forces are of the kind of hydrogen bonds. Although surface tension is present at all interfaces (solid, liquid and gas interfaces), it is more important for liquids. Molecules at the liquid surface in contact with a gas or vacuum have weaker binding than molecules at the bulk. The missing

(negative) binding energy can therefore be viewed as a positive energy added to the surface itself. Since a larger area of the surface contains larger surface energy, external forces must perform positive work against internal surface forces to increase the total area of the surface. Mathematically, the internal surface forces are represented by surface tension defined as the normal force per unit of length. This concept has been exemplified in **Figure 2-10** [45].

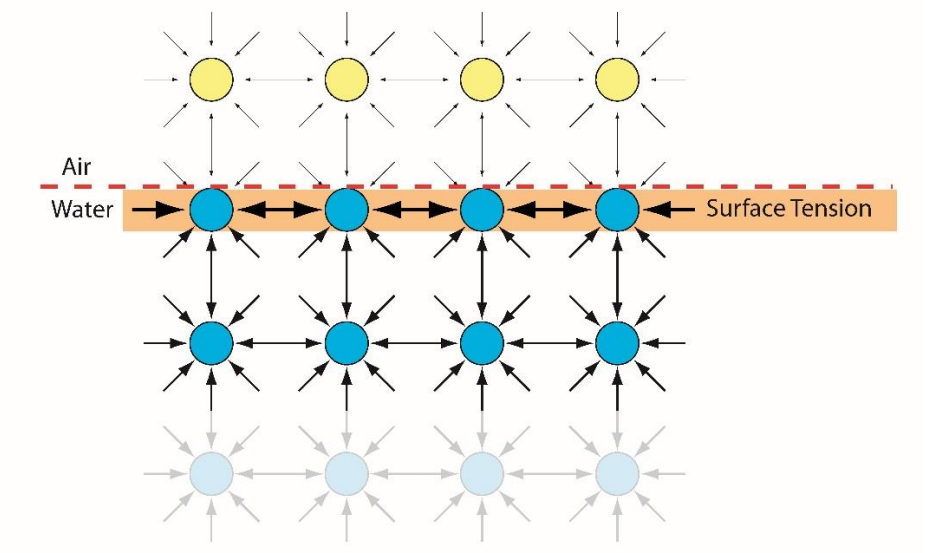

Figure 2-10. The forces acting on molecules on the surface and in the interior of a liquid.

A molecule at the surface has less bonds compared to the ones in the interior (at the bulk). The missing bond energy at the surface gives rise to a positive surface energy density, which is the cause of surface tension. As a reference, the surface tension of several liquid is presented in **Table 2-4** [45].

Table 2-4. Surface tension of common liquids.

Liquid	**Interfacial tension (α) (20 °C ; mN/m)**
Water	72.8
Mercury	488.5
Castor oil	39
Olive oil	35.8
Dodecanol	29.75
Acetic acid	27.59
Hexadecane	27.47
Ethanol	22.39

*mN/m = millinewtons per meter

The binding energy represented as ϵ considers the specific heat of evaporation of a substance (evaporation enthalpy per unit mass) and the mass of the substance. It is used to calculate the surface energy density α and therefore, to estimate the necessary work W to increase the area of an interface. This work W is then equal to the surface energy and is expressed as follows:

$$dW = \alpha\, dA$$

Where dA is the increase area of an interface.

The surface energy density associated with a liquid or solid interface against vacuum or gas, is always positive because of the missing negative binding energy of the surface molecules. The positivity of the surface energy density guarantees that such interfaces seek towards the minimal area consistent with the other forces that may be at play, for example gravity. For this reason, spontaneously liquids tend to acquire a spherical shape like raindrops. Interfaces between solids and liquids or between liquids and liquids are not required to have positive interfacial energy density. The sign depends on the strength of the cohesive forces holding molecules of a material together compared to the strength of the adhesive forces between the opposing molecules of the interfacing materials. The interface between a solid and liquid is normally not deformable, and a negative interfacial energy density has no effect. If in the other hand, the interfacial energy density between two liquids is negative, a large amount of energy can be released by

maximizing the area of the interface. The two liquids are mixed thoroughly instead of being kept separate. Fluids that readily mix with each other, such as alcohol and water, may be viewed as having negative interfacial energy density. Immiscible liquids like oil and water must on the other hand have positive interfacial energy density which makes them seek towards minimal interface area with maximal smoothness. Since an interface has no macroscopic thickness, it may be viewed as being locally flat everywhere, implying that the surface energy density cannot depend on the curvature of the interface, but only on the properties of the interfacing materials. If these are homogenous and isotropic, as they often are, the value of the energy density will be the same everywhere on the interface [45] .

2.3.2 Force and surface tension

The resistance against extension of a free substance shows that the surface has an internal surface tension, which is equal to the surface energy density α. To stretch a surface along a straight line of length L by a uniform amount dS, the surface tension is then, defined as the force that a side of the surface exerts on the other surface side along at a distance (dL) in the equilibrium. For this, the surface tension is expressed as:

$$dF = \alpha \, dL \, \eta$$

Where: dF is the surface tension, dL corresponds to the surface length, α is the internal surface tension and η the normal force in the equilibrium. At an interface between homogenous materials, surface tension does not depend on how much the interface has already been stretched, and this makes the interface quite different from an elastic membrane which like the skin of a balloon resists stretching with increasing force because elastic tension increases as the deformation grows. However, surfactants can modify this behavior and make the system act as a membrane, increasing its stability [45] .

2.3.3 Effect of temperature on surface tension

In respect to the effect of temperature over surface tension, in general; as the temperature is raised, the increased kinetic energy of the individual molecules tends to overcome the net attractive forces of the bulk liquid, resulting in increased volatility and thus, decreased the

surface tension. The molecular forces of adhesion and cohesion are considered in the formula presented above, regarding the necessary work *W* to stretch the surface tension. This work is often called *work of cohesion* if the molecules correspond to the same liquid and *work of adhesion* if the system is composed of two different liquids or interfaces. The work of adhesion will be subtracted to the work of cohesion [45].

2.3.4 Surfactants and their effect on surface activity

Surface activity is the ability of a substance to alter the nature of a surface or an interface between two substances. The surface of a pure liquid tends to contract because of surface tension forces. Packing of the surface with a surfactant favors expansion of the liquid by an amount equal to the surface pressure [46].

Surfactants are characterized by having two distinct regions (hydrophilic and hydrophobic) and are termed amphiphiles. They tend to accumulate at the boundary between two phases because of this unique physic-chemical nature. Their adsorption at various interfaces results in changes the interfaces making them of great importance in emulsion systems. Based on the nature of their hydrophilic group, surfactants are generally classified into three main categories: anionic, cationic and non-ionic surfactants. Cationic surfactants are positively charged. Examples of these are gelatin and quaternary ammonium compounds. Anionic surfactants are negatively charged, and examples include agar, tragacanth, acacia and sodium lauryl sulphate. Non-ionic surfactants are uncharged like polysorbates. This kind of surfactants are commonly found medicines. The surface activity of surfactants which is the extent to which it can reduce the surface tension of water, is usually evaluated by dissolving it in water and then determine the surface tension of the solution using a tensiometer. Several methods are available for this procedure such as: the plate method, ring method, drop weight and drop volume method and the capillary rise method. The reduction of the surface tension of water so determined is a measure of the surface activity of the surfactant [46].

2.3.5 Critical micelle concentration (CMC)

Critical micelle concentration (CMC) is the concentration above which aggregates of colloidal dimension, called micelles, are formed. To determine the CMC of a surfactant, a graph of surface tension of solutions of increasing concentration of the surfactant is plotted against natural logarithm of the concentrations. Generally, surface tension decreases with increase in surfactant concentration until a point where further increase in concentration does not affect the surface tension. This point is termed critical micelle concentration. Accumulation in surface layer and adsorption at interface are favored below CMC while micelle formation and solubilization are favored above CMC. When surface active agents are present below their CMC, they concentrate at the water surface with the hydrophobic region oriented away from the aqueous phase causing an expansion of the surface layer. This leads to reduction in the surface tension of the liquid. When they are present above the CMC, they formed micelles. The hydrophobic chains of the surfactant form a core of the micelles and are shielded from the aqueous environment by the hydrophilic chains. Formation of micelles is responsible for solubilization of water-insoluble substances. This is the principle behind the use of surface-active agents as solubilizing agents [46].

2.3.6 Hydrophile-Lipophile balance (HLB)

Hydrophile-lipophile balance (HLB) is the relative hydrophilicity or lipophilicity of a surfactant. It is characteristic of the relative polarity of the surfactant and ranges from 0 to 20. The lower the HLB value, the more hydrophobic is the surfactant and the higher the HLB value, the more hydrophilic is the substance. HLB values have been used to classify surfactants as water-in-oil emulsifiers, wetting agents, oil-in-water emulsifiers, foaming agents and solubilizing agents as seen in **Figure 2-11**. To form emulsions of oil in water, it is very frequent to use non-ionic surfactants. They are considered superior to ionic surfactants because they tend to produce stable emulsions and are less toxic than most ionic surfactants. Sometimes a combination between non-ionic surfactants may be convenient. This number is a measure of the size and strength of the two opposite groups (hydrophilic moiety and lipophilic moiety) in an emulsifier molecule. Though it does not indicate the overall efficiency of the emulsifier, the HLB number indicates what kind of an emulsion or product to expect [47].

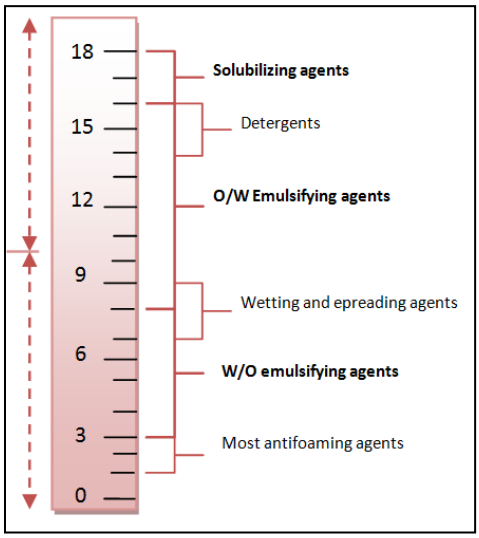

Figure 2-11. HLB values of non-ionic surfactants and their applications.

Surfactants with a HLB number beyond 20 are solubility promoters for aqueous systems; Surfactants with low HLB values are use for W/O emulsions, as well as those ones with high values are for O/W emulsions.

The optimal HLB number has been shown to be in the range 10 – 12, also it is better to use a mixture of surfactants than one with the same HLB number. Nevertheless, there is an optimum difference in HLB number to formulate emulsifier blends of intermediate HLB numbers to produce stable emulsions. A good approximation of the additives of the weighted HLB number could be obtained by the following formula: [47]

$$N^{\text{mix HLB}} = N^{(1)}_{\text{HLB}}\, w + N^{(2)}_{\text{HLB}}\, W^{(2)}$$

Where:

$N^{(i)}_{HLB}$ is the HLB number of surfactant (i), and $W^{(i)}$ its weight percentage. The values of HLB are available in literature [47]. As reference common surfactant HLB values have been listed in **Table 2-5**.

Table 2-5. HLB values and molecular structure of common surfactants.

Surfactant	Commercial name	HLB
⌖ Sorbitane trioleate	Span 85	1.8
⌖ Polyethylene glycol sorbitan Monooleate sorbitan monooleate, Polysorbate 80	Tween 80	15
⌖ Magrogolglycerol ricinoleate PEG-35 castor oil	Kolliphor El Cremophor El	13

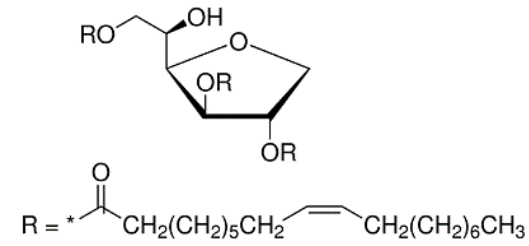

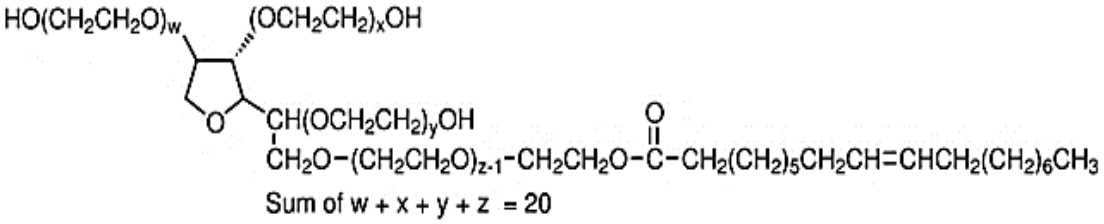

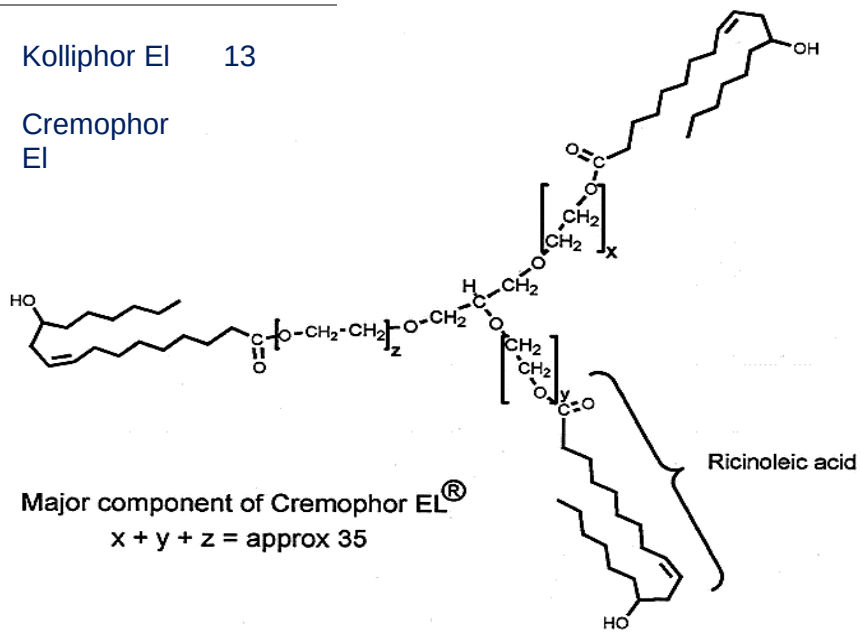

After having discussed the importance of phase change materials in thermal energy storage and the application of emulsion systems for their encapsulation, it's interesting to discuss the way emulsions have been used to synthetized new porous materials by polymerization encapsulating at the same step phase change materials, resulting in solid-monoliths with encapsulated phase change materials.

Developed research projects concerning this field have been presented in the following chapters.

2.4 Emulsion templating polymerization

Emulsion templating polymerization is a effective technique for the encapsulation of tiny drops of PCM occurs, without modifying or affecting its properties and at the same time, creating a solid matrix capable of protecting and keeping it. The material elaborated is then, possible to be used for thermal insulation without any kind of packaged. The principle of preparation of emulsion-templated materials lies on the mixing of two non-miscible fluids, leading to the formation of an emulsion from which the external (continuous) phase is generally converted into a polymeric structure and the internal phase is removed leaving behind voids often called cavities. **Figure 2-12** exemplifies these steps showing the cavities as seen in the microscope. These porous materials showing a specific structure are known under the general acronym of poly-HIPE (for polymerized High Internal Phase Emulsion) and are very well documented [48-51].

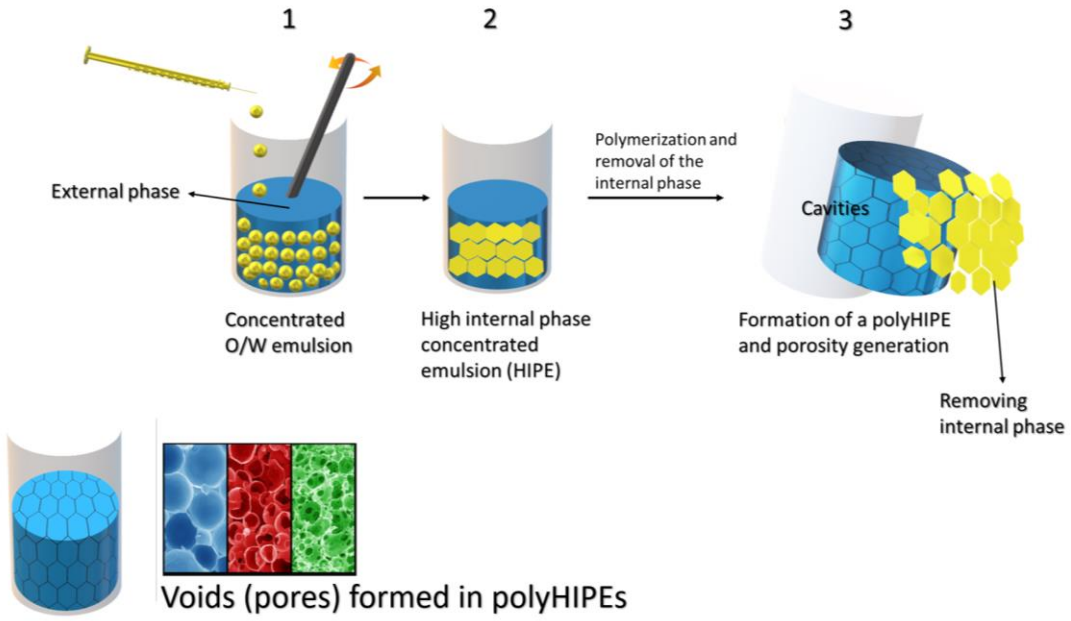

Figure 2-12. Preparation of porous materials polyHIPE and cavities observed in the microscope after internal phase removal.

High Internal Phase Emulsions (HIPEs) are concentrated systems with a volume fraction (Φ) of at least 0.74 of internal or dispersed phase. At $\Phi < 0.74$, dispersed phase droplets are arranged in a compacted way with a sphere shape of the same diameter size, these systems are known as Low Internal Phase Emulsions (LIPEs). If the case if of: $\Phi > 0.74$ of internal or dispersed phase, droplets are deformed acquiring a polyhedral shape to occupied as much space as possible (**Figure 2-13**). Droplets are then separated by a thin film of continuous phase and surfactants that avoids the coalescence of the system. This film is usually flexible to resist shape changes but strong enough to avoid ruptures. Polymer materials can easily be prepared from HIPEs if one or the other (or both) phases of the emulsion contain monomeric species. This process yields a range of products with widely differing properties [48-52].

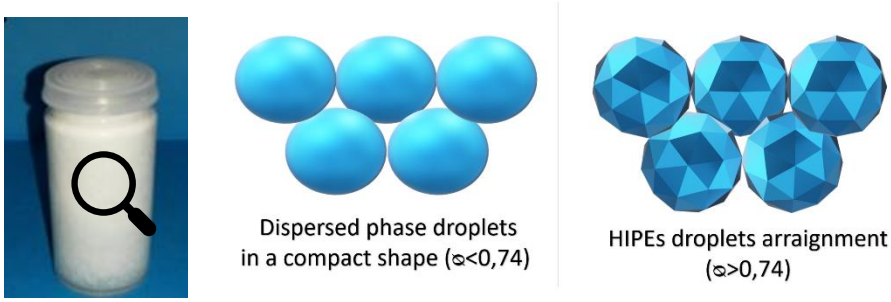

Figure 2-13. LIPEs and HIPEs droplet arraignments in emulsion systems.

Physical properties like higher viscosity, non-Newtonian rheologic behaviour and a darker colour have been determined for HIPEs better than for low internal phase emulsions (LIPEs), the reason is the arraignment of their droplets [53]. Porosity generation occurs because of the internal phase removal, after polymerization a three-dimensional structure is obtained because of the presence of monomer or polymer precursors [53.] In the cases, more rarely reported, where the inner phase is also polymerized, polymer-polymer composites are obtained [54-56]. Materials where the internal phase remains intact after the final treatment also remains little studied [57.]

Pullulan was the object of study during this research since a polyHIPE with a pullulan high concentration was synthetized. Pullulan properties will be presented in the following section.

2.5 Pullulan produced by microorganisms

Exopolysaccharides (EPSs) produced by a number of microorganisms are chemically well defined and have attracted worldwide attention due to their novel and unique physical properties. These are rapidly emerging as new and industrially important source of polymeric materials, which are gradually becoming economically competitive. Microorganisms that produce large amount of slime have the greatest potential for commercialization, since EPSs can be recovered from the fermentation broth easily. Microbial EPSs have become available for use in many applications that are not only compatible with human lifestyle but also are friendly to the environment. Many microorganisms overproduce EPSs with an interesting rate of chemical and physical properties, some of them are presented in **Table 2-6** [58.]

Table 2-6. Commercially available microbial exopolysaccharides (EPSs).

EPS	Producer organism
Xantham	*Xanthomonas campestris*
Dextran	*Leuconostoc* *Mesentroides* *Streptococcus mutans* *Acetobacter sp.*
Curdlan	*Alcaligenes faecalis*
Gellan	*Pseudomonas elodea*
Scleroglucan	*Sclerotium glutanicum*
Pullulan	*Aerobasidium pullulans* *Tremela mesenterica* *Cytaria harioti* *Cytaria darwinii* *Cryphonectria parasítica* *Teloschistes flavicans* *Rhodototula bacarum*

Although many microorganisms are known to produce EPSs, most of the research effort has been directed to the α-glucan pullulan, produced by *A. pullulans*, a yeast-like fungus with impressive metabolic and ecological versatility [58].

2.5.1 Pullulan historical outline

The basic structure of pullulan was discovered during the 1960's, it was observed that the enzyme pullulanase specifically hydrolyzes *α-(1→6)* linkages in pullulan and converts the polysaccharide to maltotriose. On this basis, pullulan is commonly viewed as *α-(1→6)* linked polymer of maltrotriose subunits, as it can be seen in **Figure 2-14** [58-60].

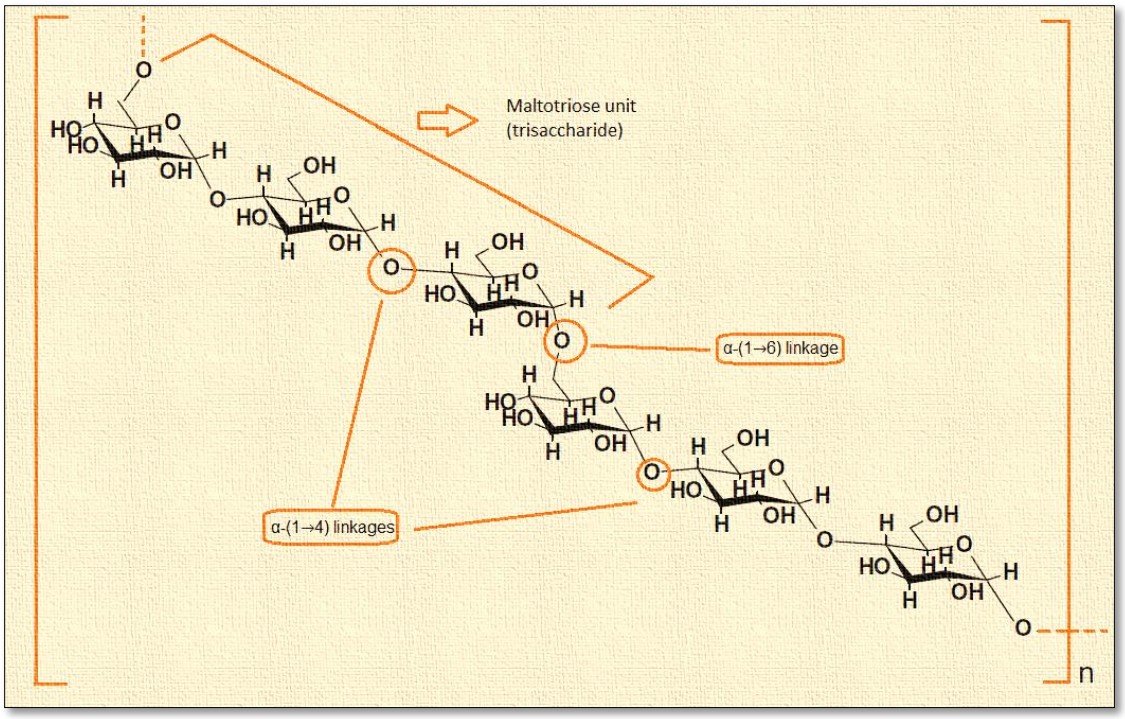

Figure 2-14. Chemical form of pullulan.

This polysaccharide is viewed as a succession of α-(1→6)-linked (1→4)- α-D-triglucosides like maltotriose G_3. However, pullulan can be considered to be a polymer of panose or isopanose subunits, which may reflect more accurately the biosynthetic origins of the molecule. There is also a minor percentage of randomly distributed maltotetraose subunit [60] .

2.5.2 Biosynthesis of pullulan

Little has been stablished about the mechanism of pullulan biosynthesis, it is occurring intracellularly and secreted by *A. pullulans*, involving UDP-glucose, ATP and proceeds through lipid intermediates. *A. pullulans* incorporates ^{14}C-labeled glucose into lipid-linked glucose, isomaltose, panose and isopanose through a reaction mechanism in which pullulan is formed by the polymerization of either panosyl or isopanosyl moieties. An occasional direct linkage of panosyl and isopanosyl moieties would form the minor maltotetraosyl elements. However, none of the enzymes involved have been characterized. Commercial production of pullulan began in 1976 by the Hayashibara company in Japan, selling it as starch syrup. The company remains the principle commercial source in nowadays [60].

2.5.3 Industrial production of pullulan by fermentation

In general, the production of pullulan can be exemplified by **Figure 2-15**.

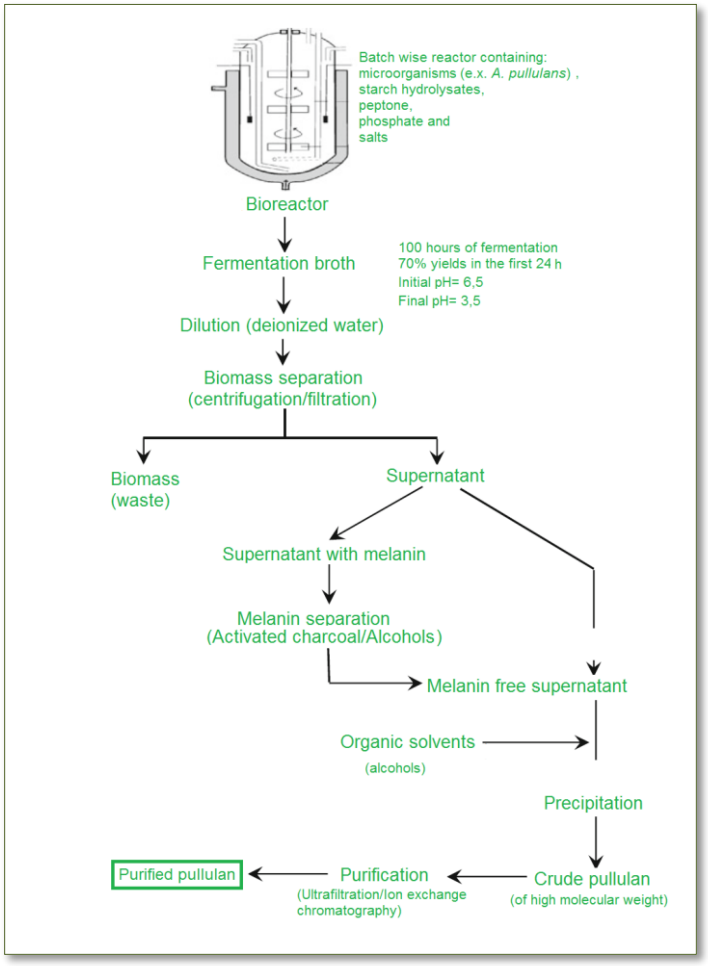

Figure 2-15. Industrial processing of pullulan by fermentation.

Briefly, a fermentation process occurs in a batch wise reactor with the corresponding microorganisms, phosphates, starch, peptones and salts, obtaining yields of 70% in the first 24 h. Fermentation is followed by dilution, filtration, precipitation and purification steps in which; melanin is separated from pullulan with activated charcoal and later purified through by ultrafiltration and ion exchange resins. Finally, purified pullulan of high molecular weight is obtained. The industrial production of pullulan does not demand a higher economic inversion than the common reactor-batch mechanisms, its price production however; comes mainly from melanin removal and its limited production by a Japansse industry. More factors are listed in **Table 2-7** and information regarding its price can be find in **Table 2-8** [58-60] .

Table 2-7. Factor that increase costs in the production of pullulan.

Factors	Consequence
Melanin removal	Main problem contributing to production cost.
Enzymes coming from microorganisms	Cause a degradation of pullulan reducing its molecular weight. As a result, more feedstock is needed increasing costs.
Feedstock	Tendency in reducing production cost is identifying less expensive feed.
Fermentation	Developing alternative fermentation schemes would contribute to reduce costs.
Limited production	Pullulan is produced in a small-scale sell by a Japanese industry. As it is not produced worldwide, this represents the main issue regarding its price.

Table 2-8. Pullulan price in Japan

Production per year	**Food grade usage**	**Pharmaceutical grade (deionized)**
300 metric tons	US $20 per kg	US $25 per kg.

2.5.4 Physicochemical properties

The regular occurrence of α-(1→6) linkages in pullulan interrupts what would otherwise be a linear amylase chain. This unique linkage pattern is believed to be responsible for its structural flexibility and solubility, resulting in distinct film and fiber-forming characteristics not exhibited by other polysaccharides. Although more expensive than these plastics, pullulan products are edible and biodegradable, and underivatized pullulan is highly water-soluble [58-60]. Its main quality parameters are listed in **Table 2-9**.

Table 2-9. Physicochemical characteristics of pullulan.

Parameter	Specification
Appearance	White/yellowish white
Water solubility (25°C)	High
Organic solvents solubility	Poor or non Except: dimethyformamide and dimethylsulfoxide
Polypeptides (%)	Maximum 0,5
pH of solution	5-7 and stable in a wide value range
Mineral residue-ash (sulphated, %)	Maximum 3
Moisture (loss on drying, %)	Maximum 6
Molecular weight (range, kDa)	100-250
Viscosity in water solutions	Proportional to pullulan's molecular weight
Toxicity	Biodegradable Biocompatible

2.5.5 Applications

Microbial polymers are known to possess useful physical properties, even then currently only a small number of biopolymers are produced commercially on large scale. A few fungal EPSs have been reported so far that possess appealing industrial applications. Pullulan, a water-soluble biopolymer from *A. pullulans* is one of them. Numerous applications of pullulan in food industry, pharmaceutics, cosmetics, oral care products, electronics, etc. have been proved and being used. In many sectors its application seems to be maintained over the years and growing for different sectors. Main of its industrial interesting properties are shown in **Table 2-10**.

Table 2-10. Main applications of pullulan by type of industrial sector.

Applications	Properties
Food industry Low-viscosity agent filler in beverages and sauces. Stabilizer in mayonnaise formulations Food-paste to adhere nuts to cookies Food coating agent Decorative chips for bakery Protective glaze directly in food Binder and stabilizer in pastes Production of glucose and maltose syrups from starch.	Easily dissolved in hot or cold water. Non-hygroscopic, Non-toxic, Non-mutagenic, odorless, tasteless and edible.
Cosmetics Additive in lotions and shampoos Emulsions for anti-aged cream creating a *lift-up* effect.	Capacity to form solutions from low to high viscosity similarly to gum arabic.
Pharmaceutics Denture adhesive products Wound healing compositions Pill-coatings Oral care products (ex. Listerine films) Promising as a non-toxic agent for vaccines, facilitating liposome delivery Protective agent for oxidized vitamins and fats Additive in food for diabetic patients	Adhesive capacity. Films-forming agent (5-60 µm), flexible and soluble in water, resembling to certain synthetic polymers derived from petroleum. Low caloric content Promotes prebiotic function
Others Photographic and electronic. Pullulan based hydrogels. Manufacturing industry as flocculant, adhesive and binder. In wraps and plastic containers. Sizing agent for paper.	Form stable solutions to heating, changes in pH and most metal ions (including sodium chloride). Biodegradable.

Most pullulan derivatizations are intended to reduce its water solubility or to introduce charged or reactive groups for functionality. The water solubility of pullulan can be progressively reduced esterification or etherification. Hydrogenation increases the heat stability of pullulan and carboxylation enhances its solubility in cold water. Crosslinked pullulan beads are useful in gel permeation chromatography, and polyanionic and cationic derivatives have been

prepared. Cyanoethylated pullulan has potential uses in electronic devices. Pullulan has been sulfated, chlorinated, sulfinethylated and chloroalkylated. Azidopullulan and siloxane derivatives have been prepared [58-60].

2.5.6 Outlooks and perspectives

Pullulan is a unique polysaccharide with a multitude of demonstrated practical applications. The major constraint on the use of pullulan appears to be its price. As shown in **Figure 2-16**, many of the earliest pullulan patents concern bulk industrial applications, for example as a flocculating agent or in the production of paper or paint [58-60].

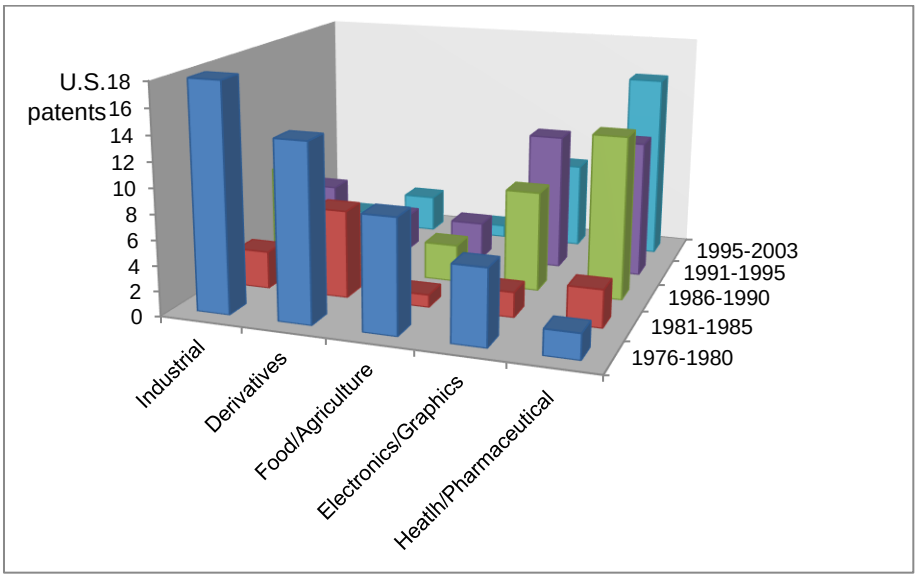

Figure 2-16. United States patents (1976-2003) basing in pullulan as a principal ingredient, by application field.

Similarly, pullulan is too expensive for many of these potential uses, including those in which it serves as biodegradable replacement for petroleum derived polymers. Although pullulan is efficiently produced by fermentation of relatively inexpensive substrates, it currently sells approximately three times the price of dextran or xhanthan, other microbial gums produced by fermentation. Perhaps, accordingly more recent patents have increasingly concerned higher value applications for pullulan, especially those related to human health. Technical improvements in pullulan production, such as engineering innovations or improved production strains, could reduce the cost of production. Molecular genetic approaches to improved production are currently limited by a lack of fundamental knowledge about pullulan

biosynthesis. Costs may be determined to a large extent by the modest production scale of pullulan. Pullulan production levels have been fairly stable for a number of years, with specialty food applications as a major market. The recent commercialization of pullulan-based oral care products is encouraging for the future of pullulan, although competing formulations have appeared. Another emerging market may be in the pharmaceuticals. Increased demand for pullulan could justify expanded production, resulting in new viable market niches for this unique biopolymer [58-60].

3 Synthesis of pullulan hydrogels by polymer crosslinking with sodium trimetaphosphate

Crosslinking of homopolymers or copolymers itself leads to a three-dimensional network connected by physical or chemical crosslinks like the one shown in **Figure 3-1**. When the polymer is solubilized and crosslinked in an aqueous phase the obtained material is commonly called: hydrogel, it has a hydrophilic behavior as main characteristic. Hydrogels are known for their properties to transport active substances and response to changes in pH or temperature developing a stimuli-responsive kind material [61] .

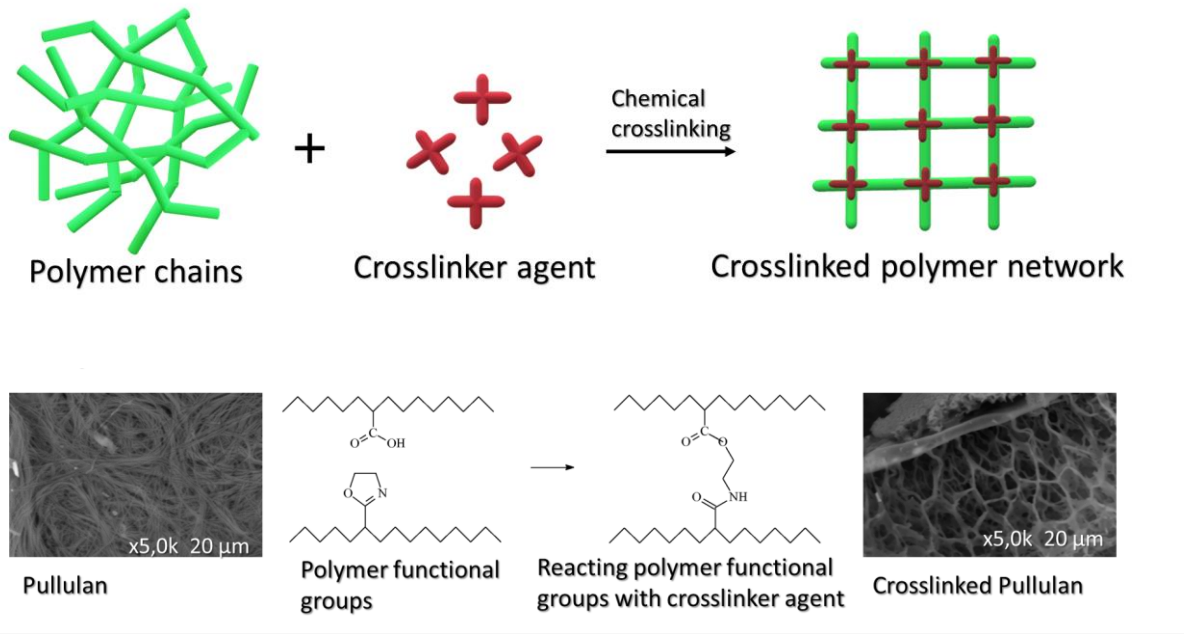

Figure 3-1. Polymer crosslinking to produce a three-dimensional network with improved properties.

(a) Non-crosslinked polymer chains; (b) Crosslinker chemical agent; (c) Three-dimensional network formation after chemical crosslinking. Polymer functional groups creates covalent bonds with the ones of the crosslinker to give a more performant structure; (d) Polymer pullulan chains seen at the microscope before crosslinking; (e) Exemplification of crosslinking by functional group links; (f) Crosslinked pullulan.

Some of the main properties that make them important for industrial, medical and agricultural applications are shown in **Figure 3-2**.

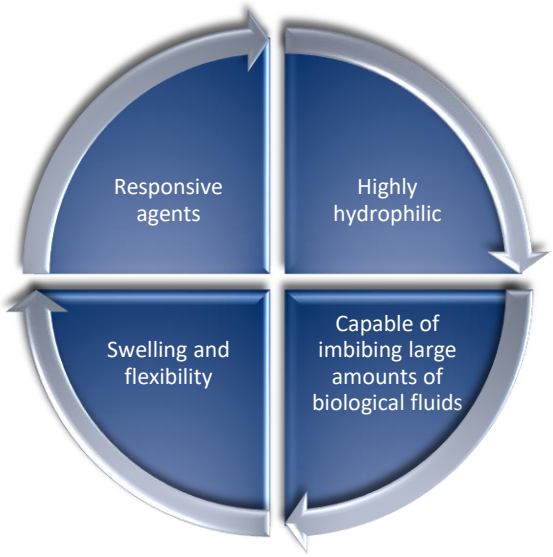

Figure 3-2. Hydrogel properties.

Their compatibility with water makes them flexible and allows them to swell in an aqueous media instead of dissolving (this main aspect explain their ability to mimic natural living tissues opening interesting ways towards biological or pharmaceutical applications). Swelling can be seen as the temporary change that happens to a sponge when it is immerse in water and squeeze out, as it is indicated in **Figure 3-3** [62].

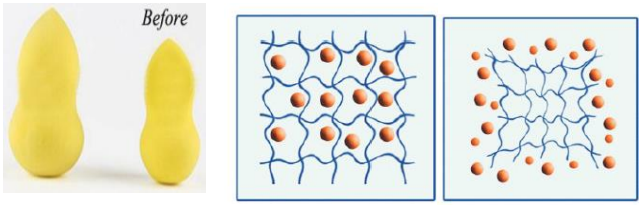

(a) (b)

Figure 3-3. Swelling and deswelling behavior of hydrogels.

(a) One can visualize it as what happens to a sponge once it has been put in water, taken out and squeezed out; (b) When an active ingredient is contained by a hydrogel, it is realized by changes in the environments as pH and temperature. This is seen as shrinkage in hydrogel's structure.

Hydrogels respond to external stimuli by swelling. It is in this way that applications like: controlled drug delivery, separation/concentration process or agricultural carriers are possible. Their ability to respond to external stimuli depends on ionic forces and the nature of the polymers used. Changes in pH, temperature or the presence in electric or magnetic fields will have a consequence on the swelling behavior [63].

3.1 Swelling behavior

The presence if ions will create a differential of chemical potential in the solution, causing the hydrogels to swell or shrink (to take or release water). Depending of the nature of these ions is the tendency of behavior of the hydrogel. Two main types or ions have been recognized:
a) Chaotropes; and b) kosmotropic [64].

a) Chaotropes also called *salting in ions* or *water structure breakers*

Chaotropes have a large radius size and present high polarizabilities. Consequently, they have weak electric fields (short charge density) and they lose their hydration layer easily, in contrast with kosmotropic ions [64].

b) Kosmotropic also called *salting out ions* or *water structure makers*

These kinds of ions are known for helping to stabilize proteins, they have a small radius size (consequently a large charge density) and present low polarizabilities. Since they have high electric fields at short distances, they do not lose their hydration layer easily. Examples of each kind are exemplified in **Figure 3-4** [64].

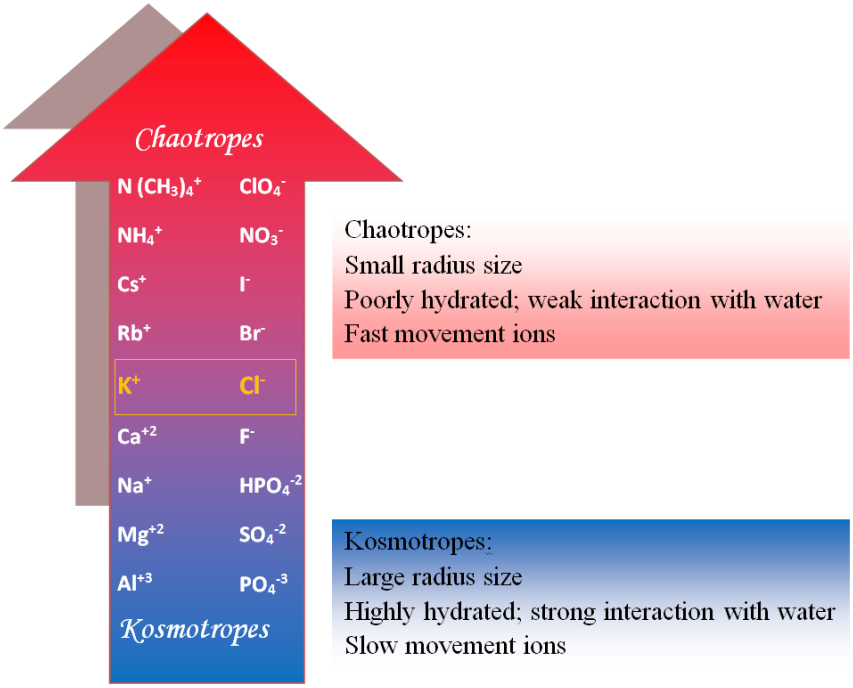

Figure 3-4. Ions classifications according to their tendency to interact with water.

a) Kosmotropes and; b) chaotropes. The tendency of interaction at the level of K^+ and Cl^- is negligible. An ion has both tendencies, but one is stronger than the other.

From bottom to the upper part of the arrow, in the bottom part the tendency of behavior is stronger for water interaction (kosmotrope behavior), as one starts to move to the upper part, this tendency decreases. The upper part of the arrow corresponds to a weak interaction with water (chaotrope behavior). In other words, an ion will have both tendencies, but one will be stronger than the other [64].

3.2 Effect of surfactant over hydrogels

A hydrogel is influenced not only for the ionic interaction with water, but also because of the presence of a surfactant. The nature of the surfactant and the type of ion present in a hydrogel will create a stronger or weaker bonding between them. Depending of which force is the predominant, the system will be less or more stable in terms of: water absorption (swelling), shrinkage, resistant to temperature, viscosity, etc. In order to facilitate the study of this complex, a classification of surfactants has been made. This classification matches the type of surfactant headgroup that will have a stronger and more stable bonding with a specific type of ion. That is; anionic surfactant headgroups are chaotropic or kosmotropic. According to this classification

the chaotropicity of surfactant headgroups increases or decreases as it can be seen in **Figure 3-5** [64].

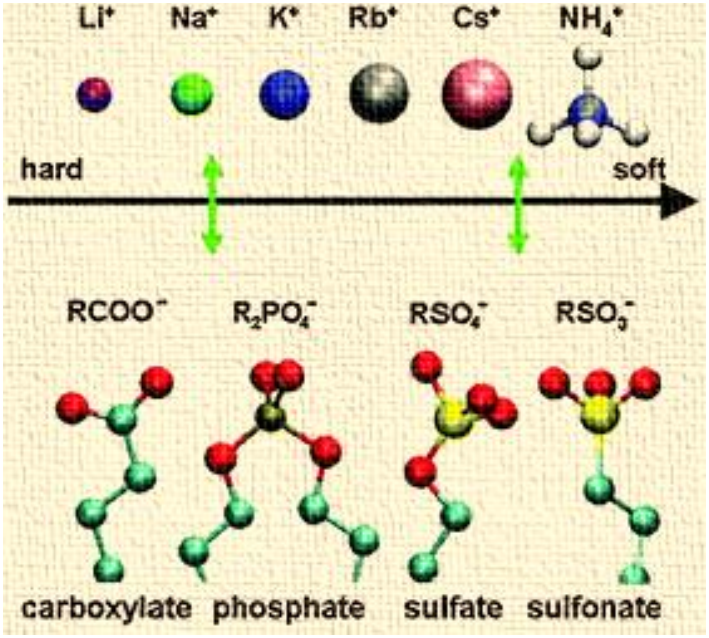

Figure 3-5. Anionic surfactant headgroups classification and their respective counterions regarding their capability to form close electron-pairs.

(the green arrow means strong interactions).

For carboxylate groups for example, the tendency to form ion pairs would decrease along the series: $Li^+ \geq Na^+ \geq K^+ \geq Rb^+ \geq Cs^+$. A reversed cation series would be expected for sulfonate surfactants. The same concept can be used to understand and predict the binding of ions to cationic surfactant headgroups and to protein charged groups. The list of hydrogels made from polysaccharides seems to be increasing, since properties are being discovered. They have been widely, mainly for electronics, pharmaceutics and medical applications, some of them commercially available are presented in **Table 3-1** [64].

Table 3-1. Common polysaccharides for hydrogels synthesis and their common applications.

Polysaccharide	Characteristics	Applications	Crosslinker agents
Hyaluronic acid **(Prepared from bacterial fermentation and present in human tissues)**	Viscoelastic Immunogenicity Drug carrier Biocompatible pH stability Clinical tissue reconstruction	Viscoelastic material in ophthalmologic surgery Injectable solution for the treatment of joint diseases in orthopedics.	1,3 diamminopropane
Pullulan **(Homo-polysaccharide originated from *Aurebasidium pullulans)***	High flexibility Forms clear highly oxygen-impermeable films with excellent mechanical properties High stability over time, pH and temperature	Food and drinks additive Coating agent Fiber-film forming (electronic devices) Drug carrier for hydrophobic substances as anticancer drugs	Sodium trimetaphosphate
Xanthan	Discover in the 50's. Thermo-responsive agent Homogeneous porous network	Tablets excipient and drug releaser in combination with other polysaccharides	Citric acid
Alginate **(Source: algae fermentation)**	Interacts with acid carboxylic pH responsive Forms hard gels with a fast-kinetic reaction Mucoadhesive Porous	Excipient in tablets with modulated drug delivery dosage Potential use in tissue regeneration Ocular drug delivery	Sodium tripolyphosphate
Carrageenan **(from red-seaweeds, Ireland)**	Sensible to the presence of hydrophobic drugs by changing its diffusion.	Drug release systems by regulated diffusion Electrostatic interactions	Genipine

3.3 The crosslinking of hydrogels

Hydrogels can be classified according to their nature, which is as: natural or synthetics. Natural hydrogels include collagen fibrin, bovine fibrinogen, fibrin, hyaluronic acid, derivatives polysaccharides like chitosan and alginate, etc. Due to their origin their composition may vary from one batch to the other, making difficult their applications in terms of reproducibility, control of mechanical properties and swelling. There is also a dependency on the hydrolysis method. However, the situation with synthetic hydrogels is different [65].

Synthetic hydrogels like poly (ethylene glycol) diacrylate, poly (acryl amide), poly (vinyl alcohol), etc. are more reproducible giving the opportunity to have more control over their properties and behavior. Although their structure depends on polymerization conditions, being necessary to control their protocol of preparation, temperature, pH and all other parameters regarding each type of hydrogel. The advantages over natural hydrogels are that, synthetic allows to produce a more flexible material with better mechanical properties as well as temperature and pH resistivity, manipulate certain parameters like: concentration of precursor material and type of crosslinker agent in order to modify their final properties. They also can be selected to be hydrolysable or biodegradable over variable periods of time. A physical crosslinked occurs thanks to hydrophobic interactions between chains, ionic interactions between a polyanion and a polycation (complex coacervation) or ionic interactions between a polyanion and a multivalent cation (ionotropic hydrogel). The chemical crosslinks occur by ultraviolet radiation, heating or by a precursor causing (**Figure 3-6**) high interactions between the polymer, water and precursor.

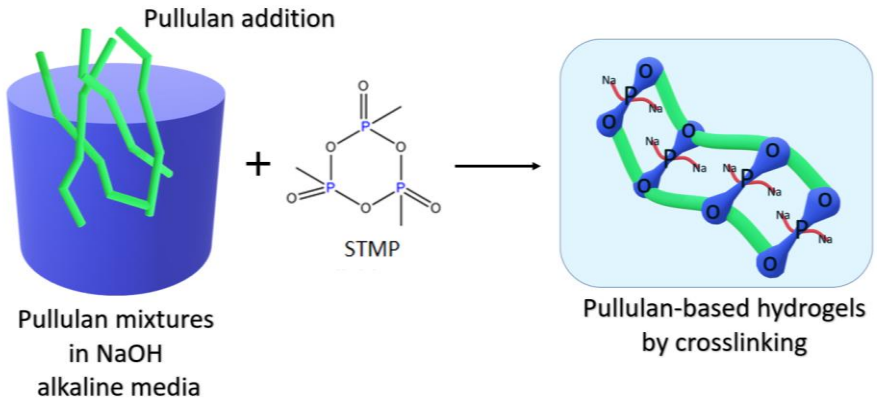

Figure 3-6. Diagram of the process steps (pullulan mixtures preparation in NaOH 1M aqueous solutions and STMP addition until crosslinking in achieved).

By controlling the degree of crosslinking is possible to tune the property of the material and optimize it for many different applications, in this way; a wide spectrum of possibilities opens starting from the same original polymer [65].

3.4 Objectives

3.4.1 General objective

Synthesis of based-pullulan hydrogels with STMP at different crosslinking yields to identify the STMP concentration that leads to a hard material different in properties to common hydrogels.

Study the crosslinking reaction of pullulan hydrogels by changes in viscosity and infrared spectrometry.

Determine pullulan hydrogels pasting properties

3.5 Materials and methods

3.5.1 Materials

Pullulan was obtained from Carbonsynth Limited Company. Trisodium trimetaphosphate (STMP) of high technical grade and NaOH were obtained from Sigma Aldrich chemicals. Deionized water was used throughout the work.

A Brookfield viscometer (L3, 5 rpm) and infrared spectroscopy were used to characterize samples. All samples were prepared at room temperature.

3.5.2 Methodology

3.5.2.1 Synthesis of pullulan hydrogels

In a typical experiment, several aqueous solutions of sodium hydroxide (100 mL; 1M) were placed in cylindrical, round-bottomed reactors at room temperature. Pullulan was added directly to each one at a concentration of 50 % (w/w) in relation to the aqueous phase under constant stirring at approximately 300 rpm with a rod fitted with one radial and one axial two blades impellers, connected to an overhead stirrer motor. After complete homogenization of the mixtures; STMP was added directly to each one to give concentrations of 5%, 10%, 13%, 15%, 17% and 20 % (w/w) in relation to pullulan concentration and stirring continued for 3 hours. Obtained samples were stored in plastic containers at room temperature until characterization studies.

3.5.2.2 Determination of hydrogel's pasting properties

Synthetized hydrogels were placed in cylindrical, round-bottomed reactors under constant stirring at approximately 150 rpm with a rod fitted with one radial and one axial two blades impellers, connected to an overhead stirrer motor and a temperature controller. A Rotation Viscometer VISCOELITE-R was adapted to the glass reactors by the introduction in each one of a rotating L3 size spindle fixed at a 5.3 rpm rate.
A heating and cooling cycle was programmed as follows: Samples were heated from 20 °C to 90 °C (corresponding to heating cycle) and then cooling went from 90 °C to 20 °C (cooling cycle), in every case temperature was hold for 5 minutes every 10 °C. Viscosity was measured during each cycle 5 minutes after samples reached a temperature.
Pasting parameters such as peak viscosity, holding strength, final viscosity, breakdown and set back were determined according to the following definitions:

-Peak viscosity is the highest viscosity during the heating step;
-Holding strength is the lowest viscosity at the end of the 90 °C heating step;
-Final viscosity is the viscosity at the end of 50 °C cooling step;
-Breakdown is the ratio of changing in viscosity from peak viscosity to holding strength;
-Set back is the changing in viscosity from holding strength to final viscosity.

Heating and cooling cycles for each sample were represented in a curve plotting viscosity vs time for each temperature tested.

3.5.2.3 Viscosity measurements

Viscosities were measured using a Rotation Viscometer VISCOELITE-R at 25 °C. Briefly, 10 g of sample were placed in a 50 mL glass-container, and the spindle was inserted until the corresponding height was achieved. Measures were performed with spindle size L3, at a rate of 5.3 rpm.

3.5.2.4 Infrared spectroscopy

Obtained hydrogels were analyzed by infrared spectrometry after 3 days of crosslinked. For comparison, Infrared spectrums were obtained of a commercial sample of unmodified pullulan.

3.6 Results

Pasting properties of synthetized hydrogels are presented in **Table 3-2**. Highest and lowest viscosity measures reached during heating – cooling cycle and final viscosity at the end of cooling were used to determine the breakdown and set back values for each sample.

Table 3-2. Pasting properties of pullulan hydrogels.

	Viscosity measurements during heating – cooling cycles (Pasting Properties)				
Pullulan hydrogels	Highest viscosity (mPa, s) during heating (20-90 °C)	Lowest viscosity (mPa, s) at the end of heating (20-90°C)	Final viscosity (mPa, s) at the end of cooling (90-20°C)	Breakdown ($V_{highest\ heating} - V_{lowest}$)	Set back ($V_{lowest} - V_f$)
$P_{50}S_5$	10	2	7	8	5
$P_{50}S_{10}$	24	3	20	20	17
$P_{50}S_{13}$	34	7	45	27	38
$P_{50}S_{15}$	89	14	78	76	65
$P_{50}S_{17}$	96	18	184	78	167
$P_{50}S_{20}$	41	5	21	36	15

Viscosity of samples increased according to STMP concentration because of the generation of more grafted pullulan chains by mono-phosphate covalent bonds coming from the cycle opening of STMP by the action of Na^+ ions (table x, highest viscosity during heating cycle). This behavior was observed in all samples except for $P_{50}S_{20}$ in which viscosity decreased.

A decrease in viscosity indicates that less pullulan chains were grafted, in this case not because of the lack of STMP agent but on the contrary because of an excess. STMP introduces phosphate negative ions to the system creating a repulsion ionic force, the one is stabilized with Na^+ ions. When there are not free positive ions and more negative forces are introduced, the repulsion force predominates over attractive forces. In this case, deprotonation of grafted pullulan chains occurs as an effort to set free positive ions and compensate negative forces. Then a less ordered system is produced and thermodynamically stable. This might indicate a STMP limit concentration for pullulan crosslinking.

Viscosity reached its lowest value at the temperature of 90 °C, at this point the heating cycle ended and the cooling began as indicated in **Figure 3-7**.

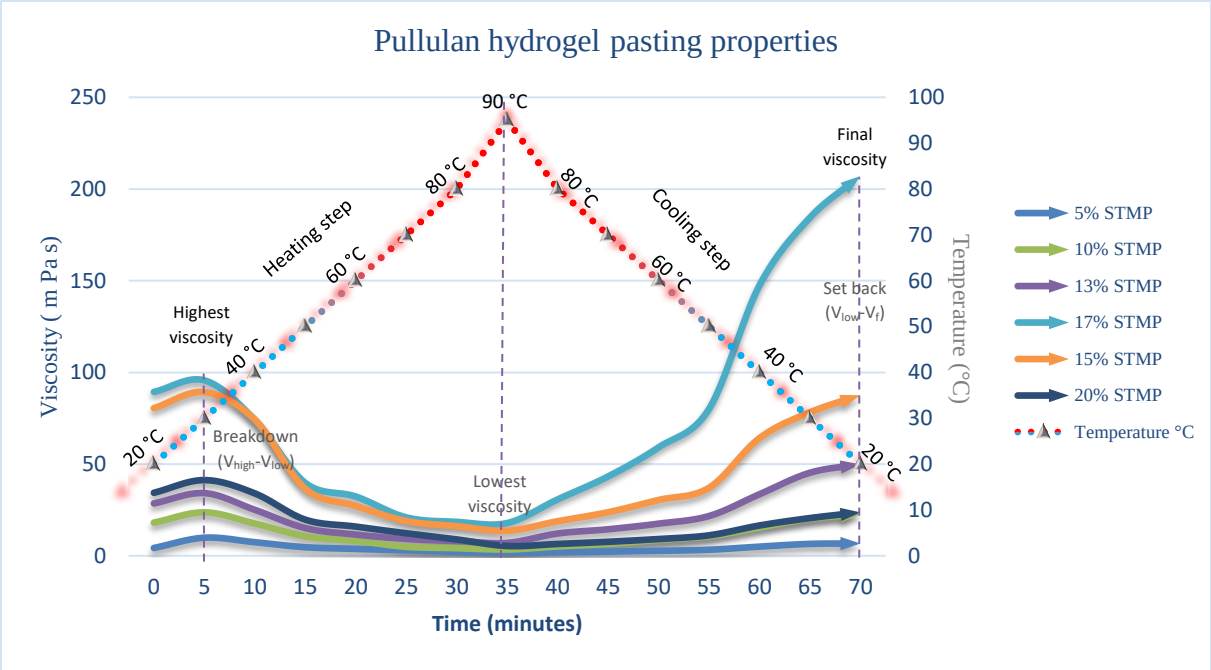

Figure 3-7. Pullulan hydrogels pasting properties.

The lowest viscosity value was reached because of the rupture of pullulan granules and crosslinking bonds. It's interesting to note that most samples reached a similar lowest value between 2 and 10, this occurred because of the degradation of pullulan granules forcing the hydrogels to expand and take more water. In the contrary, 15% and 17 % samples kept values of 14 and 18 m Pa S. this might show the better resistance of this samples to brake their phosphate covalent bonds and ungraft pullulan chains.

Cooling step (**Figure 3-7**) showed the increase of viscosity until a maximum at 20 °C. samples with better temperature resistance because of more grafted chains had the highest viscosity at the end of the cycle, presenting a different ordered of their structure with the intake of more water. samples with low values indicate the break of pullulan granules and bonds all from the exterior to the internal material phase. Showing less flexibility and weaker bonding force.

Sample with 20% of STMP had similar behavior as that of 10% STMP while 17% STMP showed more resistance and better stability. This shows a non-Newtonian behavior in pullulan materials and that not necessarily a high STMP concentration improves the materials crosslinking.

Infrared spectrum was obtained from a pullulan solution previously prepared and hydrogels $H_{50}P_{17}$, $H_{50}P_{15}$, $H_{50}P_{13}$, $H_{50}P_{10}$. Pullulan solution spectrum is presented in **Figure 3-8**. It consists of hydroxyl and alkyl functional groups.

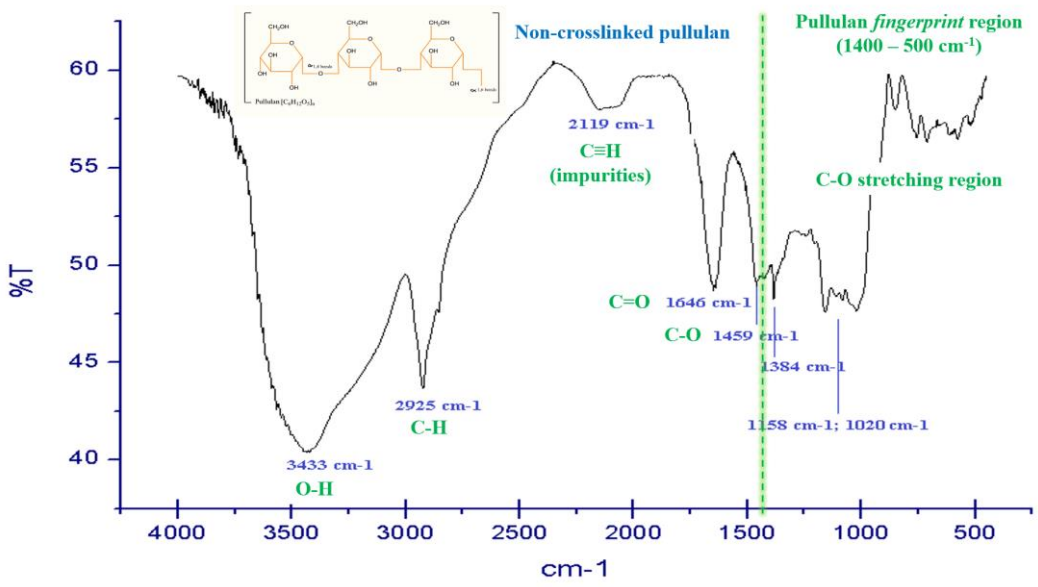

Figure 3-8. Non-crosslinked pullulan infrared spectrum.

Non-modified pullulan showed infrared functional groups O-H and C-H in wavelengths 3433 cm^{-1} and 2925 cm^{-1}, signal in 2119 cm^{-1} and 1646 cm^{-1} correspond to impurities since sample was utilized directly as received. Signals from 1646 cm^{-1} to 1020 cm^{-1} correspond to C-O functional groups characteristic of this compound.

Spectrum of hydrogel $H_{50}S_{17}$ is presented in **Figure 3-9** and its corresponding functional groups signals.

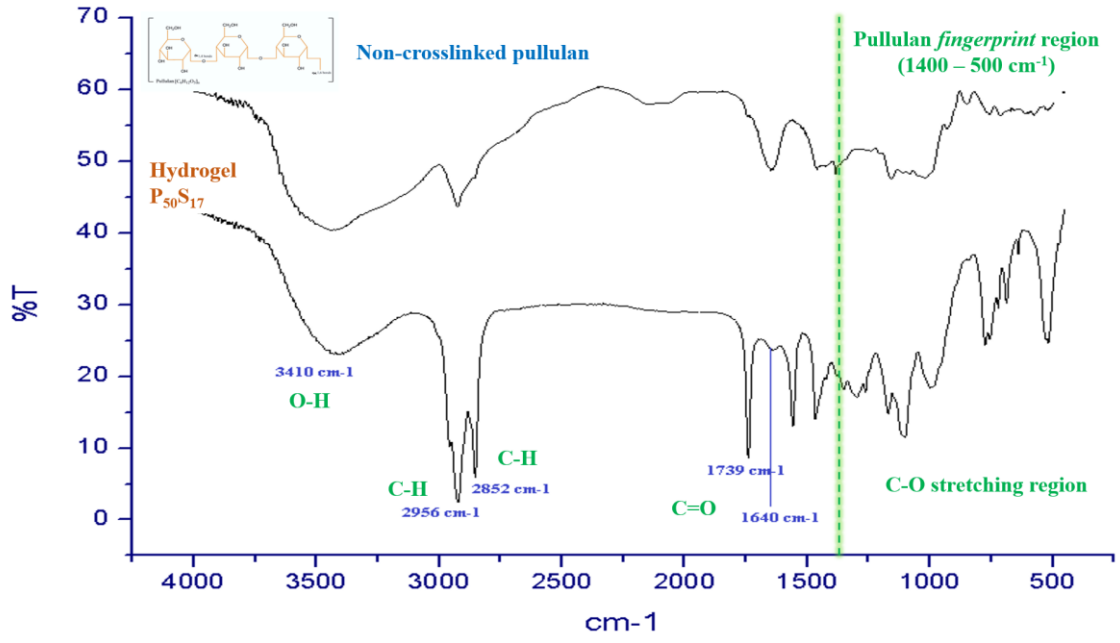

Figure 3-9. Infrared spectrum of hydrogel 17% STMP.

Signals corresponding to alcohol (O-H, 3410 cm^{-1}) and alkanes (C-H, 2956 and 2852 cm^{-1}) were affected by crosslinking. Those signals correspond to the pullulan grafting and the formation of alcoholate groups by STMP. Signals in 1739 and 1640 cm^{-1} correspond to impurities. The same signals presented changes in samples with lower STMP concentrations ($H_{50}S_{15}$, $H_{50}S_{13}$ and $H_{50}S_{10}$) as shown in **Figure 3-10**.

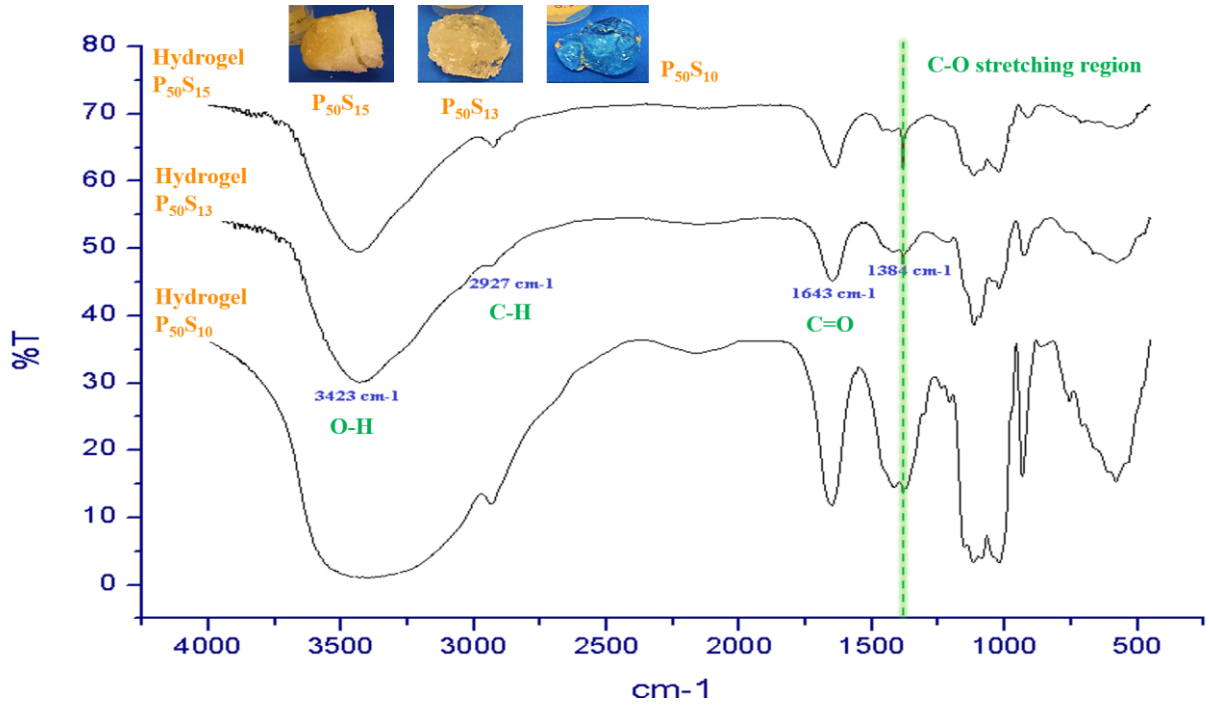

Figure 3-10. Infrared spectrum of hydrogels $P_{50}S_{15}$, $P_{50}S_{13}$ and $P_{50}S_{10}$.

A stretching of signal 3423 cm^{-1} occurs when STMP concentration increase, but the concentration was not enough to observed stretching of C-H signals at 2927 cm^{-1}. Infrared spectrums could be used to identify the obtention of better crosslinked samples.

3.7 Conclusions

Viscosity and grafting of pullulan with STMP have a direct relation, an increase of viscosity indicates better grafting yields.

STMP crosslinker agent added in excess leads to a rupture of grafted pullulan chains.

An optimal STMP concentration to graft pullulan hydrogels resistant to heating and cooling cycles was determined.

Pullulan hydrogels showed non-Newtonian properties with a non-linear increase of viscosity.

Infrared spectrum signals 2956 cm^{-1} and 2852 cm^{-1} appeared in the case of better crosslinked pullulan hydrogels, in terms of temperature resistance.

4 Pullulan monoliths as encapsulating PCM matrices

4.1 Introduction

It is well–established that the use of phase change materials (PCMs) presents numerous advantages in terms of energy storage efficiency [66]. PCMs compensate temperature peaks and increase thermal comfort in buildings, improve climate conditioning and reduce heating and cooling demands [67, 68]. However, PCMs have to be encapsulated in order to find practical applications. Encapsulation consists in the coating of liquid droplets by sealed rigid shells [69]. Encapsulation technique is widely used for pharmaceutical, biomedical, cosmetics, perfumes and food applications as it provides a transportation and protection media for substance of interest [70, 71]. Encapsulation also allows separating incompatible components, functionalizing active ingredients and converting liquid components into solid systems [72]. Encapsulation is of special interest for phase change materials [73] .

The principle of preparation of emulsion-templated materials lies on the mixing of two non-miscible fluids, leading to the formation of an emulsion from which the external (continuous) phase is generally converted into a polymeric structure and the internal phase is removed leaving behind voids often called cavities. These porous materials showing a specific structure are known under the general acronym of polyHIPE (for polymerized High Internal Phase Emulsion) and are very well documented [74-77]. In the cases, more rarely reported, where the inner phase is also polymerized, polymer-polymer composites are obtained [78-80]. Materials where the internal phase remains intact after the final treatment also remains little studied [81].

The present work reports the encapsulation of a bio-based PCM - butyl stearate - onto a polysaccharide – pullulan - rigid matrix using the emulsion templating approach. Polysaccharide-based polyHIPEs have been the subject of numerous studies because of their biodegradable properties that can find many biomedical applications. However, in most of the reported studies the polysaccharide chains (pullulan or dextran), are chemically modified to make them polymerizable by a radical route in water-in-oil emulsion [82]. More recently pullulan was inserted in the continuous aqueous phase of water-in-oil HIPE for final material reinforcement [83]. To our knowledge, no examples of the use of native pullulan as the constituent of the continuous phase of an oil-in-water emulsion in view to prepared emulsion-templated porous material have been reported.

Pullulan is a commercially available highly water-soluble polysaccharide purified from the fermentation medium of the fungus-like yeast *Aureobasidium pullulans* (originally *Pullularia pullulans*) [84, 85]. Pullulan can commonly be viewed as *α-(1→6)* linked polymer of maltotriose subunits; this type of bonding is responsible for a great chain flexibility inducing quite particular film forming and fiber formation characteristics not usually encountered with other polysaccharides [86]. Most applications of pullulan deal with food, pharmaceutics and cosmetics markets, mainly as a stimuli-responsive material [87]. Pullulan products are edible and biodegradables [88] . Emerging markets propose its use in cancer therapy as a carrier and releaser of cytotoxic molecules and in bio-remediation as a releaser of nutrients in soil and water [89]. Sodium trimetaphosphate (STMP) is of special interest as crosslinking agent as it is non-toxic and able of crosslink a wide variety of polysaccharides at moderate temperatures (50 to 70 °C) [90], under strong alkaline conditions. Crosslinked hydrogels obtained turn into consistent pastes with good resistance to heat, acid and shearing [91, 92].

Butyl stearate can be easily produced out of butanol and stearic acid, both of them renewable, and it is commercially available at a low cost. Furthermore, its thermal characteristics (F = 27°C) [93], are such that it is used as PCM in building insulation [94-96].

The main advantages of our approach are: i) The chemicals used: a fatty acid ester, food grade polysaccharide and crosslinking agent, a bio-based PCM and water, allows to consider the process as sustainable; ii) Since this process is done in only one step, the encapsulation is simpler than the methods usually reported; iii) Encapsulation is performed using a low energy processes; iv) The matrix is chemically stable and nontoxic; v) The monolithic shape of the resulting material allows to use it directly in most of applications.

4.2 Materials and methods

4.3 Materials

Pullulan (M_w = 200-300 kD) was a gift from Hayashibara-Nagase (Europa) GmbH, Düsseldorf, Germany). Butyl stearate, Span 85, Tween 80, trisodium trimetaphosphate (STMP), sodium hydroxide and ethanol were obtained from Sigma Aldrich chemicals. Butyl acetate was provided by Alfa Aesar. Deionized water was used throughout the work. Chemicals were used without further purification.

4.4 Methodology

4.4.1 Preparation of butyl stearate-in-pullulan emulsions

Oil-in-Water (O/W) emulsions containing different concentrations of pullulan in the continuous phase were synthesized as follows: Alkaline solutions (NaOH 2.5 mol. L^{-1}, 35g), were placed in cylindrical, round-bottomed reactors thermostated at 30 °C equipped with a rod fitted with axial/radial two blades impellers connected to overhead stirrer motors. Different amounts of pullulan (7, 9, 11 and 13 g) were then added to each stirred mixture until complete homogenisation. Different amounts of Tween-80 were then added to achieve the same surfactant concentration in each emulsion (7% w / w vs. continuous phase). The solutions were then homogenized under stirring at approximately 300 rpm. Subsequently, the dispersed phase composed of butyl stearate and span-85 (7 % w/w relative to butyl stearate), was added at 30°C using a syringe pump at a rate of $1mL \cdot min^{-1}$ until no more oil insertion was possible. Aliquot of each emulsion was kept in separate glass-containers for viscosity measurements.

4.4.2 Synthesis of emulsion-templated monoliths by crosslinking with STMP

Crosslinking was performed by rapid addition of sodium trimetaphosphate (17% w/w relative to pullulan content) to the stirred emulsions at 30°C. The resulting emulsions were placed in closed PTFE cylindrical moulds ($Ø_{in}$ = 35 mm, h = 45 mm) and stored in an oven at 60 °C during 12 h. As-synthesized wet monoliths were obtained after careful removal from the moulds.

4.4.3 Viscosity measurements

Viscosities were measured using a Rotation Viscometer VISCOELITE-R at 25 °C. Briefly, 10 g of sample were placed in a 50 mL glass-container, and the spindle was inserted until the corresponding height was achieved. Measures were performed with spindle size L3, at a rate of 5.3 rpm.

4.4.4 Water-drying of PCM/Pullulan hydrogel composites

As-synthesized wet monoliths cylinders were used for water removal studies. Different approaches were investigated: i) Drying at atmospheric pressure in an oven at 60°C; ii) Freeze-drying using a Heto Power Dry LL3000 Freeze Dryer; and, iii) Water-ethanol exchange done by gently stirring the samples at 10°C on a large amount of ethanol (1 L), ethanol-filled samples being then placed in an oven at 60 °C. The total duration of the drying step was 168 hours in every case.

4.4.5 Solvent-extraction of encapsulated butyl stearate

Butyl stearate was extracted from water-dried monoliths by n-butyl acetate using a Soxhlet extractor for 3 days. Evaporation of n-butyl acetate was then performed at 60 °C at atmospheric pressure in an oven to give dried pullulan matrices.

4.4.6 Scanning Electronic Microscopy

Morphology of fully dried monoliths was analyzed by Scanning Electron Microscopy (SEM) using a Hitachi TM-1000 microscope (Tokyo, Japan) by mounting a piece of sample of approximately 36 mm^2 and 2 mm in height on a carbon tab to ensure good conductivity. To estimate the cell and window diameters, manual measurements were done over a population of 30 units from the 100x and 300x micrographs, respectively.

4.4.7 Mercury Intrusion Porosimetry

Porosity of fully dried monoliths was estimated by Mercury Intrusion Porosimetry (MIP) analysis using a Micromeritics Autopore IV 9500 porosimeter (Norcross, GA, USA), with the parameters: contact angle of 130°, Hg surface tension of 485 $mN \cdot m^{-1}$, maximum intrusion pressure of 124 MPa.

4.4.8 Differential Scanning Calorimetric

Thermal analysis was conducted using a µDSC3 EVO (SETARAM). Dried-monolith samples of 60 to 250 mg were encapsulated in a Hastelloy C cell. Modulated DSC measurements were carried out in the temperature range from 5 to 35 °C. The test was carried out at a heating and cooling rate of 0.2 $K.min^{-1}$.

4.4.9 Mechanical tests

Uniaxial compressive loadings have been performed using a universal testing machine Inspekt 50 (Hegewald & Peschke, Nosse, Germany). A load cell of 5 kN has been used to get force and to calculate nominal stress. Temperature range was fixed between 20 and 23 ° C and controlled by a thermocouple. Nominal strain was calculated thanks to the stroke, considering the rigidity negligible compared to the one of the specimens. The compression-release programme was as follows :Velocity = 10.8 mm/min (strain rate ~0.01. s^{-1}) Method : 1) compression 5% (displacement ~1 mm), 2) unloading to 0 N, 3) compression 10% (displacement ~2 mm), 4) unloading to 0 N, 5) compression 30% (displacement ~6 mm), 6) unloading to 0 N, 7) compression 60% (displacement ~12 mm), 8) unloading to 0 N. A digital camera was positioned in front of the specimen to follow its deformation at a frequency of one frame *per* second. Dried monolith samples were cylindrically-shaped with a diameter of 18 mm and a height of 7 mm.

4.5 Results and discussions

4.5.1 Determination of optimal concentration of pullulan and butyl stearate weight fraction

Concentrations of pullulan and butyl stearate in emulsions (as continuous and internal phase, respectively), are the most prominent parameters of the formulation. Therefore, our first concern was to determine the optimal levels for these two values. Combining the addition in the dispersed phase of a hydrophobic surfactant such as Span-85 (HLB = 1.8) with the presence of a hydrophilic one (Tween-80, HLB = 15) in the strongly alkaline continuous phase was found to provide the best stabilization of the emulsion system [97, 98].

In the perspective of energy storage devices development, synthesis of materials with the highest concentration possible of encapsulated PCM is desirable. Relationship between pullulan concentration and PCM insertion ratio in the emulsions as well as the corresponding viscosities of the final emulsions are reported on **Table 4-1**. From these data, it clearly appears that the rapid increase of viscosity represents the main limit to the insertion of PCM. Therefore, the pullulan content of the continuous phase is limited to 24%w/w and the insertion of PCM into the emulsion to about 30-35%.

Table 4-1. Relationship between pullulan concentration and PCM insertion ratio in emulsions

Emulsion	Concentration of pullulan in aqueous phase (% w/w)	Maximum quantity of PCM inserted in emulsion (% w/w)	Viscosity of the emulsion measured at 30 °C (kPa.s)
E16	16	36	17
E20	20	33	22
E24	24	30	24
E27	27	25	> 24[a]

[a]Viscosity over the limit of measurement of the instrument

4.5.2 Synthesis of polyLIPE by crosslinking with STMP

Sodium trimetaphosphate (STMP) was selected as crosslinking agent to convert emulsions into pullulan monoliths encapsulating butyl stearate. Crosslinking of polysaccharides with STMP has already being reported in numerous papers [90, 91]. Its mechanism has been thoroughly studied using ^{31}P-NMR [92]. Briefly, the first step of the reaction is the grafting of sodium tripolyphosphate moieties ($STPP_g$) on the polysaccharide (i.e. pullulan) through the STMP ring opening on basic conditions (**Figure 4-1**, step 2). The stable sodium tripolyphosphate (STPP) by-product is simultaneously produced in these conditions (**Figure 4-1**, step 2). $STPP_g$ is then attacked by the base on the α-phosphate inducing a crosslinking with a second polysaccharide chain through a phosphate diester P_c (**Figure 4-1**, step 3).

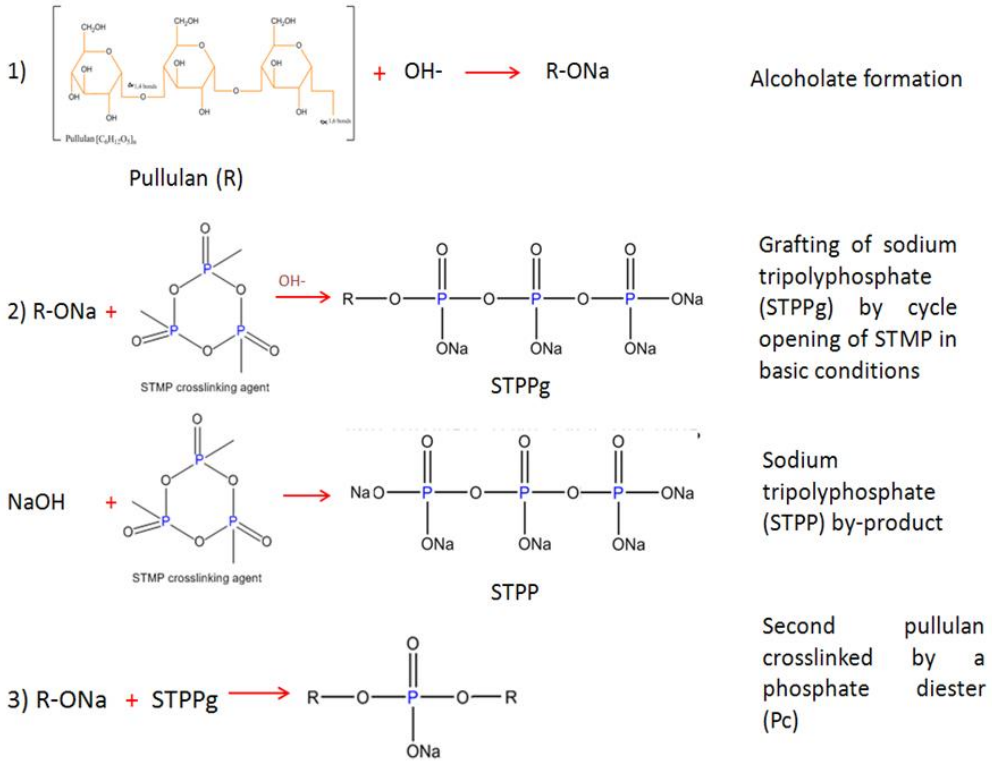

Figure 4-1. Schematic reaction crosslinking of pullulan with STMP in alkaline media (NaOH) .

The pH of the medium plays a major role on the efficiency of the crosslinking. A pH value in the range of 10 - 13.5 is the best choice for the reduction of by-products formation.

In this work, the amount of crosslinking agent was set at 17% w/w relative to the pullulan amount in order to assure the maximum yield of crosslinking without destabilizing the emulsion due to negative charges that come with the reaction.

Self-standing, white monoliths M16, M20 and M24, presenting a regular cylindrical shape ($Ø_{in}$ = 35 mm, h = 45 mm) were synthesized from their corresponding precursor emulsions (**Figure 4-2**). The ratio of butyl stearate (internal phase) in the composite being around 30-35% w/w, these materials may be called polyLIPE [92].

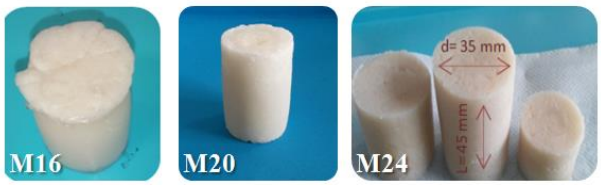

Figure 4-2. Optical photography of the different pullulan monoliths filled with butyl stearate before drying.

Monoliths M16, M20 and M24 dimensions were: d= 35 mm, L= 45 mm.

Monoliths M16 and M20, prepared with low levels of pullulan, present some shrinkage at mid-height of the cylinder; on the contrary, the monolith M24, having the highest level of pullulan, reproduces exactly the internal shape of the original mold.

4.5.3 Water removal from butyl stearate-encapsulated pullulan monoliths

As-synthesized composite monoliths contained a large amount of water (35% w/w). In view of future applications in heat storage and for the good aging of the material, it would be advantageous to remove this water as much as possible without leakage of the encapsulated PCM. Different approaches were investigated in this view. Details of these methods are reported in the Material and Methods section. The effect of the water removal method on the visual aspect of the monoliths is shown in **Figure 4-3**.

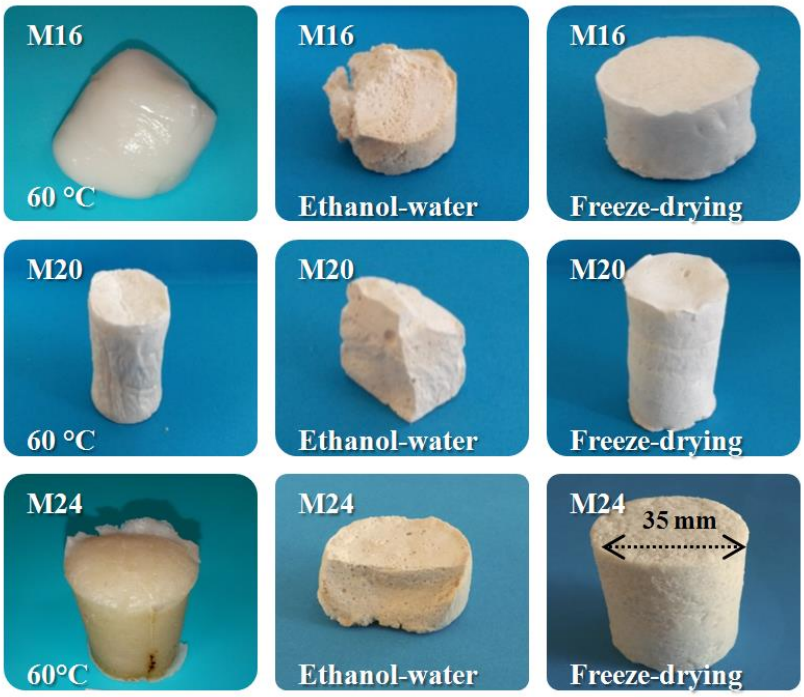

Figure 4-3. Optical photography of dried monoliths M16, M20 and M24 after water removal according to the three different methods employed.

After direct removal of the water by drying in an oven at atmospheric pressure at 60 ° C (Fig. 3, first column), all the samples present significant cracks and shrinkage. The ethanol-water exchange prior to drying in the oven (Fig. 3, second column), do not improve significantly the visual aspect of the monoliths obtained after removal of the solvents with always significant shrinkage of their initial shape. When freeze-drying is used (**Figure 4-3**, third column), the monoliths M16 and M20 present deformations of their initial shape, while M24 retains, after water removal, its initial cylindrical structure. Thus, the formulation of the monolith M24 and the use of freeze drying seem to be the best combination for the encapsulation of butyl stearate onto a pullulan matrix.

It is of prime interest to control that the maximum amount of water is removed from the pullulan matrix without reducing the amount of encapsulated butyl stearate. Weight loss evolutions were then conducted on monolith M24 using the different drying methods tested in this work. Results are reported in **Figure 4-4.**

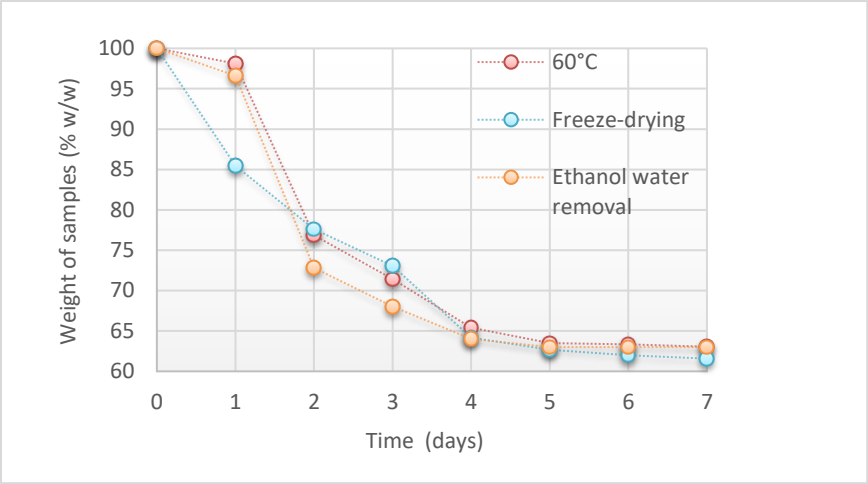

Figure 4-4. Comparative efficiency of different drying methods tested on monolith M24: a) direct evaporation at 60 °C, b) freeze drying and, c) water-ethanol exchange followed by drying at 60°C.

All drying methods tested allowed to reach a weight loss plateau corresponding to the removal of about 35% w/w of the initial monolith weight. Most of the loss occurs during the first two days of drying. This result indicates that, whatever the drying method employed, all the water was removed from monolith M24 without altering significantly the amount of butyl stearate encapsulated.

4.5.4 *Solvent extraction from pullulan polyLIPE*

Butyl stearate used as the dispersed phase for the preparation of the different composites was extracted to obtain fully dried emulsion-templated pullulan matrices for morphological analysis. Visual observation of dried samples indicates a good conservation of the cylindrical shape after extraction (**Figure 4-5**).

Figure 4-5. Optical photography of fully dried monolith M24 after PCM-extraction.

4.5.5 SEM analysis

Scanning electron microscopy (SEM) analyses of fully dried monoliths were conducted. In the case of samples M16 and M20, it can be seen that fibers of pullulan crosslinked by STMP forms a thin and heterogeneous open-cell network. (**Figure 4-6**, upper line).

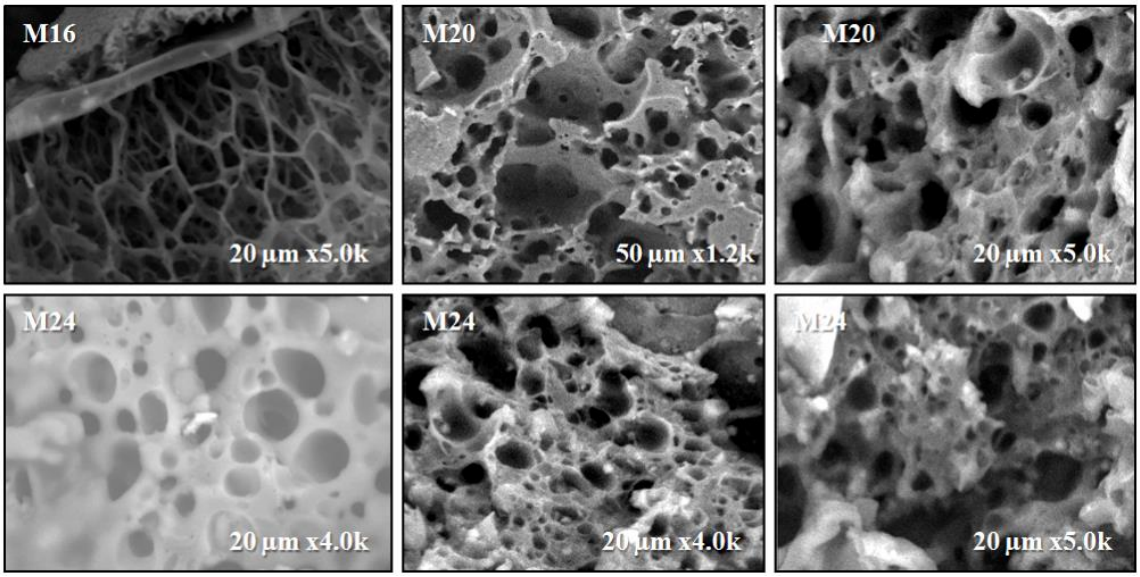

Figure 4-6. Porous pullulan structure (MEB) of PCM-emptied monoliths M16, M20 and M24.

An increase in pullulan concentration gradually increases the fibers diameter leading to a denser network after crosslinking, as it is observed for monolith M24 (Figure 4-6, lower line). Its structure appears thicker with more homogeneous pore interconnections. These differences in structure could be attributed to the difference in pullulan concentration as already reported in the literature [35-36].These observations confirm that the highly alkaline medium used during emulsification is necessary to obtain an effective STMP crosslinking of pullulan chains.

4.5.6 Porosity measurement

Mercury intrusion porosimetry (MIP) and helium pycnometry (HePyc) were used to determine the porosity and densities of fully dried pullulan matrices (**Table 4-2**).

Table 4-2. Porosity skeletal and bulk densities of pullulan matrices.

Sample	Skeletal density ($g.cm^{-3}$)[a]	Skeletal density ($g.cm^{-3}$)[b]	Porosity (%)[a]	Bulk density ($g.cm^{-3}$)[a]
M16	1.52 ± 0.05	1.54 ± 0.01	47 ± 1	0.81 ± 0.05
M20	1.55 ±0.05	1.56 ± 0.01	46 ± 1	0.84 ± 0.05
M24	1.66 ±0.05	1.62 ± 0.01	44 ± 1	0.88 ± 0.05

[a] Determined by Mercury Intrusion Porosimetry, b Determined by Helium Pycnometry.

Data presented in **Table 4-2** indicate an excellent correlation between the skeletal density values determined by MIP and HePyc. These relatively high values for crosslinked pullulan can be explained, in part, by the presence of sodium ions. The porosity values of all polyLIPE are around 45%. This value is to be compared with the concentration of the initial emulsions (30% w / w). The difference can be attributed to the presence of air bubbles in the pullulan matrix caused by some foaming during emulsification. However, these high values indicate that the crosslinked pullulan network did not significantly collapse during the various solvent extraction steps. The apparent density values, determined from the above data, appear relatively high because of the high value of the skeletal density of the pullulan network. Finally, it is clear that the content of pullulan in the continuous phase of the precursor emulsion has almost no influence on the porosity of the final materials.

Interconnections-size distribution in monoliths M24 was also examined by MIP. Samples dried by the three different methods discussed above were investigated. Results are reported in **Figure 4-7**.

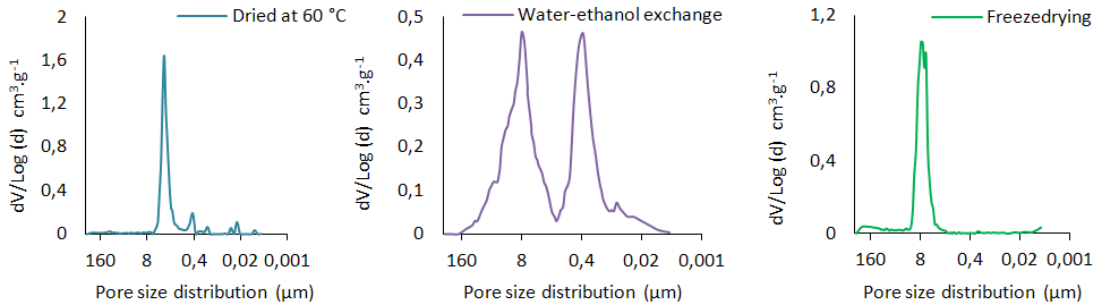

Figure 4-7. Interconnections-size distribution of monolith M24 dried by: a) direct evaporation at 60 °C; b) water-ethanol exchange followed by drying at 60 °C and; c) freeze drying.

Different interconnections-size distributions are observed according to the drying method used. Mean interconnections-size are centered at 2.19 µm and 8 µm for samples dried at 60 °C and freeze-dried, respectively (**Figure 4-7**, a and c). A bimodal mean interconnections-size distribution centered at 8 µm and 0.4 µm is observed for samples dried by water-ethanol exchange (**Figure 4-7**, b). A gentle drying process under low temperatures (freeze-drying), prevent the collapse of the porous network and allows to maintain higher mean interconnections-size (8 µm) than a harsher process such as direct drying at 60 °C (2 µm).

4.5.7 Differential scanning calorimetry (DSC) analysis

DSC thermograms were preformed between 15°C and 35°C on: a) pure butyl stearate, b) fully dried pullulan matrix M24 and, c) pullulan dried monoliths M24 encapsulating butyl stearate (30 % w/w). Endothermic (melting point) and exothermic peaks (solidification) were obtained for experiments. Results are reported in **Figure 4-8**.

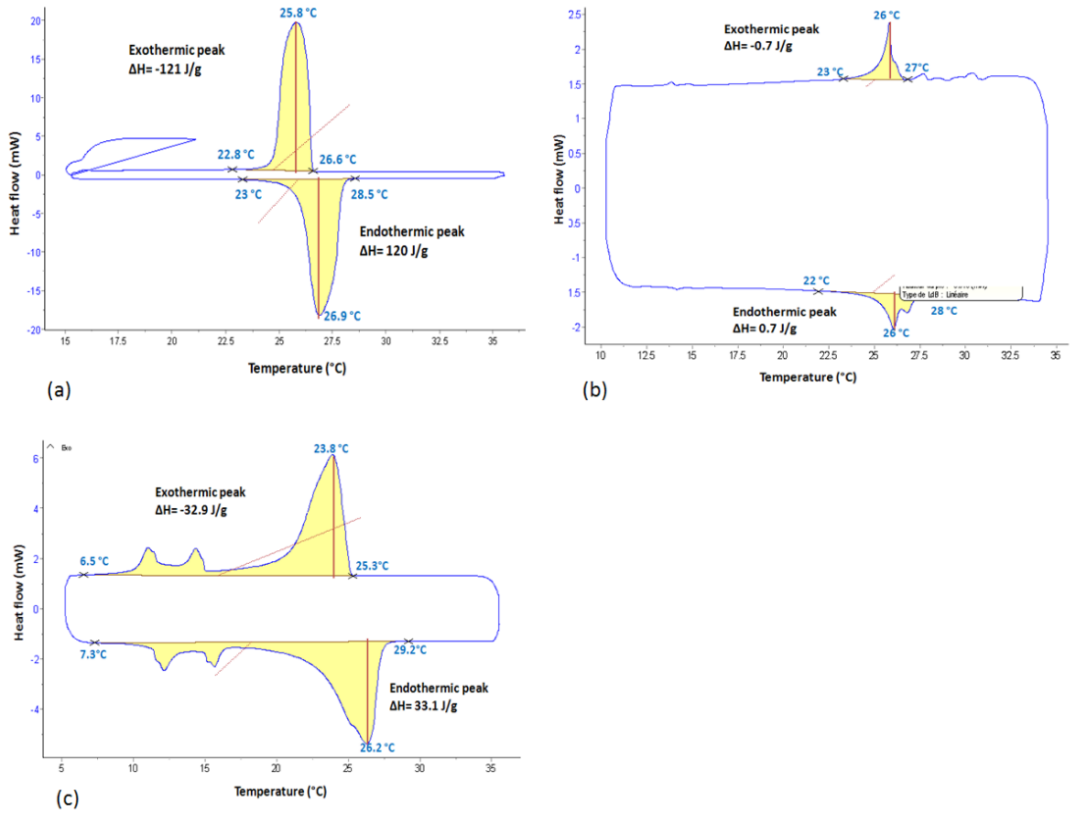

Figure 4-8. DSC curves of: a) pure butyl stearate, b) pullulan matrix, c) pullulan matrix encapsulating butyl stearate (30% w/w).

DSC curve of pure butyl stearate (**Figure 4-8**.a) indicates an endothermic (melting point) at 26.9°C and an exothermic peak (solidification point) at 25.8°C. The enthalpie of fusion is ΔH = 120 $J.g^{-1}$. These values are consistent with the data of the literature [99,100]. DSC curve of pullulan matrix (**Figure 4-8**-b) indicates a weak endothermic peak at 26 °C and another weak exothermic peak at 26 °C. The enthalpie of fusion is ΔH = 0.7 $J.g^{-1}$. These data are probably due to some butyl stearate remaining after soxhlet treatment of the monolith. DSC curve of pullulan matrix encapsulating butyl stearate (**Figure 4-8**-c) indicates an endothermic peak at 26.2 °C and an exothermic peak at 23.8 °C. The enthalpie of fusion is ΔH = 33 $J.g^{-1}$. The phase change temperatures are close from that of pure butyl stearate, the enthalpie of fusion value correspond to 27.4 % of the value for pure butyl stearate. This result is consistent with an encapsulation level of 30 % w/w.

Solidification and melting point of butyl stearate are not significantly affected by its encapsulation. However, phase change DSC peaks of butyl stearate become wider after encapsulation (**Figure 4-8**-c), with the apparition of secondary peaks between 10 °C and 15 °C.

This phenomenon can be explained by the presence of pullulan matrix. During the heating-cooling cycle, polymer changes from a vitreous to a viscous or rubbery state and vice versa, this transition induces to poorly define thermal exchanges giving a rise to small and large peaks.

4.5.8 Mechanical tests

A uniaxial loading-unloading compression test of the encapsulated butyl stearate dried material (sample M24), was performed at temperature range of 20 and 23 °C (**Figure 4-9**).

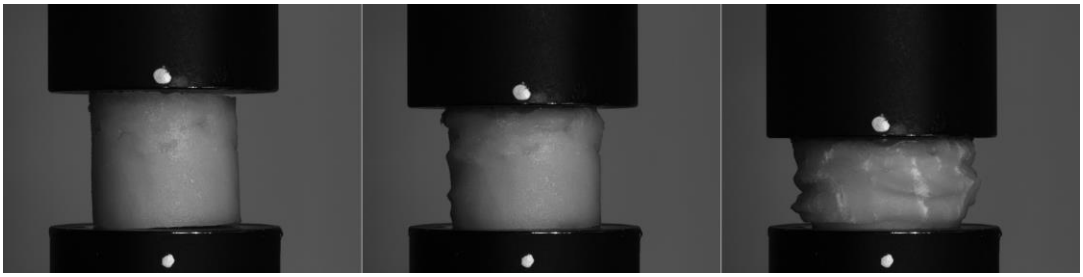

Figure 4-9. Evolution of the PCM-encapsulated pullulan polyLIPE sample M24 during uniaxial compression for a nominal strain of 0% (left), 10% (middle), and 30% (right).

During the first 10% of the deformation, the sample retains its shape with the exception of a few small swellings. Therefore, a modulus of elasticity can be calculated [101]. An average value for the Young's modulus of E = 15 ± 7 MPa could be evaluated, however, a large diffusion of the results is observed between the samples. Beyond this limit of deformation, the sample is not only subjected to uniaxial compression: a certain tension appears on the external surface. The encapsulated liquid (butyl stearate) begins to seep on the walls. When 30% of the deformation is reached, some vertical defects occur in the sample, which means that the tension on the outer surface is sufficient for the rupture. More MCP is exfiltrated. This experiment shows the fragile behavior of the material, however, a certain ability to maintain the PCM inside the matrix until fairly large deformations is also highlighted.

Additionally, the response of the material to mechanical compression was filmed and showed in a video included in this document. It can be observed the initial formation of fissures in material walls until a complete deformation occurred.

4.6 Conclusions

Pullulan polyLIPEs encapsulating butyl stearate has been synthesized by emulsion- templating, followed by crosslinking and drying process. The concentration of pullulan in the continuous phase is the limiting parameter because very viscous emulsions are rapidly reached during the slow insertion of butyl stearate. Stable emulsions containing 30% w / w in the internal phase have thus been obtained (LIPE). A highly alkaline media for continuous phase is a fundamental parameter to control in order to obtain an effective crosslinking reaction of pullulan by the STMP. The process used to remove water from the continuous phase of monoliths has a direct impact on their morphology. Freeze-drying is the best method: it provides gentle drying conditions to protect the pullulan network from physical damage caused by too abrupt extraction of water. DSC analysis has shown that butyl stearate thus encapsulated does not lose any of its thermal characteristics of Phase Change Material usable near ambient temperature.
Therefore, emulsion-templating appears as an attractive way to Phase Change Materials encapsulation.

5 Emulsion-templated Black Liquor monoliths as Phase Change Materials encapsulating matrices

5.1 Introduction

Energy efficiency technologies are a prime objective for the sustainable development at a regional, national and international level since its positive impact in the environment and global markets is increasing within time [102]. The construction sector is a great opportunity area for the applications of these technologies considering that forty percent of the produced primary energy in the U.S. and E.U. is consumed by commercial buildings and domestic residences [103], while studies indicate a maintain increase of the worldwide energy demand coming from these sectors for the coming years (according to studies done in 2007 and 2016 considering the population growth over the past decades [102-104].

Among energy efficiency technologies, latent heat storage systems through phase change materials (PCMs) have a great potential in reducing cooling loads in buildings contributing to thermal comfort, especially because of their interesting properties such as a high-energy storage density and an isothermal storage process. Their wide range of melt and solidify temperatures, make them attractive in many application fields (like in heat pumps, solar engineering and spacecraft thermal control) [105] . Moreover, research concerning their utilization in buildings has increased during the past decade [105-107] owed to promising obtained results; simulations studies in a commercial building in California, U.S. with encapsulated paraffin wax embedded in wallboards done by [103] showed a clear reduction of temperature peaks leading to energy savings and pointed the need of more studies regarding this topic; while [108] indicated a reduction in cooling loads of about 30 % in the case of an house-attic containing PCM-enhanced insulation wall.

The encapsulation of phase change materials for their utilization in thermal energy storage is a well-known technique, research done in the year 1987 [109] indicates the use of polyethylene glycol as a PCM encapsulated in a condensation polymeric shell for this application, furthermore studies in 2017 proposed a more sophisticated method for the utilization of this PCM [110], finally in previous research we develop a pullulan network for the same purpose. In general, the PCM is coated with a reactive monomer (for example ethylene diamine) or with a

polymeric material, then a crosslinker agent is added (such as isocyanate) to form condensation polymeric shells. The best coating material would be one with enough mechanical strength, thermal stability and compatibility with the PCM [111]. The encapsulated phase change material has no significant change of its heat of fusion due to its encapsulation while it can be implemented directly in wall covering materials being part of the building structure even for light weight buildings. Encapsulation creates PCM containers that protect them from the external environment [111] .

Among the wide available PCMs, butyl stearate has interesting properties due to its phase change temperature and relatively high heat storage capacity; therefore, it can be used as an effective thermo-regulating material at ambient temperature in insulating materials such as foams after being encapsulated or as an additive in indoor and outdoor coating [111].

Finally, the synthesis of materials by emulsion-template polymerization has numerous advantages (light weight, unique mechanical, acoustic and thermal properties, large surface to volume ratios, etc.) [112] and it has been widely utilized for the preparation of porous materials [113-117] showing interesting results regarding material mechanical properties, porosity and thermal stability comparable to commercial materials like polyurethane foams [118] .

Kraft paper waste black liquor has been reported as an interesting coating polymer to synthesized resistant materials though regeneration of the lignin and hemicelluloses fibers contained in it by chemical crosslinking with Epichlorohydrin [119-120]. It has been seen that the resulting crosslinked material has good mechanical properties and temperature resistance. Epichlorohydrin has been widely use in the synthesis of polymeric bases for different applications (manufacture of solvents, surfactants, solvents, surface active agents, dyestuff intermediate, etc). Nevertheless, studies have pointed it as potentially hazardous to humans because of its clastogenic action in experimental systems and have been classify as probably carcinogenic to humans by the Environmental Protection Agency [121-122] even though more studies are necessary to determine its toxicological effects. Sodium trimetaphosphate (STMP) in the contrary is a safe and non-toxic crosslinking agent legally use in the USA for having no effects on humans, commonly utilized in food starches, polysaccharides matrixes and even konjac glucomannan for colon targeting drug delivery applications, it leads to consistent pastes with good resistance to heat, acid and shearing [123-125] . The crosslinking reaction occurs through

the hydroxyl groups of the polysaccharide and led to ester linkages, this property is an important advantage since it leaves the polymer carboxylic groups free for further modification, a reaction mechanism has been proposed as a result of studies made by high resolution NMR spectroscopy [126] . In a first step, sodium tripolyphosphate is grafted on a polysaccharide. The extremity of tripolyphosphate reacts with a second polysaccharide alcoholate to produce a crosslinked phosphate network. Tripolyphosphate could lead through hydrolysis to a monophosphate on the chain.

Valorization of lignin and hemicelluloses contained in black liquor to synthetize monoliths with encapsulated phase change materials through emulsion-templating is proposed in this research, with the utilization of a non-toxic crosslinking agent STMP.

5.2 Materials and methods

5.2.1 Materials

Crude Kraft black liquor collected from a local paper mill (Smurfit Kappa, Cellulose du Pin Kraft paper mill, Biganos, France) was used as received. Butyl stearate, Epichlorohydrin, Kolliphor® EL, sodium trimetaphosphate (STMP) and ethanol were purchased from Sigma-Aldrich and used as received. N-butyl acetate 99% was provided by Alfa Aesar and used without further purification. The as-received Kraft black liquor comes as a viscous, black liquid. Its major physic-chemical properties are: dynamic viscosity μ = 7000 mPa s at 23 °C; pH = 14 (solution diluted to 5 % dry matter); density ρ = 1.3 g mL^{-1}; dry matter amount = 50 wt%.

5.2.2 Methodology

5.2.2.1 Preparation of butyl stearate-in-Black liquor emulsions

In the following, emulsions have been abbreviated E_xT_y, where x represents the weight percent of surfactant in the continuous phase, T the nature of the crosslinking agent (STMP) and y the weight percent of crosslinking agent employed. For example, E_{20} T_{15} refers to an emulsion formulated with 20% w/w of surfactant in the continuous phase and 15% w/w of STMP.

$M_{20}T_{15}$ refers to the corresponding crosslinked monolith.

5.2.2.2 Emulsions and materials prepared with different amounts of surfactant.

Oil-in-Water (O/W) emulsions containing different concentrations of surfactant in the continuous phase were synthesized as follows: a solution of black liquor (50 % of dry matter; 150 g), was placed in cylindrical, round-bottomed reactors thermostated at 50 °C equipped with a rod fitted with axial/radial two blades impellers connected to overhead stirrer motors. Different amounts of Kolliphor® EL (5, 10, 15 and 20 %w/w, vs. black liquor solution) were then added to each stirred mixture until complete homogenisation. The solutions were then homogenized under stirring during 1 hour at approximately 450 rpm. Subsequently, the dispersed phase composed of butyl stearate was added at 30°C using a syringe pump at a rate of 1 $mL \cdot min^{-1}$ until no more was possible to be inserted, reaching a concentration of 30 % w/w over the total emulsion. Crosslinking was performed by rapid addition of STMP (20 %w/w vs. black liquor) to the stirred emulsions at 50°C and homogenization continued for 3 hours. The resulting emulsions were placed in closed PTFE cylindrical moulds ($Ø_{in}$ = 35 mm, h = 45 mm) and stored in an oven at 60 °C for 3 days. As-synthesized wet monoliths were obtained after careful removal from the moulds. Samples M_6S_{20}, $M_{10}S_{20}$, $M_{15}S_{20}$ and $M_{20}S_{20}$ were obtained.

5.2.2.3 Emulsions and materials prepared with different crosslinking agent

Emulsions of the E_{20} series, formulated with (20 %w/w, vs. black liquor solution) of surfactant were crosslinked similarly as above with different concentrations of STMP (5, 10, 13, 15 and 20 %w/w vs. black liquor solution). Samples: $M_{20}S_5$, $M_{20}S_{10}$, $M_{20}S_{13}$, $M_{20}S_{15}$, and $M_{20}S_{20}$ were obtained.

5.2.2.4 Solvent-extraction of encapsulated butyl stearate

Butyl stearate was extracted from water-dried monoliths by n-butyl acetate using a soxhlet extractor for 3 days. Evaporation of n-butyl acetate was then performed at 60 °C at atmospheric pressure in an oven to give dried matrices.

5.2.2.5 Scanning Electronic Microscopy

Morphology of fully dried monoliths was analyzed by Scanning Electron Microscopy (SEM) using a Hitachi TM-1000 microscope (Tokyo, Japan) by mounting a piece of sample of approximately 36 mm^2 and 2 mm in height on a carbon tab to ensure good conductivity. To estimate the cell and window diameters, manual measurements were done over a population of 30 units from the 100x and 300x micrographs, respectively.

5.2.2.6 Mercury Intrusion Porosimetry

Porosity of fully dried monoliths was estimated by Mercury Intrusion Porosimetry (MIP) analysis using a Micromeritics Autopore IV 9500 porosimeter (Norcross, GA, USA), with the parameters: contact angle of 130°, Hg surface tension of 485 $mN \cdot m^{-1}$, maximum intrusion pressure of 124 MPa.

5.2.2.7 Differential Scanning Calorimetric

Thermal analysis was conducted using a µDSC3 EVO (SETARAM). Dried-monolith samples of 60 to 250 mg were encapsulated in a Hastelloy C cell. Modulated DSC measurements were carried out in the temperature range from 5 to 40 °C. The test was carried out at a heating and cooling rate of 0.2 $K.min^{-1}$.

5.3 Results and discussions

5.3.1 Crosslinking of lignin and hemicelluloses in Black liquor monoliths

PCM was encapsulated in a solid, un-soluble network formed by crosslinked fibers of lignin and hemicelluloses contained in a black liquor matrix (concentrated at 50 % w/w of dry matter). The network was crosslinked with STMP through phosphate ester covalent bonds in the phenolic groups in the case of lignin, and in the hydroxyl groups in the case of hemicellulose. The concentration of STMP agent was a fundamental parameter to regenerate the fibers and formed a suitable network for encapsulation, therefore crosslinked black liquor monoliths were synthetized at different STMP yields and the obtention of phosphate ester bonds as the principal reaction product was studied. Their formulation is shown in **Table 5-1** and their physical appearance in **Figure 5-1**.

Table 5-1. Monoliths composition

Samples	$M_{20}S_5$	$M_{20}S_{10}$	$M_{20}S_{13}$	$M_{20}S_{15}$	$M_{20}S_{20}$
Black liquor-based composition	150 g in every case (at 50 % of dry matter)				
Kolliphor EL®	20 % w/w (in relation to black liquor)				
STMP (% w/w in relation to black liquor)	5	10	13	15	20
Dispersed phase PCM: butyl stearate	30 % w/w (in every case)				

Black liquor is composed mainly of lignin and hemicelluloses fragments (70 % w/w of its solid matter) dissolved in an alkaline aqueous solution (pH ≈ 14 approximately) containing salts of NaOH, Na_2S and Na_2CO_3 [114-119]. These last components are the responsible of its high alkalinity, property that facilities its crosslinking with STMP agent without the necessity to modify its pH at any time during the crosslinking reaction since pH becomes a primordial parameter, as was determined by [125-126]. Black liquor aqueous phase was concentrated up to 50 % (w/w) of dry matter to obtain an enough dense network in terms of lignin and hemicellulose moieties and yet with a PCM insertion of 30 % (w/w) as dispersed phase under a sustainable alkaline pH value through crosslinking reaction. Indeed, higher concentrated black liquor

solutions (55 % and 60 % w/w) lead to the obtention of more viscous aqueous phases. Consequently, the dispersed phase was inserted in a more compacted system; therefore, higher stirring rates and time were necessary to obtain a homogeneous emulsion. Thereby water evaporated more rapidity leading to emulsion destabilization due to a phase separation of the surfactant with emulsion overwhipping. In contrast, at low concentrated black liquor solutions (<40 %), the obtained low-density system was not suitable for PCM encapsulation. The concentration chose, and our observations are in accordance with [113, 119, 120].

Nonionic surfactant Kolliphor El in combination with inorganic salts present in black liquor enhance stability of the system without causing precipitation, it contributed to a fine PCM dispersion and thereby improved it absorption and distribution through the bulk. As a result, O/W emulsions were obtained containing different concentrations of Kolliphor El. Subsequently to study the surfactant effect over PCM distribution, hard solid monoliths were obtained at different surfactant concentration and characterized by scanning electron microscopy and mercury intrusion porosimetry (results in section 5.3.3).

PCM butyl stearate was of interest because of its high latent heat of fusion, superior to most organic PCMs [127, 128] and its melting temperature range (between 26 and 29 °C) [129] that allows its utilization for future applications in building thermal insulation.

Self-standing wet black liquor monoliths $M_{20}S_5$, $M_{20}S_{10}$, $M_{20}S_{13}$, $M_{20}S_{15}$ and $M_{20}S_{20}$ presented a regular cylindrical shape as shown in **Figure 5-1**, with a butyl stearate ratio (dispersed phase) of 30 % (w/w).

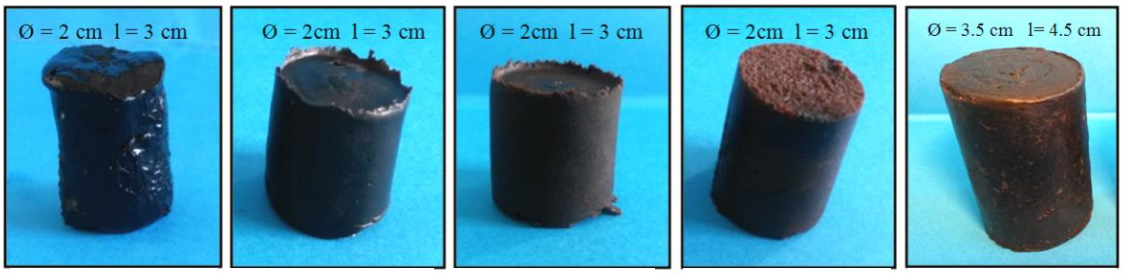

Figure 5-1. Synthesized monoliths at 5, 10, 13, 15 and 20 % (w/w) in relation to black liquor concentration in the aqueous phase.

Synthesized wet monoliths had significant changes regarding their surface-texture from smooth and shiny to rough and opaque along with a harder and better-defined body-structure

comparable to the given mould-shape dimensions (diameter Ø = 2 and 3.5 cm; height 3 and 4.5 cm), as a result of crosslinking-optimization with STMP. Moreover; their dark-brown color was similarly to concentrated black liquor solutions.

Drying was optimized through freeze drying removing a maximum of 10 % of water in 5 days without sample damage in any case (**Figure 5-2**.a), whereas via temperature at 60 and 80°C the quantity removed varied between 20 and 30 % in the same given time along with sample shrinkage located in the middle body part (**Figure 5-2**.b) and fractures generated over its surface. These defects might be responsible for the loss of reticulated water with a higher change in weight.

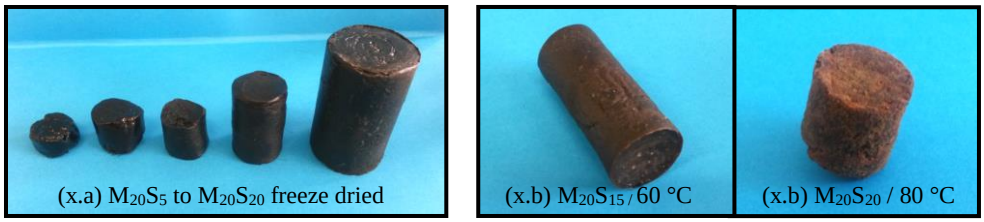

Figure 5-2. Monoliths after (x.a) 5 days freeze drying and (x.b) dried at 60 and 80 °C for 5 days.

Additionally, temperature dried samples presented a slight color changed; while those freeze-dried remain comparable to wet monoliths.

5.3.2 Crosslinking study

A strong insoluble network was created by the regeneration of polysaccharides contained in black liquor, allowing in this way the encapsulation of PCM. The regenerated network was crosslinked with STMP by the mechanism proposed in

Figure 5-3.

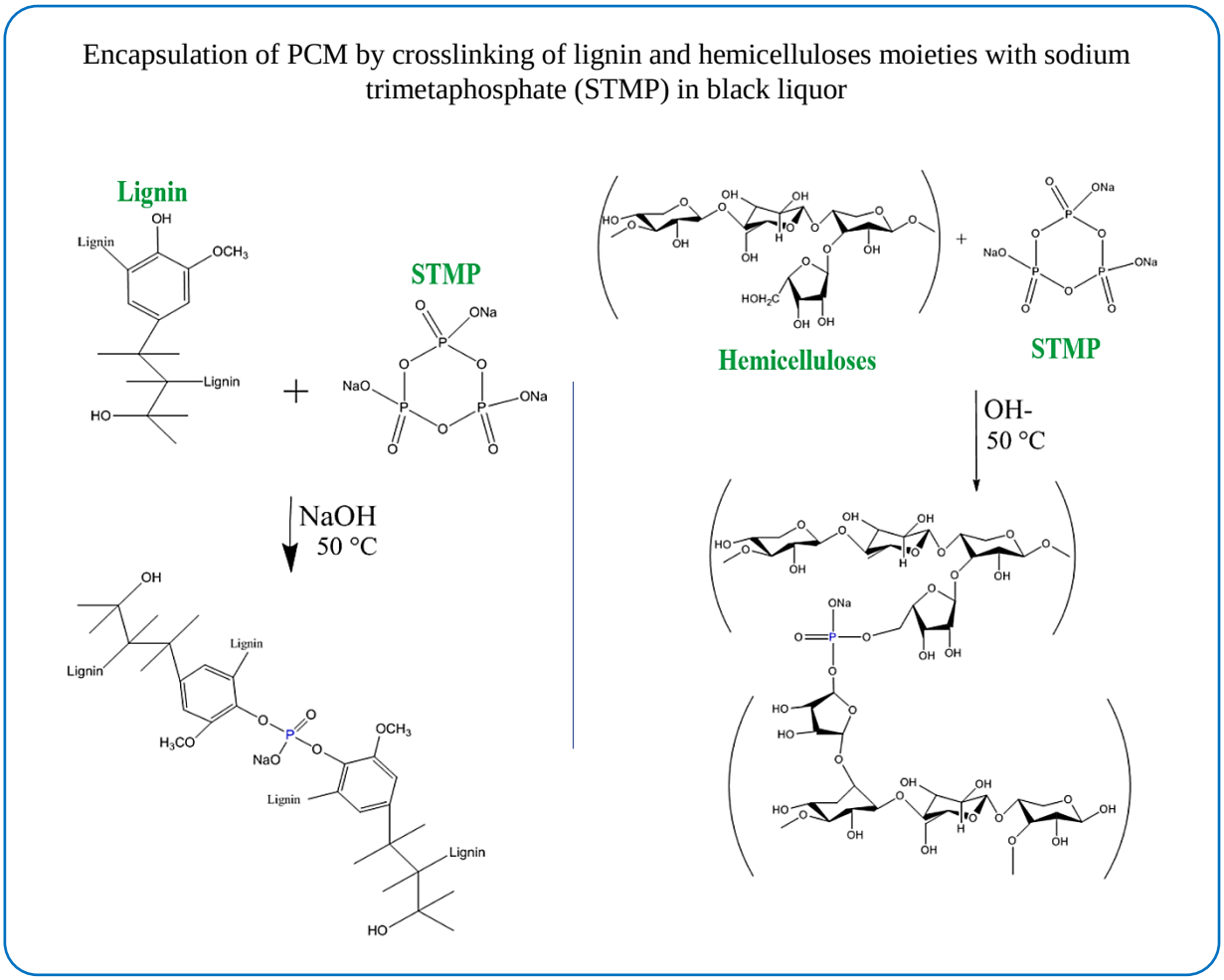

Figure 5-3. Production of phosphate diester (Pc) crosslinking product between: lignin and hemicelluloses with STMP agent.

The crosslinking reaction with epichlorohydrin has been widely studied [113, 115, 119] it requires an alkaline pH, introduces negative charges and creates covalent links of the ester type through the hydroxyl groups present in the polysaccharide. These characteristics occur also in the case of STMP; with the difference that this agent introduces phosphate groups in the ones the links between polysaccharides occurs as shown in **Figure 5-3** [119, 124, 126].

Crosslinking mechanism with STMP leads to the formation of phosphate diester (Pc) and phosphate monoesters (Pg). Pc has been identified in common STMP reaction products in the contrary of Pg, its presence has not always been observed or reported and It indicates: **1)** the total consumption of STMP; **2)** an aggressive alkaline media and; **3)** high polymer grafting yields plus the conversion of Pc into Pg. Nevertheless, reported synthesis conditions does not occur at a high enough alkaline pH to maintain its value through the whole grafting reaction, in consequence Pg is rarely produced or studied by chemical characterization. The objective of

this study was to identify this product along with Pc by solid NMR characterization and relate the presence of Pc and Pg with a better PCM encapsulation, because encapsulation depends of the grafting of lignin and hemicellulose fibers. Besides, it possible to obtain: sodium polyphosphates (STPPg), sodium tripolyphosphates (STPP) and sodium pyrophosphates grafted to a sugar, as indicated by [124, 125, 130]. Results are shown in **Figure 5-4**.

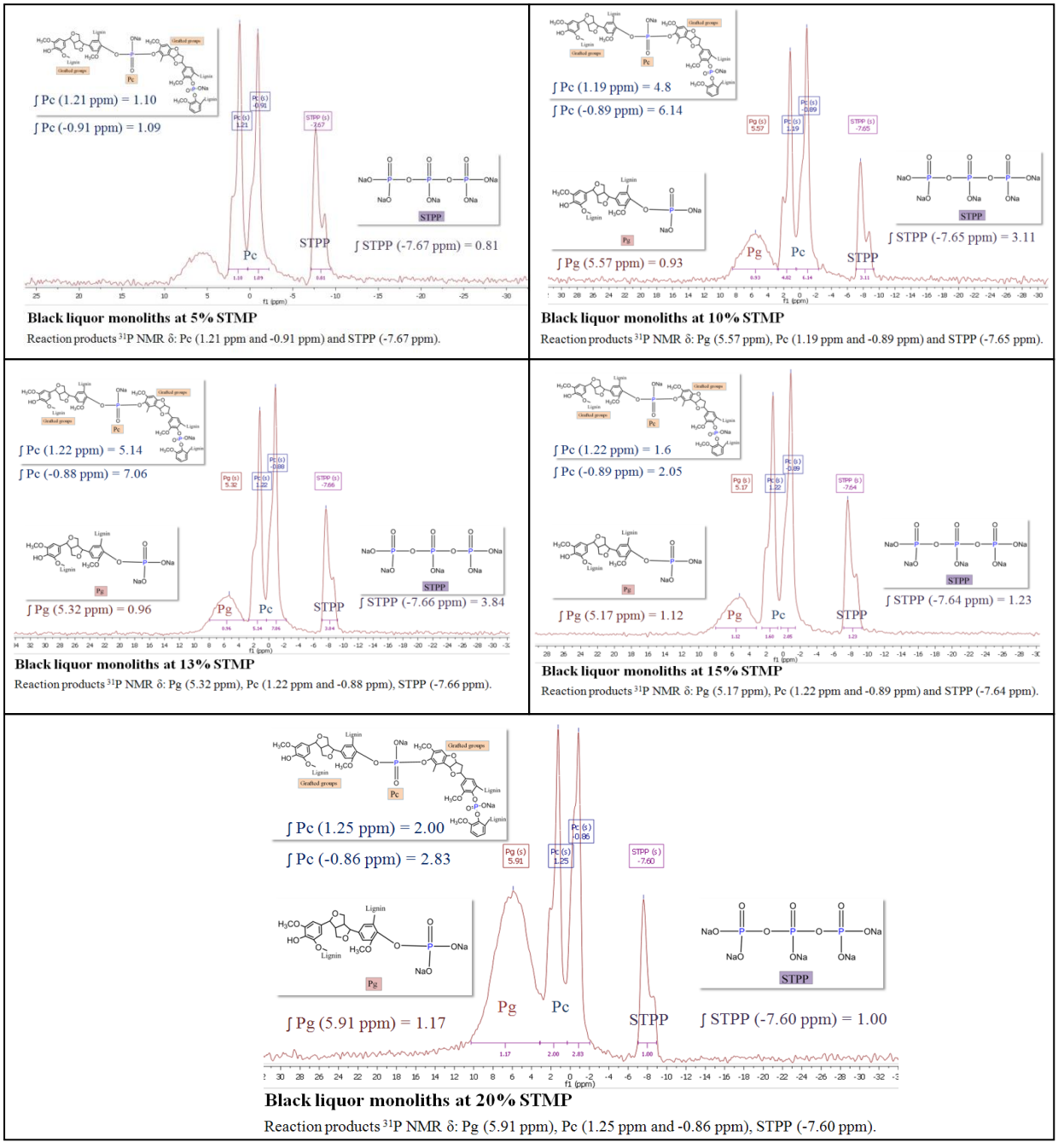

Figure 5-4. Solid state ^{31}P-NMR reaction products of black liquor based-monoliths crosslinked with 5, 10, 13, 15 and 20 % of STMP

It seems that STMP was immediately hydrolyzed giving Pc, Pg and STPP. In all samples grafting of lignin and hemicellulose occurred but the presence of Pg starting from $M_{20}S_{10}$ sample could indicate a better yield. The absence of intermediate species such as STPPg occurred because of the aggressive alkaline media. According to studies done by [123] this only could occur in the case of a very strong alkaline media when all STMP has been consumed and STPPg is consumed in favor of Pc as fast as it is produced. This observation is confirmed considering the alkalinity of black liquor and the absence of STMP signal in every case as observed in **Figure 5-4.**

Ratio between Pc and Pg was not the same as seen in **Table 5-2**.

Table 5-2. Ratio of the ∫ NMR spectra integral signal of Pc, Pg and STPP crosslinking products.

Sample	Integral value of NMR Pc and Pg signals		∫Pc : ∫Pg Ratio
	Pc	*Pg*	
$M_{20}S_5$	1.10	-	α
	1.09	-	α
$M_{20}S_{10}$	4.8	0.93	5
	6.14		7
$M_{20}S_{13}$	5.14	0.96	5
	7.06		7
$M_{20}S_{15}$	1.6	1.12	1
	2.05		2
$M_{20}S_{20}$	2.00	1.17	2
	2.83		2

[α] Pg not detected

For sample $M_{20}S_5$ there is no ratio since Pg was not detectable. For $M_{20}S_{10}$ and $M_{20}S_{13}$ it was the same possibly because the production of Pg did not increase, but for $M_{20}S_{15}$ and $M_{20}S_{20}$ it was lower with close values for both samples. This could indicate the stabilization of the production of Pc and Pg grafting products. The effect of different grafting yields over PCM-encapsulation was studied by DSC characterization in section 5.3.5.

5.3.3 SEM analysis

Monoliths M_5S_{20}, $M_{10}S_{20}$, $M_{15}S_{20}$ and $M_{20}S_{20}$ were synthesized at different concentrations of Kolliphor El to test its effect over pore size distribution, porosity and samples morphology, their composition is shown in **Table 5-3**.

Table 5-3. Monoliths composition

Samples	M_5S_{20}	$M_{10}S_{20}$	$M_{15}S_{20}$	$M_{20}S_{20}$
Black liquor-based composition	150 g for all (at 50 % of dry matter)			
Kolliphor EL®	5	10	15	20
STMP (% w/w in relation to black liquor)	20 % w/w (in relation to black liquor)			
Dispersed phase PCM: butyl stearate	30 % w/w (in every case)			

The efficacy of surfactant Kolliphor El as an emulsifier agent and to increase lignin solubilization was tested in PCM-black liquor emulsions, expecting to obtain a uniform pore size distribution with small sizes. Materials were synthesized with different concentrations of kolliphor (5, 10, 15 and 20 % w/w), after the removal of encapsulated PCM, scanning electron microscopy observations were done on samples. Obtained micrographs are shown in **Figure 5-5**.

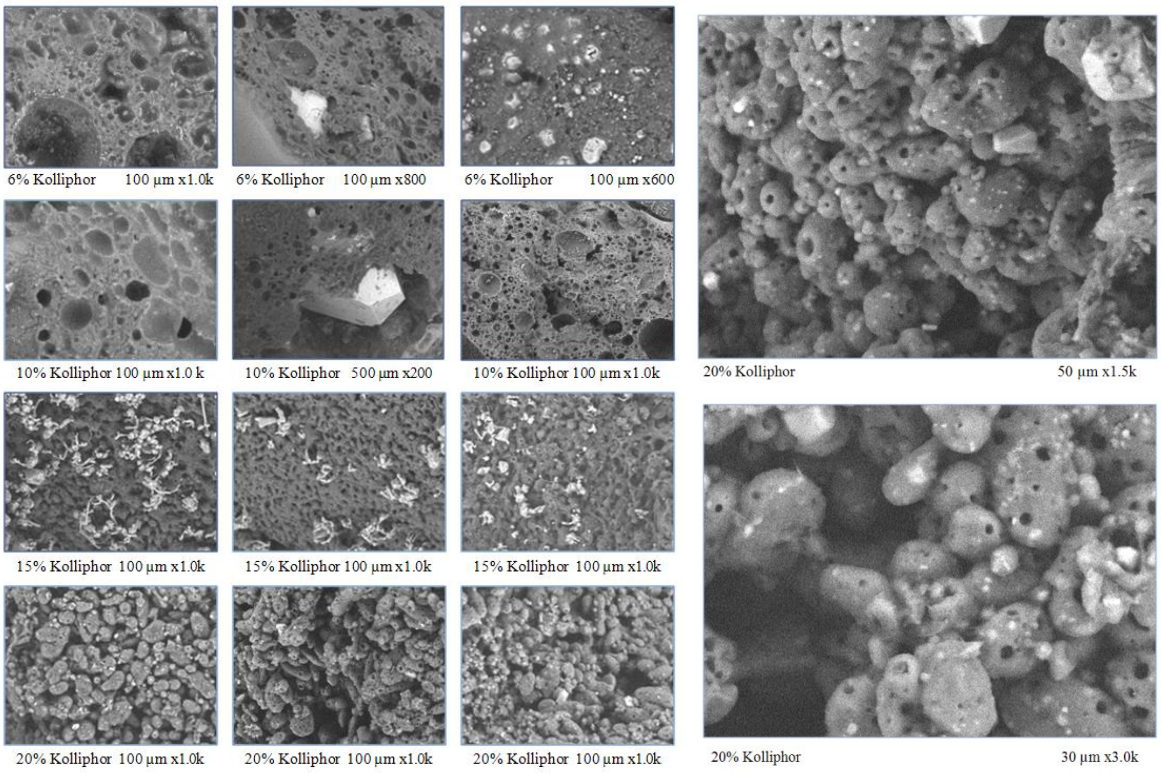

Figure 5-5. Scanning electron microscopy micrographs, crosslinked lignin and hemicelluloses in black liquor

Solubility of lignin and hemicelluloses contained in black liquor is improved at high surfactant concentrations. In samples M_5S_{20} and $M_{10}S_{20}$ SEM micrographs, crystals were seen entrapped in the matrix causing holes and ruptures, this effect was been identified in MIP measurements (**Figure 5-5**) as bigger pore size distribution. While the surfactant concentration increases, crystal salts are separated from the matrix obtaining smaller pore sizes. For sample $M_{15}S_{20}$ pore size uniformity increased, and salt crystals were found over the surface. Finally, for $M_{20}S_{20}$ pore size measured was the smallest and crystal salts were over the surface. These observations show the importance of surfactant concentration to control materials morphology and help to establish a concentration range.

PCM-encapsulation occurred in a crosslinked matrix like the one shown in **Figure 5-5**. The matrix with 20 % (w/w) of STMP is crosslinked as a series of granules joined to each other with empty channels between them, granules with small cavities where PCM used to be. Encapsulation does not occur like in common porous materials with a well-defined pores structure.

5.3.4 Porosimetry measurement

Mercury intrusion porosimetry (MIP) and helium pycnometry (HePyc) were used to determine the porosity and densities of fully dried black liquor matrices (**Table 5-4**).

Table 5-4. Porosity skeletal and bulk densities of pullulan matrices.

Sample	Skeletal density MIP($g.cm^{-3}$) [a]	Skeletal density He-Pyc($g.cm^{-3}$) [b]	Porosity (%) [a]	Bulk density ($g.cm^{-3}$) [a]
M_5S_{20}	1.29 ± 0.05	1.28 ± 0.01	25 ± 1	0.96 ± 0.05
$M_{10}S_{20}$	1.31 ± 0.05	1.30 ± 0.01	17 ± 1	1.1 ± 0.05
$M_{15}S_{20}$	1.47 ± 0.05	1.51 ± 0.01	44 ± 1	0.82 ± 0.05
$M_{20}S_{20}$	1.72 ± 0.05	1.90 ± 0.01	55 ± 1	0.77 ± 0.05

[a] Determined by Mercury Intrusion Porosimetry, b Determined by Helium Pycnometry.

Skeletal density and porosity (%) values increased within the Kolliphor concentration showing a most significant difference at the highest concentrations tested. This might indicate that high Kolliphor concentrations were effective to disperse PCM into small droplets giving more and smaller uniform pore sizes, greater porosity with thicker lignin and hemicelluloses walls contributing to a better PCM encapsulation. On the contrary, low Kolliphor concentrations lead to bigger PCM droplets observed as big pore sizes easily visible in scanning electron micrographs with lower density values due to thinner lignin and hemicelluloses walls.

Interconnections-size distributions on monoliths M_5S_{20}, $M_{10}S_{20}$, $M_{15}S_{20}$ and $M_{20}S_{20}$ were examined by MIP, results are presented in **Figure 5-6**.

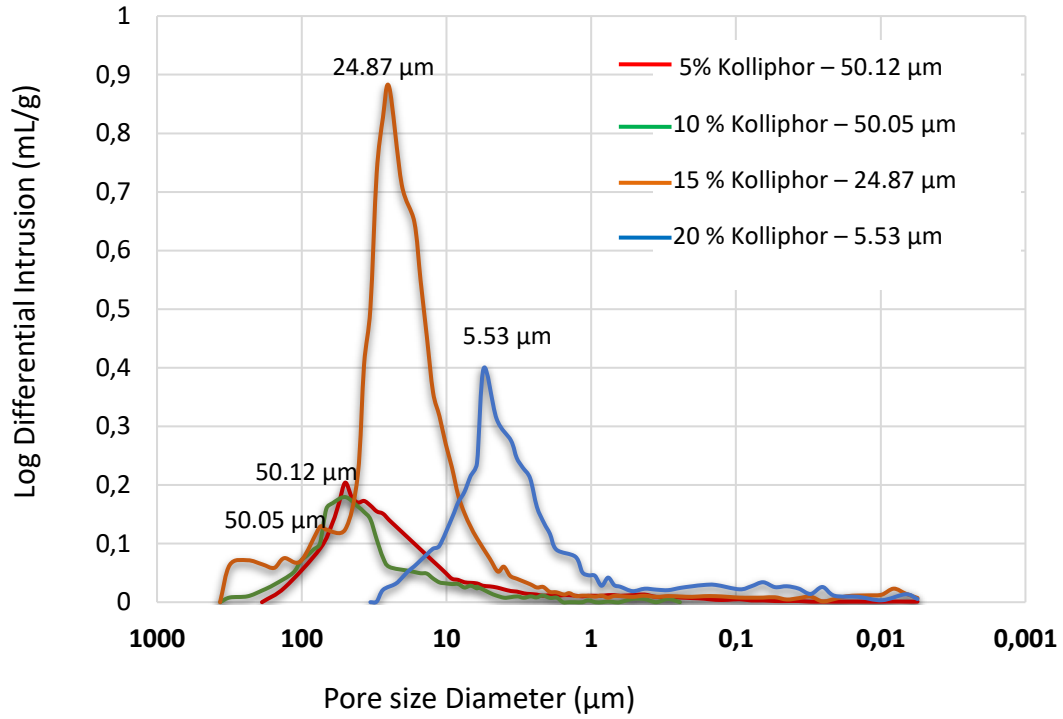

Figure 5-6. Interconnected-pore sizes of monoliths M5S20, M10S20, M15S20 and M20S20

Pore size diameter was highly sensitive to kolliphor concentrations, passing from 50 µm (for samples M_5S_{20} and $M_{10}S_{20}$) to 5 µm ($M_{20}S_{20}$). This was attributed first to a better solubilization of lignin and hemicellulose in black liquor allowing the movement of salt crystals from the bulk to the surface in this way they do not contribute to the formation of pores and second, to a better PCM distribution through the bulk, reducing the surface tension thus increasing emulsion stability over time at relatively high temperatures.

5.3.5 Differential scanning calorimetry (DSC) analysis

Differential scanning calorimetry analysis were done to butyl stearate encapsulated in samples $M_{20}S_{10}$, $M_{20}S_{13}$, $M_{20}S_{15}$ and $M_{20}S_{20}$. **Figure 5-7** shows the phase transition temperature of encapsulated PCM, monoliths were submitted to a temperature cycle in the range from 5 °C to 40 °C expecting to observed PCM phase transition from solid to liquid and liquid to solid in the mentioned range.

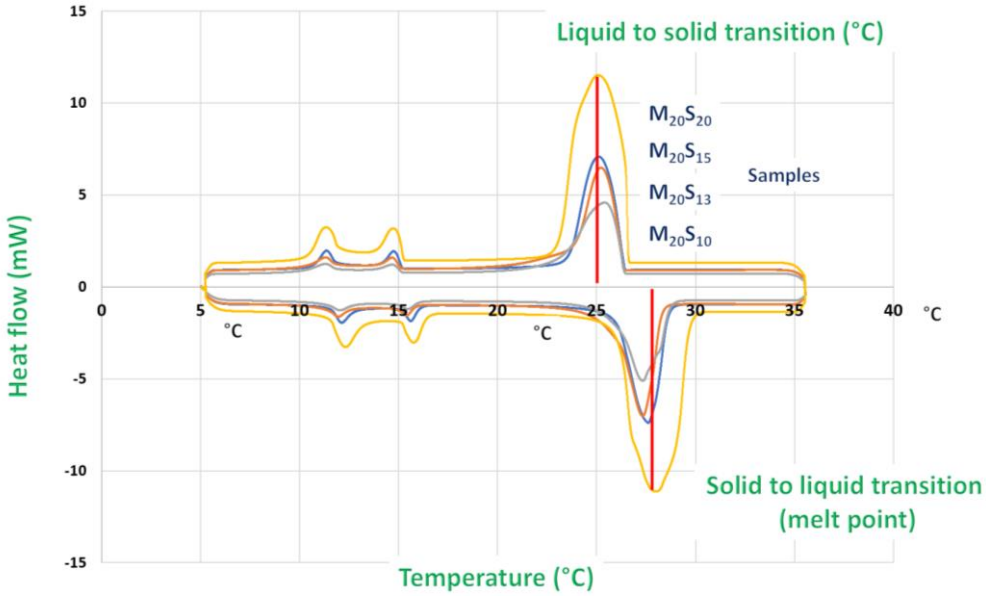

Figure 5-7. Differential scanning calorimetry characterization of encapsulated PCM.

In all cases temperature PCM phase transition was the same (27 °C for solid to liquid phase transition and 25 °C for liquid to solid), similar to the temperature phase transition measured in the PCM before its encapsulation (**Figure 5-8**). Encapsulation did not affect its thermal properties.

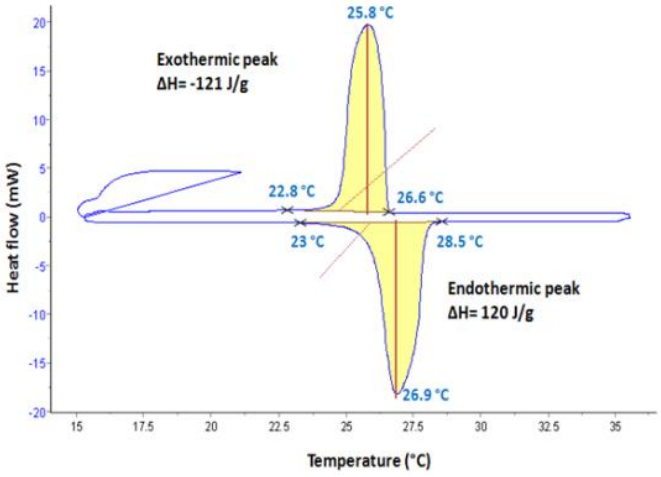

Figure 5-8. Butyl stearate not encapsulated PCM.

The measured heat flow in **Figure 5-7** could be related to the PCM quantity encapsulated in every case. Probably not all matrix encapsulated all the dispersed PCM otherwise they would have the same height and peaks will overlap. It's important to consider that similar quantities of samples were chosen for the analyses (between 0.12 and 0.19 g). Monolith with STMP 10% crosslinking yield ($M_{20}S_{10}$) gave the lowest heat flow, the increase of STMP crosslinking yields resulted in a higher heat flow every time until it reached it maximum height for $M_{20}S_{20}$. It's possible that imperceptible PCM losses occurred during samples manipulation because no weight loss was measured during synthesis nor after water removal (no other than that of water).

Nevertheless, it's possible to consider that encapsulation occurs in granules from the insides of the matrix to superficial layers. It could be through these superficial layers that PCM losses could have occurred.

To discuss the change in heat (ΔH), **Figure 5-8** is presented, it shows the DSC characterization analyses of every samples individually.

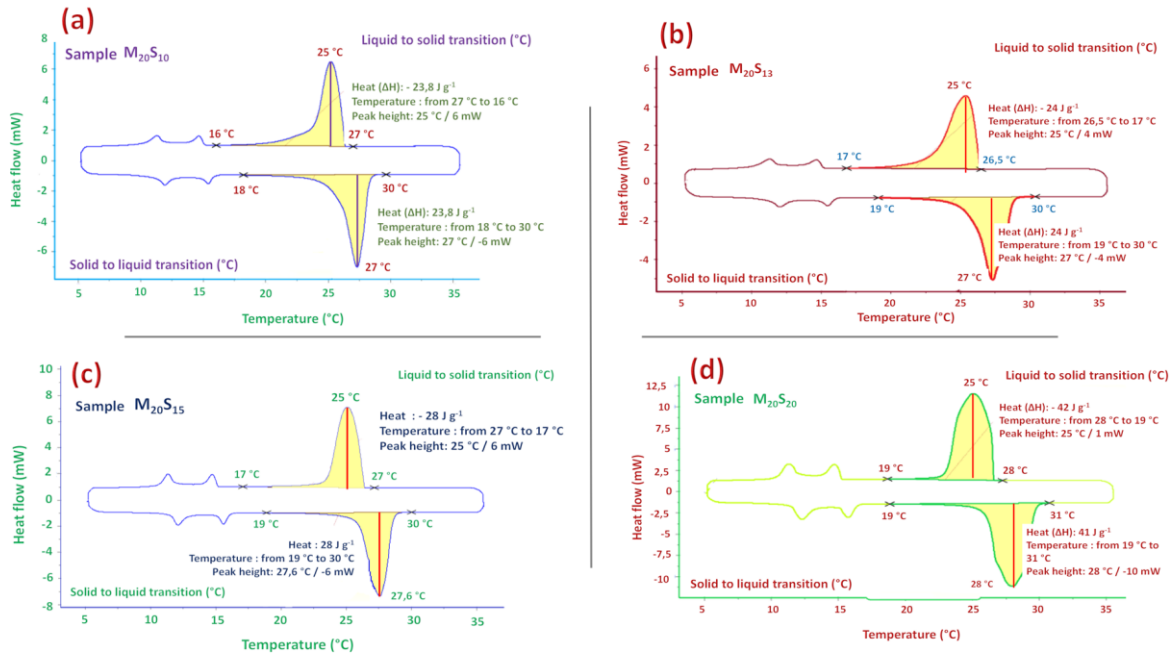

Figure 5-9. DSC characterization results of samples 10%, 13%, 15 and 20% STMP crosslinking yield.

Pure butyl - stearate PCM has a heat flow of 120 $J.g^{-1}$ as shown in **Figure 5-8**. Considering a 30% of encapsulated PCM the expected value for all samples tested is near 36 $J.g^{-1}$. In all samples near values were obtained (**Figure 5-9**: 23 $J.g^{-1}$ for sample M_5S_{10}, 24 $J.g^{-1}$ for $M_{20}S_{13}$, 28 $J.g^{-1}$ for $M_{20}S_{15}$ and 40 $J.g^{-1}$ for $M_{20}S_{20}$). This shows small PCM losses except for sample $M_{20}S_{20}$. This could be related to a better encapsulation with higher yields.

5.3.6 Mechanical tests

Monoliths $M_{20}S_{13}$, $M_{20}S_{15}$, $M_{20}S_{20}$ and $M_{20}S_{20}$ (0% PCM) was tested, results are tested in **Figure 5-10**.

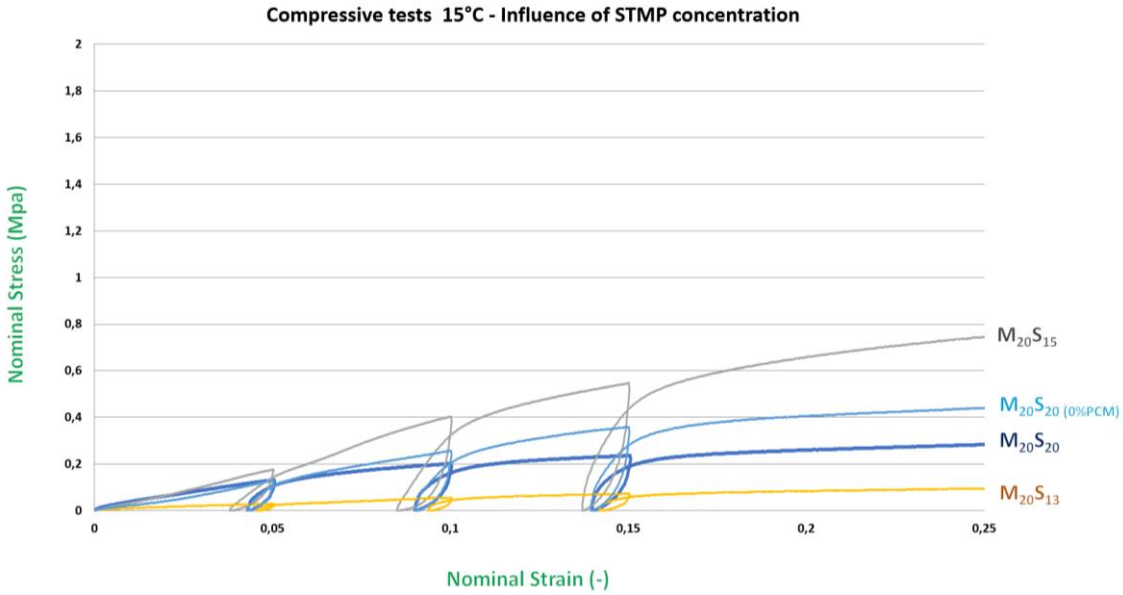

Figure 5-10. Nominal stress of STMP crosslinked monoliths.

All monoliths presented an elastic behavior seen by the nods formed at three different moments during the test. Finally, an elastic limit was determined around 0.1 value of nominal strain, beyond this point fractures appeared just before complete sample break. It is difficult to determine the elastic limit in compression and therefore the stress plateau for some specimen mechanically tested, in this case it was fixed at 0.1. Nevertheless, STMP crosslinking yields seem not to have an influence over mechanical stress nor the presence of PCM in solid phase (this test was performed at 15 °C to assure the solid phase of PCM). It's interesting to notice than sample $M_{20}S_{20}$ (0 % PCM) was in the same range of resistance, so PCM might not have a direct influence over mechanical properties.

As reference and for comparison, the same test was done for monoliths synthetized with epichlorohydrin crosslinking agent (**Figure 5-11**).

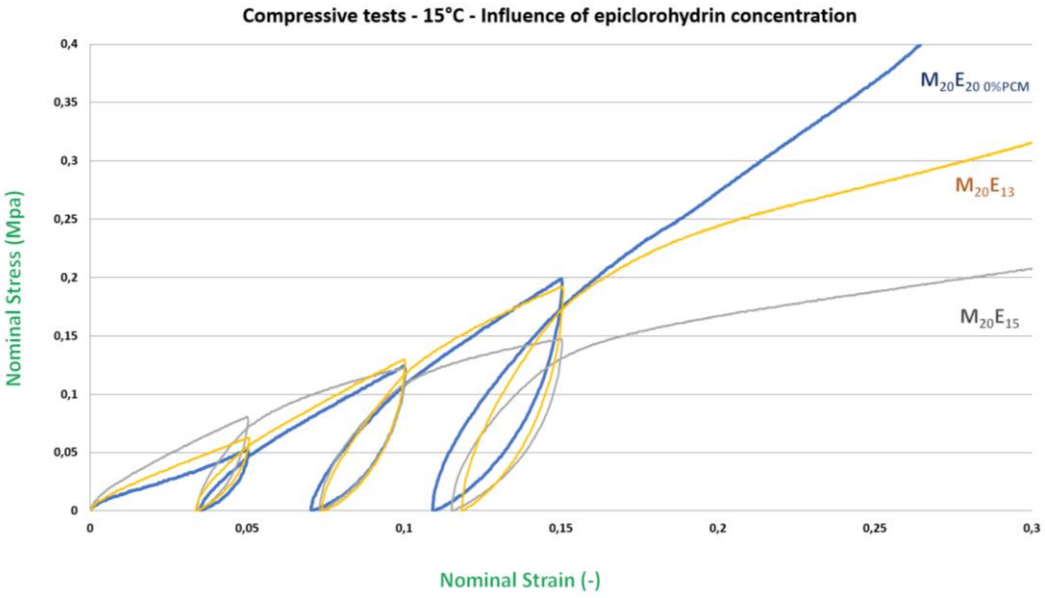

Figure 5-11. Nominal stress of epichlorohydrin crosslinked monoliths

At 15 °C (PCM in solid phase) nominal stress did not seem to be widely different than that with STMP and the same elastic modules are present, possible characteristic of these kind of crosslinked samples. No references of these properties have been reported as far as we are aware of, so no comparison with reported articles were possible to be done.

The elastic modulus has been measured for $M_{20}S_{20}$ and for comparisons purposes a sample synthetized with epichlorohydrin $M_{20}E_{20}$ (same composition as $M_{20}S_{20}$). Results are shown in **Figure 5-12**.

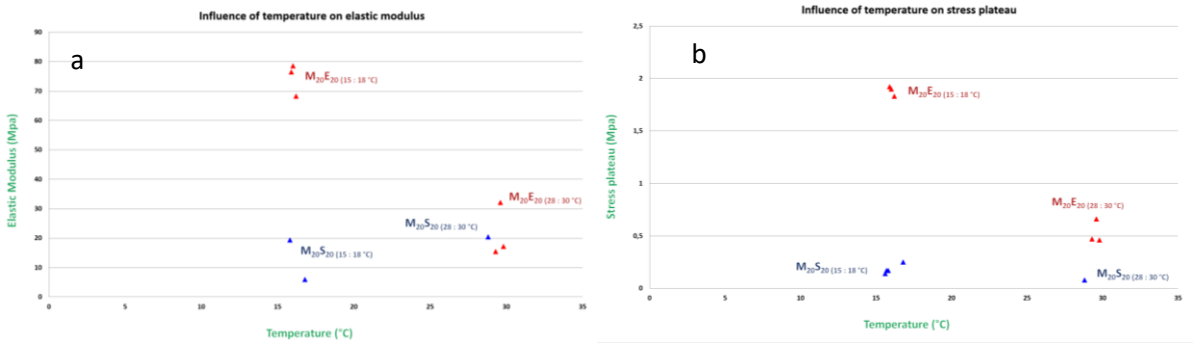

Figure 5-12. Elastic modulus measured from 0 to 35 °C temperature range for black liquor monoliths.

Figure 5-12-a shows the elastic modulus for two temperature values, about 15 and 30 °C. PCM at 18 °C is found in solid phase, significant difference is observed at this temperature while at 30 °C elastic modulus seems to be similar for both. This could indicate that for exterior panels applications, this type of materials did not have a wide range of resistance to stress in

comparison with wood (10-20 GPa), concrete (20-50 GPa) or expanded polystyrene (3-4 GPa). Their resistance to deformation before they fracture completely (**Figure 5-12**-b) was once higher for epichlorohydrin samples at 18 °C, dropping at 28 °C reaching similar STMP samples values. This could indicate the effect of liquid PCM on the materials resistance to external forces contributing to the materials strength when solid but not in liquid phase.

Regarding the effect of crosslinking yields at 15 °C (solid PCM phase) over the elastic modulus of samples results are presented in **Figure 5-13**.

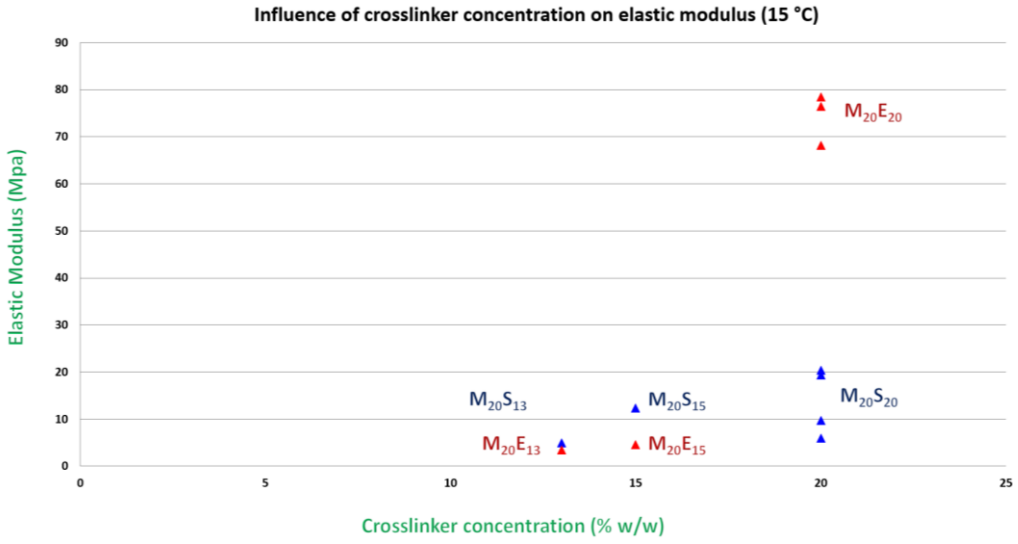

Figure 5-13. Elastic modulus at 15 °C of STMP and epichlorohydrin black liquor matrices.

It can be seen that samples have a better resistance to stress without experiencing deformations with epichlorohydrin only at a 20 % crosslinking yield. While with STMP, the yield did not modify significantly their resistance.

5.4 Conclusions

Black liquor monoliths for PCM encapsulation though the crosslinking of lignin and hemicelluloses moieties with STMP is a promising new material expecting it to have a positive impact in the efficiency use of energy.

Mechanically strong materials were synthesized with the nontoxic agent STMP, proposing its utilization in place of toxic or possible toxic crosslinking agents for the syntheses of new materials while keeping a high performance.

Emulsion templating polymerization keep showing advantages and potential opportunities for materials science, since it allows the utilization of many kinds of polymeric bases, easy addition of compounds, test the influence between chemical species and form a network by crosslinking.

Solid state ^{31}P-NMR was a valuable technique for the study of crosslinking in a polymeric base allowing the identification of intermediate and final reaction products. Alkalinity and STMP concentration were fundamental parameters during crosslinking to obtain higher yields measured by Pc and Pg relation.

Pore size distribution as a measurement of PCM dispersion during emulsion formation was affected directly by surfactant concentration; at higher concentrations smaller pores were observed. Surfactant concentration was a fundamental parameter to control materials morphology.

6 General conclusion

A sustainable development regarding energy storage systems applied in buildings offer great advantages, through the encapsulation of phase change materials it's possible to improve energy efficiency in buildings, dependency of one source (electricity) represents an opportunity to look for other options such as solar energy.

Phase change materials encapsulation in crosslinked polymer matrices is at the moment a barely explored area with great potential. Polymer matrices could be turned into size adaptable panels to be included in wall buildings, ceilings and floors in a permanent or movable way, and by phase change materials encapsulation, these panels will represent an economic, nontoxic, environmentally friendly material to contribute to energy efficiency.

This thesis has explored in a challenging field (storage energy systems) and represents the beginning of future research to achieve the synthesis of panels able to be applied in buildings.

Encapsulation of phase change materials in polymer based matrices is possible, however many parameters need to be improve before their in situ utilization, for example finding a method to determined more precisely a polymer based crosslinking yield, determine the exact amount of encapsulated PCM, improved the aqueous and dispersed phase mixing while materials synthesis and perform studies related with the utilization of solid particles dispersed in materials aqueous phase to improve mechanical resistance in final materials. Furthermore, propose the synthesis of panels and a characterization methodology since recent techniques have specific size requirements not always possible to achieve under common synthesis technology.

It necessary to have more polymer bases in order to test their potential for PCM encapsulation, pullulan for example is an interesting matrix, however its price and disponibility could not always be convenient for industrial applications. Its plastic behavior revealed after mechanical properties characterization, indicates that without any kind of particles added it might not resist a daily contact in field scenarios. On the other hand, the synthesis technique allows to improve its formulation and the addition of substances as well the utilization of other bases.

7 References

1. **Pavel, C. C., Darina Blagoeva, D. T.** *Competitive landscape of the EU's insulation materials industry for energy-efficient buildings.* Publications office of the European Union, Luxembourg. 2018. ISBN 978-92-79-74069-5.

2. **Rai, Amit.** *Thermal insulation: properties and applications in housing.* United Nations Industrial Development Organization (UNIDO), Vienna. 2017. pp. 5-34, Technical manual.

3. **Research, Grand View.** *Building thermal insulation market size, share and trends. Analysis report by product, (glass wool, mineral wool, EPS, XPS); by application; by end-use; by region and segment forecasts, 2018-2025.* State of California at Grand view resarch, Inc. U.S. State of California, U.S. 2018. p. 185. GVR-1-68038-338-6.

4. **Francesco Asdrubali, Francesco D'Alessandro, Samuele Schiavoni.** *A review of unconventional sustainable building insulation materials* 07 2015, Sustainable Materials and Technologies, Vol. 4, pp. 1-17.

5. **European Commission DG. United Nation Environment Program 2007.** Buildings and climate change: current status, challenges and opportunities. *UNEP.* https://wedocs.unep.org/handle/20.500.11822/7783.

6. **Anthony Zimmer and Haksoo Ha.** Buildings and Infrastructure from a Sustainability Perspective. *Sustainable and Healthy Communities Program - Theme 4.1.1.* https://www.epa.gov/sites/production/files/2016-09/documents/buildingsandinfrastructurefromasustainabilityperspective.pdf. Inernal EPA report (EPA/600/X-14/369).

7. **Official Journal of the European Union.** *Directive 2010/31/EU of the European Parliament and of the Council on the Energy Performance of Buildings.* [https://eur-lex.europa.eu/LexUriServ/LexUriServ.do?uri=OJ:L:2010:153:0013:0035:EN:PDF] 06 18, 2010. L 153/13.

8. **PR Newswire.** Growth opportunities in the global building thermal insulation market 2016-2021: trends, forecast and opportunity analysis. https://www.prnewswire.com/news-releases/growth-opportunities-in-the-global-building-thermal-insulation-market-2016-2021-trends-forecast-and-opportunity-analysis-august-2016-300381158.html. 4111744.

9. **Advanced thermal solutions, INC.** Thermal fundamentals. *Understanding thermal conductivity.* www.qats.com/Download/Qpedia_Feb07_Understanding_Thermal_Conductivity.ashx.

10. **Pont, Ulrich.** *A comprehensive approach to web-enabled, optimization-based decision support in building design and retrofit.* s.l., Vienna, Austria : Faculty of Architecture and Regional Planning, University of Technology of Vienna, 08 2014. Thesis dissertation.

11. **Ich-Long Ngo, Sangwoo Jeon, Chan Byon.** *Thermal conductivity of transparent and flexible polymers containing fillers: A literature review.* 07 2016, International Journal of Heat and Mass Transfer, Vol. 98, pp. 219-226. https://doi.org/10.1016/j.ijheatmasstransfer. 2016.02.082.

12. **Heindl, Eduard.** *Hydraulic Hydro Storage Systems for Self Sufficient Cities***.** Germany. 12 2014, Energy Procedia , Vol. 46, pp. 98-103.

13. **RWE Power AG. Spohr's Büro.** *Adiabatic Compressed-Air Energy Storage For Electricity Supply***.** 01 2010.

14. **Phase Change Materials Products, Inc.** *ThermalEnergy Systems (TES) Design Guide.* Mere View Industrial State. Yaxley, Cambridgeshire, PE7 3HS, UK 32 Unit. 2011.

15. **Karunesh Kant, A. Shukla, Atul Sharma, Anil Kumar, Anand Jain.** *Thermal energy storage based solar drying systems: a review.* 04 2016, Innovative food science and emerging technologies , Vol. 34, pp. 86-99.

16. **B. Akhmetov, A. G. Georgiev, A. Kaltayev, A. A. Dzhomartov, R. Popov, M. S. Tungatarova.** *Thermal energy storage systems - review.* 2016, Bulgarian chemical communications , Vol. 48, pp. 31-40.

17. **Guruprasad Alva, Lingkun Liu, Xiang Huang, Guiyin Fang.** *Thermal energy storage materials and systems for solar energy applications.* 1, 2017, Renewable and sustainable energy reviews, Vol. 68, pp. 693-706.

18. **V. V. Tyagi, S.C. Kaushik, S.K. Tyagi, T. Akiyama.** *Development of phase change materials based microencapsulated technology for buildings: A review.* 15, 2011, Energy Reviews, pp. 1373-1391.

19. **Benoit Stutz, Nolwenn Le Pierres, Frederic Kuznik, Kevyn Johannes, Elena Palomo del Barrio, Jean-Pierre Bedecarrats, Stephane Gibout, Philippe Marty, Laurent Zalewski, Jerome Soto.** *Storage of thermal solar energy.* 7-8, 2017, Comptes Rendus Physique , Vol. 18, pp. 401-414.

20. **Sarada Kuravi, Jaime Trahan, D. Yogi Goswami, Muhammad M. Rahman, Elias K. Stefanakos.** *Thermal energy storage technologies and systems for concentrating solar power plants.* 4, 2013, Progress in energy and combustion science, Vol. 39, pp. 285-319.

21. **Ali Fallahi, Gert Guldentops, Mingjiang Tao, Sergio Granados-Focil, Steven Van Deseel.** *Review on solid - solid phase change materials for thermal energy storage: Molecular structure and thermal properties.* 2017, Applied Thermal Engineering, Vol. 127, pp. 1427-1441.

22. **Jingyu Huang, Shilei Lu, Xiangfei Kong, Shangbao Liu, Yiran Li.** *Form-stable phase change materials based on eutectic mixture of tetradecanol and fatty acids for building energy storage: preparation and performance analysis*2013, Materials, Vol. 6.

23. **G. Saville.** Heat and mass transfer and fluids engineering. 2017.

24. **Duncan, W.A., Swinton, F.L.** *Thermodynamic properties of binary systems containing hexafluorobenzene*, 1965, Dept. of Pure and Applied Chemistry, Vol. 1, pp. 1082-1089.

25. **M. Karthikeyan, T. Ramachandran.** *Review of thermal energy storage of micro and nano encapsulated phase change materials.* 7, 11 2014, Materials research innovations, Vol. 18, pp. 541-553.

26. **Hamman Umer, Hemlata Nigam, Asif M. Tamboli, M. S. M. Nainar.** *Microencapsulation: process, techniques and applications.* 2, 01 2011, International journal of research in pharmaceutical and biomedical sciences, Vol. 2, pp. 474-481.

27. **A. Jamekhorshid, S. M. Sadrameli, M. Farid.** *A review of microencapsulation methods of phase change materials (PCMs) as a thermal energy storage (TES) medium .* 03 2014, Renewable and sustainable energy reviews, Vol. 31, pp. 531-542.

28. **Dingcai Wu, Fei Xu, Bin Sun, Ruowen Fu, Hongkun He, Krzyszof Matyjaszewski.** *Design and preparation of porous polymers.* 7, 2012, Chemical Reviews, Vol. 112, pp. 3959-4015.

29. **Borislav D. Zdravkov, Jiri J. Cermak Sefara, Josef Janku** *Pore clasification in the characterization of porous materials: a perspective.* 2, 2007, Central European Journal of Chemistry, Vol. 5, pp. 385-395.

30. **Barbara, Imane.** *Synthése de polyméres macroporeux par polymérisation par étape en émulsion concentrée.* Université de Bordeaux. Bordeaux : Ecole doctorale des sciences chimiques, 20117. p. 173, These.

31. **Garvin, Karen S.** Sciencing. *What are the advantages of the transmission electron microscope?.* 04 24, 2017. www.sciencing.com/advantages-transmission-electron-microscope.com.

32. **Andrzej Kownacki, Ewa Szarek-Gwiazda, Olga Woznicka.** *The importance of scanning electron microscopy (SEM) intaxonomy and morphology of chironomidae.* 1, 2015, European journal of environmental sciences, Vol. 5.

33. **Swapp, Susan.** Scanning electron microscopy (SEM). *Geochemical instrumentation and analysis .* https://serc.carleton.edu/research_education/geochemsheets/techniques/SEM.html.

34. **Justin, H.** Why are electron microscopes important? www.sciencing.com/electron-microscopes-important.

35. **Rogers, Michael Armin.** *Naturally ocucuring nanoparticles in food.* 1, 02 2016, Current opinion in food science, Vol. 7, pp. 14-19.

36. **Hadi, J. N., Norazian M. Hassan, Kausar Ahmad.** *Natural surfactants for pharmaceutical emulsions.* University of Malaysia. 2018.

37. **Becher, Paul.** *Emulsions: Theory and Practice.* American Chemical Society. 3er. Washington, D.C. : Oxford University Press, 2001.

38. **Lee D. Wilson, Inimfon A. Udoetok, John V. Headley.** *Stabilization of pickering emulsions by iron oxide nanoparticles.* National Research Council of Italy. 08 30, 2016. Advanced Marterial Science.

39. **Philippe Riachy, Marie-José Stébé, Bénédicte Lebeau, Andreea Pasc, Loïc Vidal.** *Nano-emulsions as imprints for the design of hierarchical porous silica through a dual templating mechanism.* 1, 2016, Microporous and Mesoporous Materials, Vol. 221, pp. 228-237.

40. **Wei Lu, Alan L. Kelly, Song Miao.** *Emulsion-based encapsulation and delivery systems for polyphenols* 1, 2016, Trends in Food Science and Technology, Vol. 47, pp. 1-9.

41. **Claire Forgacz, Marc Birot, Hervé Deleuze.** *Synthesis of porous emulsion-templated monoliths from a pulp mill by-product.* 2013, Journal of Applied Polymer Science.

42. **S. Tesch, Ch. Gerhards, H. Schubert.** *Stabilization of emulsions by OSA starches* 2002, Journal of Food Engineering , Vol. 54, pp. 167-174.

43. **Ali Barkat, Akhtar Naveed, Haroon Khan.** *Basics of pharmaceutical emulsions: a review.* 25, 2011, African journal of pharmacy and pharmacology , Vol. 525, pp. 2715-2725.

44. **Santosh Nemichand Kale, Sharada Laxman Deore.** *Emulsion micro emulsion and nano emulsion: a review* 1, 01 2017, Systematic Reviews in Pharmacy , Vol. 8, pp. 39-47.

45. **Lautrup, Benny.** *Physics of continuous matter.* Second edition. CRC Press, 2011. p. 696. Vol. 1.

46. **Olorunsola EO, Adedokun MO.** *Surface activity as basis for pharmaceutical applications of hydrocolloids: A review***.** 10, 2014, Journal of applied pharmaceutical science, Vol. 4, pp. 110-116.

47. **P. Schalbart, M. Kawaji, K. Fumoto.** *Formation of tetradecane nanoemulsion by low energy emulsification methods*8, 2010, International Journal of Refrigeration. Vol. 33, pp. 1612-1624.

48. **Silverstein, M. S.** *Emulsion-templated polymers: Contemporary contemplations.* 2017, Polymer, Vol. 126, pp. 261-282.

49. **Silverstein, M. S.** *Emulsion-templated porous polymers: A retrospective perspective.* 2014, Polymer, Vol. 55, pp. 304-320.

50. **N. Brun, S. Ungureanu, H. Deleuze, R. Backov.** *Hybrid foams, colloids and beyond: From design to applications.* 2011, Chem. Soc. Rev., Vol. 40, pp. 771-788.

51. **Cameron, N. R.** *High internal phase emulsion templating as a route to well defined porous polymers.* 2005, Polymer, Vol. 46, pp. 1439-1449.

52. **Cameron N. R., Sherrington D. C.** *High internal phase emulsions (HIPES): Structure, properties and use in polymer preparation.* Berlin, Heidelberg Springer. 1996, Biopolymers Liquid Crystalline Polymers Phase Emulsion. Advances in Polymer Science, Vol. 126, pp. 163-214.

53. **Q. Jiang, A. Menner, A. Bismarck.** *Emulsion-templated macroporous polymer/polymer composites with switchable stiffness.* 2014, Pure Appl. Chem., Vol. 86, pp. 203-213.

54. **S. Kovacic, K. Jerabek, P. Krajnc.** *Responsive Poly(acrylic acid) and Poly(N-isopropylacrylamide) monoliths for high internal phase emulsions (HIPEs).* 2011, Templating Macromol. Chem. Phys., Vol. 212, pp. 2151-2158.

55. **T. Gitli, M. S. Silverstein.** *Emulsion templated bicontinuous hydrophobic-hydrophilic polymers: Loading and release.* 2011, Polymer, Vol. 52, pp. 107-115.

56. **N. Shirshova, A. Bismarck, J. H. G. Steinke.** *Ionic liquids as internal phase for non-aqueous PolyHIPEs.* 2011, Macromol. Rapid Commun., Vol. 32, pp. 1899-1904.

57. **Singh R. S., Sainin G. K.** *Biosynthesis of pullulan and its applications in food and pharmaceutical industry.* 2012, Research gate. Microorganisms in sustainable agriculture and biotechnology, Vol. 24, pp. 509-545.

58. **J., Catley B. J. Whelan W.** *Observation on the structure of pullulan.* 1971. Archives of biochemistry and biophysics, Vol. 143, pp. 138-142.

59. **Leathers, L. D.** *Biotechnological production and applications of pullulan.* 2003, Applied Microbiological Biotechnology, Vol. 62, pp. 468-473.

60. **Ahmed, Enas M.** *Hydrogel: Preparation, characterization, and applications: A review.* 2015, Journal of advanced research, Vol. 6, pp. 105-121.

61. **Peppas N.A., Bures P., Leobandung W., Ichikawa H.** *Hydrogels in pharmaceutical formulations.* 2000, European Journal of Pharmaceutics and Biopharmaceutics, Vol. 50, pp. 27-46.

62. **Blasques Bueno V., Bentini R., Catalani L. H., Freitas D.** *Synthesis and swelling behavior of xanthan-based hydrogels.* 2, 02 15, 2013, Carbohydrates polymers, Vol. 92, pp. 1091-1099.

63. **Salis A., Ninham B. W.** *Models and mechanisms of Hofmeister effects in electrolyte solutions, and colloid and protein systems revisited.* 21, 08 06, 2014, Chemical Society Reviews, Vol. 43, pp. 7358-7377.

64. **Chirani N., Yahia L., Gritsch L., Motta F. L., Chirani S., Faré S.** *Hystory and applications of hydrogels.* 2:13, 10 02, 2015, Journal of biomedical sciences, Vol. 4.

65. **V. V. Tyagi, S. C. Kaushik, T. Akiyama.** *Development of phase change materials based microencapsulated technology for buildings: a review.* 2011, Renewable and sustainable energy reviews, Vol. 15, pp. 1373-1391.

66. **M. Karthikeyan, T. R.** *Review of thermal energy storage of micro and nanoencapsulated phase change materials.* 2014, Mater. Res. Innov., Vol. 18, pp. 541-553.

67. **T. Khadiran, M. Z. Hussein, Z. Zainal, R. Rusli.** *Advanced energy storage materials for buildings applications and their thermal performance characterization: a review.* 2016, Renew. Sust. Energy Rev., Vol. 57, pp. 916-928.

68. **Risch, S. J.** *Encapsulation: overview of uses and techniques.* 1995, ACS Symposium series, pp. 2-7.

69. **M. Peanparkdee, S. Iwamoto, R. Yamauchi.** 2016. *Microencapsulation: a review of applications in the food and pharmaceutical industries*, Rev. Agri. Sci. , Vol. 4, pp. 56-65.

70. **H. Umer, H. Nigam, A.M. Tamboli, M.S.M. Nainar.** *Microencapsulation: process, techniques and applications.* 2011, Int. J. Res. Pharm. Biomed. Sci., Vol. 2, pp. 474-481.

71. **A. M. Bakry, S. Abbas, B. Ali, H. Majeed, M. Y. Abouelwafa, A. Mousa, L. Liang.** *Microencapsulation of oils: a comprehensive review of benefits, techniques and applications.* 2016, Compr. Rev. Food Saf., Vol. 15, pp. 143-182.

72. **J. Giro-Paloma, M. Martinez, L. F. Cabeza, A. I. Fernandez.** *Types, methods, techniques and applications for microencapsulated phase change materials (MPCM): a review.* 2016, Renew. Sust. Energy Rev., Vol. 53, pp. 1059-1075.

73. **N. Brun, S. Ungureanu, H. Deleuze, R. Backov.** *Hybrid foams, colloids and beyond: from design to applications.* 2011, Chem. Soc. Rezv., Vol. 40, pp. 771-788.

74. **Cameron, N. R.** *High internal phase emulsion templating as a route to well-defined porous polymers.* 2005, Polymer, Vol. 46, pp. 1439-1449.

75. **Q. Jiang, A. Menner, A. Bismarck.** *Emulsion-templated macroporous polymer/polymer composites with switchable stiffness.* 2014, Pure Appl. Chem. , Vol. 86, pp. 203-213.

76. **N. Shirshova, A. Bismarck, J. H. G. Steinke.** *Ionic liquids as internal phase of non-aqueous polyHIPES.* 2011, Macromol. Rapid Commun., Vol. 32, pp. 1899-1904.

77. **A. Barbetta, M. Dentini, M. S. De Vecchis, P. Filippini, G. Formisano, S. Caiazza.** *Scaffolds based on biopolymeric foams*2005, Adv. Funct. Mat., Vol. 15, pp. 118-125.

78. **F. Cira, E. H. Mert.** *PolyHIPE/Pullulan composites derived from glycidyl methacrylate and 1,3-butanediol dimethacrylate-based high internal phase emulsions.* 2015, Polym. Eng. Sci., Vol. 55, pp. 2636-2642.

79. **Hayashibara Co.** *Pullulan a unique functional polysaccharide.*

80. **K. .R. Sugumaran, V. Ponnusami.** *Review on production, downstream processing and characterization of microbial pullulan.* 2017, Carbohydr. Polym. , Vol. 173, pp. 573-591.

81. **R. S. Singh, G. K. Saini.** *Biosynthesis of pullulan and its applications in food and pharmaceutical industry.* India Springer. 2012, Microorganisms in sustainable agriculture and biotechnology, Vol. II, pp. 509-553.

82. **Q. Tong, Q. Wiao, L. T. Lim.** *Preparation and properties of pullulan-alginate-carboxylmethylcellulose blend films .* 2008, Food Res. Int. , Vol. 41, pp. 1007-1014.

83. **Safety evaluation of certain food.** *Pullulan.* Sixty-fifth report of the joint FAO/WHO Expert committee on food additives. Geneva : s.n., 2006. pp. 24-8.

84. **K. C. Cheng, A. Demirci, J. M. Catchmark.** *Pullulan: biosynthesis, production and applications.* 2011, Appl. Microbiol. Biotechnol., Vol. 92, pp. 29-44.

85. **F. Gao, D. Li, C. H. Bi, Z. H. Mao, B. Adhikari.** *Preparation and characterization of starch crosslinked with sodium trimetaphosphate and hydrolyzed by enzymes*2014, Carbohydr. Polym., Vol. 103, pp. 310-318.

86. **S. Lack, V. Dulong, D. Le Cerf, L. Picton, J. F. Argillier, G. Muller.** *Hydrogels based on pullulan crosslinked with sodium trimetaphosphate (STMP): rheological study.* 2004, Polymer Bull. , Vol. 52, pp. 429-436.

87. **V. Dulong, R. Forbice, E. Condamine, D. Le Cerf, L. Picton.** *Pullulan-STMP hydrogels: a way to correlate crosslinking mechanism, structure and physicochemical properties.***.** 2011, Polymer Bull, Vol. 67, pp. 455-466.

88. **A. Sari, A. Biçer, A. Karaipekli.** *Synthesis, characterization, thermal properties of a series of stearic acid esters as novel-liquid phase change materials.* 2009, Mat. Lett. , Vol. 63, pp. 1213-1216.

89. **K. Cellat, B. Beyhan, B. Kazanci, Y. Konuklu, H. Paksoy.** *Direct incorporation of butyl stearate as phase change material into concrete for energy saving in buildings.* 2017, J. Clean Energ. Technol., Vol. 5, pp. 64-68.

90. **C. Liang, X. Lingling, S. Hongbo, Z. Zhibin.** *Microencapsulation of butyl stearate as a phase change material by interfacial polycondesation in a polyurea system.* 2009, Energ. Convers. Manag., Vol. 50, pp. 723-729.

91. **T. G. Chuah, D. Rozanna, A. Salmiah, S. Y. Thomas Choong, M. Sa'ari.** *Low chain esters of stearic acid as phase change materials for thermal energy storage in buildings.* 1995, Sol. Energ. Mat. Sol. Cells., Vol. 36, pp. 311-322.

92. **Americas, ICI.** HLB system: a time saving guide to emulsifier selection. 1984.

93. **J. Jiao, D. J. Burgess.** *Rheology and stability of water-in-oil-in-water multiple emulsions containing span 83 and tween 80.* 2003, AAPS PharmaSci., Vol. 5, pp. 62-73.

94. **L. Shaofeng, X. Jianwei, Z. Zhaohuan, J. Gaopeng.** *Preparation and characterization of polyurea/polyurethane double shell microcapsules containing butyl stearate through interfacial polymerization*2011, J. Appl. Polym. Sci. , Vol. 121, pp. 3377-3383.

95. **A. Sari, A. Biçer, A. Karaipekli.** *Synthesis, characterization, thermal properties of a series of stearic acid esters as novel soli-liquid phase change materials.* 2009, Mat. Lett. , Vol. 63, pp. 1213-1216.

96. **L. J. Gibson, M. F. Ashby.** *Cellular solids: structure and properties.* Cambridge University Press. 1999.

97. **Xiaodong Cao, Xilei Dai, Junjie Liu.** *Building energy-consumption status worldwide and the state-of-the-art technologies for zero-energy buildings during the past decade.* 06 2016, Energy and Buildings, Vol. 128.

98. **Delaney, Brian James and Paul.** *Phase change materials: are they part of our energy efficient future?* U.S. 2012, Association of Computer Electronics and Electrical Engineers (ACEEE), Vol. 3, pp. 160-172.

99. **Luis Pérez-Lombard, José Ortiz, Christine Pout.** *A review on buildings energy consumption information*3, Spain, United Kingdom : s.n., March 2008, Energy and Buildings , Vol. 40, pp. 394-398.

100. **Atul Sharma, V.V. Tyagi, C.R. Chen, D. Buddhi.** *Review on thermal energy storage with phase change materials and applications.* 2, 02 2009, Renewable & Sustainable Energy Reviews, Vol. 13, pp. 318-345.

101. **Kyoung Ok Lee, Mario A. Medina, Xiaoqin Sun, Xing Jin.** *Thermal performance of phase change materials (PCM)-enhanced cellulose insulation in passive solar residential building walls.* 15, 03 2018, Solar Energy, Vol. 163, pp. 113-121.

102. **Jianqing Chen, Donghui yang, Jinghua Jiang, Aibin Ma, Dan Song.** *Research progress of phase change materials (PCMs) embedded with metal foam (a review).* 2014, Procedia Materialsl Science, Vol. 4, pp. 389-394. 8th International Conference on Porous Metals and Metallic Foams, Metfoam 2013.

103. **Jan Kosny, Som S. Shrestha, Therese K. Stovall, David W. Yarbrough.** *Theoretical and Experimental Thermal Performance Analysis of Complex Thermal Storage Membrane Containing Bio-Based Phase-Change Material (PCM).* 12 2010, Thermal Performance of the Exterior Envelopes of Whole Buildings - 11th International Conference.

104. **James C. Hatfield, St. Albans, W. Va.** *Encapsulation of phase change materials* . 4.708.812, Union Carbide Corporation, Danbury, Conn. : s.n., 11 24, 1987, United States Patent. 749.098.

105. **Marco A. Marcos, David Cabaleiro, Maria J. G. Guimarey, Maria J. P. Comunas, Laura Fedele, Josefa Fernandez, Luis Lugo.** *PEG 400-Based Phase Change Materials Nano-Enhanced with Functionalized Graphene Nanoplatelets.* 16, 12 29, 2017, Nanomaterials, Vol. 8.

106. **B. Alic, U. Sebenik, M. Krajnc.** *Microencapsulation of butyl stearate with melamine-formaldehyde resin: effect of decreasing the pH value on the composition and thermal stability of microcapsules.* 10, 2012, Express polymer letters, Vol. 6, pp. 826-836.

107. **Cosima Stubenrauch, Angelika Menner, Alexander Bismarck, Wiebke Drenckhan.** *Emulsion and Foam Templating: Promising Routes to Tailor-Made Porous Polymers.* 32, 08 2018, Angewandte Chemie International Edition, Vol. 57, pp. 10024-10032.

108. **Claire Forgacz, Marc Birot, Hervé Deleuze.** *Synthesis of Porous Emulsion-Templated Monoliths from a Pulp Mill By-Product.* 5, 01 30, 2013, Journal of Applied Polymer Science, Vol. 129, pp. 2606-2613.

109. **Juliette Merle, Marc Birot, Hervé Deleuze, Pierre Trinsoutrot, Heléne Carré, Quentin Huyette, Fatima Charrier-El Bouhtoury.** *Valorization of Kraft black liquor and tannins via porous material production.* 09 17, 2016, Arabian Journal of Chemistry. Article In press, https://doi.org/10.1016/j.arabjc.2016.09.006.

110. **Dorra Saidane, Jean-Christophe Barbe, Marc Birot, Hervé Deleuze.** *Preparation of Functionalized Kraft Lignin Beads.* 2, 12 17, 2009, Journal of Applied Polymer Science, Vol. 116, pp. 1184-1189.

111. **Robert T. Woodward, Arthur Jobbe-Duval, Sofia Marchesini, David B. Anthony, Camille Petit, Alexander Bismarck.** *Hypercrosslinked polyHIPEs as precursors to designable, hierarchically porous carbon foams.* 04 21, 2017, Polymer, Vol. 115, pp. 146-153.

112. **Imane Barbara, Marie-Anne Dourges, Hervé Deleuze.** *Preparation of porous polyurethanes by emulsion-templated step growth polymerization* . 12 06, 2017, Polymer, Vol. 132, pp. 243-251.

113. **Amandine Foulet, Marc Birot, Guido Sonnemann, Hervé Deleuze.** *The potential of Kraft black liquor to produce bio-based emulsion-templated porous materials.* 05 2015, Reactive and Functional Polymers, Vol. 90, pp. 15-20.

114. **Mohammad Jalalian, Qixiang Jiang, Marc Birot, Hervé Deleuze, Robert T. Woodward, Alexander Bismarck.** *Frothed black liquor as a renewable cost effective precursor to low-density lignin and carbon foams.* 08 03, 2018, Reactive and Functional Polymers . Article in press. https://doi.org/10.1016/j.reactfunctpolym.2018.07.027.

115. **Environmental Protection Agency.** *Health and environmental effects profile for epichlorohydrin.* Environmental criteria and assessment office; Office of research and development of Cincinnati. U.S. : s.n., 1985. https://www.epa.gov/sites/production/files/2016-09/documents/epichlorohydrin.pdf.

116. **National Center for Environmental Assessment.** *Integrated risk information system (IRIS) on epichlorohydrin.* 1999.

117. **Virginie Dulong, Renauld Forbice, Eric Condamine, Didier Le Cerf, Luc Picton.** *Pullulan-STMP hydrogels: a way to correlate crosslinking mechanism, structure and physicochemical properties.* 3, 07 2011, Polymer Bulletin, Vol. 67, pp. 455-466.

118. **Virginie Dulong, S. Lack, D. Le Cerf, L. Picton, J.P. Vannier, G. Muller.** *Hyaluronan-based hydrogels particles prepared by crosslinking with sodium trimetaphosphate. Synthesis and characterization.* 1, 08 12, 2004, Carbohydrate Polymers, Vol. 57, pp. 1-6.

119. **Stéphane Lack, Virginie Dulong, Didier Le Cerf, Luc Picton, Jean Francois Argillier, Guy Muller.***Hydrogels Based on Pullulan Crosslinked with sodium trimetaphosphate (STMP): Rheological study* 6, 12 2004, Polymer Bulletin, Vol. 52, pp. 429-436.

120. **Stéphane Lack, Virginie Dulong, Luc Picton, Didier Le Cerf, Eric Condamine.** *High-resolution nuclear magnetic resonance spectroscopy studies of polysaccharides crosslinked by sodium trimetaphosphate: a proposal for the reaction mechanism.* 7, 05 21, 2007, Carbohydrate Research, Vol. 342, pp. 943-953.

121. **Fréderic Kuznik, Damien David, Kevyn Johannes, Jean-Jacques Roux.** *A review on phase change materials integrated in building walls.* 1, 01 2011, Renewable ans Sustainable Energy Reviews, Vol. 15, pp. 379-391.

122. **Kemal Cellat, Beyza Beyhan, Berk Kazanci, Yeliz Konuklu, Halime Paksoy.** *Direct Incorporation of Butyl Stearate as Phase Change Material into Concrete for Energy Saving in Buildings.* 1, 01 2017, Journal of Clean Energy Technologies , Vol. 5, pp. 64-68.

123. **Chen Liang, Xu Lingling, Shang Hongbo, Zhang Zhibin.** *Microencapsulation of butyl stearate as a PCM by interfacial polycondensation in a polyurea system.* 3, 03 2009, Energy Conversion and Management, Vol. 50, pp. 723-729.

124. **Barbara J. Cade-Menun, Martin R. Carter, Dean C. James.** *Phosphorus Forms and Chemistry in the Soil Profile under Long-Term Conservation Tillage: A Phosphorus-31 Nuclear Magnetic Resonance Study* 1, 12 2010, Journal of Environmental Quality, Vol. 39, pp. 1647-1655.

125. **H. Ibrahim, A. llinca, J. Perron.** *Energy storage systems: characteristics and comparisons.* 5, 06 2008, Renewable and sustainable energy reviews, Vol. 12, pp. 1221-1250.

126. **Khin, Mya Mya.** *Encapsulation of phase change materials (PCMS) for heat storage.* Department of Chemical and Environmental Engineering. National University of Singapore. 2003.

127. **D. Pal, Y. K. Joshi.** *Application of phase change materials to thermal control of electronics modules: a computational study.* 1, 1997, Journal of Electronic Packaging , Vol. 119, pp. 40-50.

128. **Jiri Zach, Jitka Hroudova, Jiri Brozovsky, Zdenek Krejza, Albinas Gailius.** *Development of thermal insulating materials on natural base for thermal insulation systems*2013, Procedia Engineering, Vol. 57, pp. 1288-1294. 11th International Conference on Modern Building Materials, Structures and Techniques, MBMST 2013.

129. **Marjana Radünz, Elizabete Helbig, Caroline Dellinghausen Borges, Tatiane Kuka Valente Gandra, Eliezer Avila Gandra.** *A mini-review on encapsulation of essential oils .* 1, 01 26, 2018, Journal of analytical and pharmaceutical research, Vol. 7.

130. **Becher, Paul.** *Emulsions: Theory and Practice.* s.l. : Oxford University Press, 2001.

131. **Lee, Yuan-Tseh.** *Challenges facing human society in the 21st century.* Academia Sinica Taiwan, 2009, Conference of the national associations of the international sociological association., pp. 1-7.

132. **Güngör, Gökhan.** Thermal comfort and energy consumption of a typical office building, Gothenburg, Sweden. *Master thesis.* 2015.

133. **Ibrahim Diçer, Marc A. Rosen.** *Thermal energy storage: systems and applications.* [ed.] Wiley. 2nd edition. 2011.

134. **T. Khadiran, M. Zobir Hussein, Z. Zainal, R. Rusli.** *Advanced energy storage materials for building applications and their thermal performance characterization: A review.* 05 2016, Renewable and suistainable energy reviews, Vol. 57, pp. 916-928.

135. **PCM products Ltd company.** [Online] [Cited: 09 23, 2018.] www.pcmproducts.net.

136. **B. Alic, U. Sebenik, M. Krajnc.** *Microencapsulation of butyl stearate with melamineformaldehyde resin: effect of decreasing the pH value on the composition and thermal stability of microcapsules* 10, 2012, Express polymer letters, Vol. 6, pp. 826-836.

137. **Jean-Paul Douliez, Nicolas Martin, Thomas Beneyton, Jean-Charles Eloi, Jean-Paul Chapel, Laurence Navailles, Jean-Christophe Baret, Stephen Mann, Laure Béven.** *Preparation of swellable hydrogel containing colloidosomes from aqueous two phase pickering emulsion droplets .* 26, 04 23, 2018, Angewandte Chemie , Vol. 57, pp. 7780-7784.

138. **Marques, Helena Ma Cabral.** *A review on cyclodextrin encapsulation of essential oils and volatiles.* 1, 07 02, 2010, Flavour and fragance journal, Vol. 25, pp. 313-326. DOI 10.1002/FFJ.2019.

139. **Youngman Yoo, Carlos Martinez, Jeffrey P. Youngblood.** *Synthesis and chracterization of microencapsulated phase change materials with poly(urea-urethane) shells containing cellulose nanocrystals.* 1, 08 08, 2017, Applied materials and interfaces, Vol. 9, pp. 31763-31776.

140. **B Alič, U Šebenik, M Krajnc.** *Microencapsulation of butyl stearate with melamine-formaldehyde resin: effect of decreasing the pH value on the composition and thermal stability of microcapsules.* 10, 2012, Express polymer letters, Vol. 6, pp. 826-836. DOI: 10.3144/expresspolymlett.2012.88.

141. **Hammad Umer, Hemlata Nigam, Asif M. Tamboli, M. Sundara Moorthi Nainar.** *Microencapsulation: process, techniques and applications.* 2, 06 2011, International journal of research in pharmaceutical and biomedical sciences, Vol. 2, pp. 474-481.

142. **Bjorn Bolund, Hans Bernhoff, Mats Leijon.** *Flywheel energy and power storage systems.* 2, 02 2007, Renewable and Sustainable Energy Reviews, Vol. 11, pp. 235-258.

143. **Miriana Kfoury, David Landy, Sophie Fourmentin.** *Characterization of cyclodextrin volatile inclusion complexes: A review.* 1204, 04 30, 2018, Molecules, Vol. 23, pp. 1-23.

144. **A. Barbara, M. Dentini, M. S. De Vecchis, P. Filippini, G. Formisano, S. Caiazza.** *Scaffolds based on biopolymeric foams.* 2005, Adv. Funct. Mat., Vol. 15, pp. 118-125.

145. **F. Cira, E. H. Mert.** *PolyHIPE/Pullulan composites derived from glycidyl methacrylate and 1,3-butanediol dimethacrylate-based high internal phase emulsions.* 2015, Polym. Eng. Sci., Vol. 55, pp. 2636-2642.

146. **Feng Jiang, Chen Qian, Alan R. Esker, Maren Roman.** *Effect of Nonionic Surfactants on Dispersion and Polar Interactions in the Adsorption of Cellulases onto Lignin .* 41, 09 2017, The Journal of Physical Chemistry B, Vol. 121, pp. 9607-9620.

147. **Qinghua Zhang, Karine De Oliveira, Sebastien Royer, Francoise Jerome.** *Deep eutectic solvents: syntheses, properties and applications*12, 2012, Chemical Society Review, Vol. 41, pp. 7108-7146.

148. **CERES Greenhouse.** *Phase change materials. Passive temperature regulation.* Greenhouse solutions, Boulder Colorado U.S., 2018.